INFORMATION TO USERS

This material was produced from a microfilm copy of the original document. While the most advanced technological means to photograph and reproduce this document have been used, the quality is heavily dependent upon the quality of the original submitted.

The following explanation of techniques is provided to help you understand markings or patterns which may appear on this reproduction.

1. The sign or "target" for pages apparently lacking from the document photographed is "Missing Page(s)". If it was possible to obtain the missing page(s) or section, they are spliced into the film along with adjacent pages. This may have necessitated cutting thru an image and duplicating adjacent pages to insure you complete continuity.

2. When an image on the film is obliterated with a large round black mark, it is an indication that the photographer suspected that the copy may have moved during exposure and thus cause a blurred image. You will find a good image of the page in the adjacent frame.

3. When a map, drawing or chart, etc., was part of the material being photographed the photographer followed a definite method in "sectioning" the material. It is customary to begin photoing at the upper left hand corner of a large sheet and to continue photoing from left to right in equal sections with a small overlap. If necessary, sectioning is continued again — beginning below the first row and continuing on until complete.

4. The majority of users indicate that the textual content is of greatest value, however, a somewhat higher quality reproduction could be made from "photographs" if essential to the understanding of the dissertation. Silver prints of "photographs" may be ordered at additional charge by writing the Order Department, giving the catalog number, title, author and specific pages you wish reproduced.

5. PLEASE NOTE: Some pages may have indistinct print. Filmed as received.

Xerox University Microfilms
300 North Zeeb Road
Ann Arbor, Michigan 48106

76-9531

TROESCH, Armin Walter, 1947-
THE DIFFRACTION POTENTIAL FOR A SLENDER SHIP MOVING THROUGH OBLIQUE WAVES.

The University of Michigan, Ph.D., 1975
Engineering, marine

Xerox University Microfilms, Ann Arbor, Michigan 48106

THIS DISSERTATION HAS BEEN MICROFILMED EXACTLY AS RECEIVED.

THE DIFFRACTION POTENTIAL FOR A SLENDER SHIP MOVING THROUGH OBLIQUE WAVES

by

Armin Walter Troesch

A dissertation submitted in partial fulfillment
of the requirements for the degree of
Doctor of Philosophy
(Naval Architecture and Marine Engineering)
in The University of Michigan
1975

Doctoral Committee:

Assistant Professor Robert F. Beck, Chairman
Professor T. Francis Ogilvie
Assistant Professor William S. Vorus
Associate Professor Wei H. Yang

ACKNOWLEDGMENTS

I would like to thank Professor T. Francis Ogilvie and Assistant Professor Robert F. Beck for their support in this work and their friendly display of skepticism on the various occasions when we discussed its content.

I would like to thank Nabil Daoud and Art Reed who provided a number of invaluable suggestions concerning the numerical analyses and also Professor Masataka Fujino and Toshimitsu Kaiho who obtained and interpreted the experimental data.

The typing of this manuscript has been a laborious task, and my thanks go to Kathie Malley and Nancy Dillon who suffered through it.

Finally, I would like to thank my family for their understanding and enthusiastic support throughout my education.

ABSTRACT

The diffraction problem of a fixed slender ship in incident waves is formulated. Both the conditions of zero and constant forward velocity are considered. The waves are assumed to be of the same order as the beam of the ship and are from an oblique heading.

The boundary value problem is linearized with respect to wave amplitude and solved by the method of matched asymptotic expansions. The first order zero speed solution is described in terms of an integral representation and means for numerically evaluating it are given. The forward speed potential is solved to two orders of magnitude. The first order is just the zero speed case while the second order problem involves solving a boundary value problem with a non-homogeneous free surface condition. The solution to this second order problem is given in terms of three auxiliary potentials, each satisfying a separate part of the boundary conditions.

For zero forward speed, the sectional exciting force is calculated and compared with the commonly used integrand of the Khaskind relations. The two give different values, but when integrated over the hull both show the same total exciting force.

The pressure distribution on an ore carrier for both zero forward speed and an abbreviated form of the forward speed case are given and compared with experiments. The theory compares well with the measured pressures on the mid-ship section, and on a forward section with stern seas. However, the theory does not compare well for the case of a forward section and bow seas.

TABLE OF CONTENTS

ACKNOWLEDGMENTS ii

ABSTRACT iii

LIST OF TABLES vi

LIST OF ILLUSTRATIONS vii

CHAPTER I: INTRODUCTION 1

CHAPTER II: FORMULATION OF THE PROBLEM 5

CHAPTER III: THE ZERO SPEED PROBLEM 8

The Near Field Problem 9
The Far Field Problem 11
The Inner Expansion of the Outer Expansion 14
Matching the Expansions 22
Summary of the Zero Speed Problem 24

CHAPTER IV: METHOD OF SOLUTION FOR THE ψ_1 PROBLEM . . . 25

Formulation of an Integral Representation 25
Derivation of an Integral Equation 27
Solution of the Integral Equation 29
The Determination of the Potential 35

CHAPTER V: THE FORWARD SPEED PROBLEM 40

The Near Field Problem 41
The Far Field Problem 47
The Inner Expansion of the Far Field Expansion . . . 51
Matching the Expansion 53
Summary of the Forward Speed Problem and Its Solution 55
The Pressure and Force on the Hull 58

CHAPTER VI: NUMERICAL RESULTS 64

Pressure Distribution 65
Sectional Force Distribution 72
Total Force 81

CHAPTER VII: SUMMARY AND CONCLUSIONS 86

APPENDIX A: The Green's Function 90

APPENDIX B: The Applied Pressure Problem 95

APPENDIX C: Simplification of I(k) 104

BIBLIOGRAPHY 116

LIST OF TABLES

Table 1: Values of $I_S(k)$ for Different Ranges of k and U Equal to Zero 14

Table 2: Values of $I_D(k)$ for Different Ranges of k and U Equal to Zero 14

Table 3: Heaving Rectangular Cylinder 35

Table 4: $I_S(k)$ for Different Values of k and U Not Equal to Zero 48

Table 5: Sectional Exciting Force for a Midship Section of an Ore Carrier ($\chi = 45°$) 68

Table C1: Values of $I_S(k)$ for Different Ranges of k and U Equal to Zero 110

Table C2: Values of $I_D(k)$ for Different Ranges of k and U Equal to Zero iii

Table C3: Values of $I_S(k)$ for Different Ranges of k and U Not Equal to Zero 114

LIST OF ILLUSTRATIONS

Figure 1: The Coordinate System 5

Figure 2: Hull Surface for Finding $\frac{\partial}{\partial N}\int d\ell\sigma G$ 28

Figure 3: A Section of the Hull 30

Figure 4: The Behavior of $\frac{\partial}{\partial N} K_o(\nu r)$ as $(\xi,\eta)\rightarrow(y,z)$ . . . 32

Figure 5: The Behavior of the Source Strength for a Heaving Rectangular Cylinder 36

Figure 6: Description of dr_i 37

Figure 7: Girthwise Pressure Distribution for a Midship Section of an Ore Carrier in Oblique Seas ($L/\lambda = 1.96$, $\chi = 45°$) 66

Figure 8: Girthwise Pressure Distribution for a Midship Section of an Ore Carrier in Oblique Seas ($L/\lambda = 1.44$, $\chi = 45°$) 67

Figure 9: Girthwise Pressure Distribution for a Forward Station of an Ore Carrier in Oblique Seas ($L/\lambda = 2.0$, $\chi = 135°$) 70

Figure 10: Girthwise Pressure Distribution for a Forward Station of an Ore Carrier in Oblique Seas ($L/\lambda = 2.0$, $\chi = 45°$) 71

Figure 11: The Shadow Region of an Obstacle in Incident Waves 72

Figure 12: Sectional Force Distribution for a Series 60, $C_B = .70$ Hull Form ($L/\lambda = 3.33$, $\chi = 60°$) . . . 74

Figure 13: Sectional Force Distribution for a Series 60, $C_B = .70$ Hull Form ($L/\lambda = 2.0$, $\chi = 60°$) 75

Figure 14: Sectional Force Distribution for a Series 60, $C_B = .70$ Hull Form ($L/\lambda = 1.43$, $\chi = 60°$) . . . 76

Figure 15: Sectional Force Distribution for a Series 60, $C_B = .70$ Hull Form ($L/\lambda = 3.33$, $\chi = 30°$) . . . 77

Figure 16: Sectional Force Distribution for a Series 60, C_B = .70 Hull Form (L/λ = 2.0, χ = 30°) 78

Figure 17: Sectional Force Distribution for a Series 60, C_B = .70 Hull Form (L/λ = 1.43, χ = 30°) 79

Figure 18: Total Force for a Series 60, C_B = .70 Hull Form in Oblique Seas (χ = 120°) 83

Figure 19: Total Force for a Series 60 C_B = .70 Hull Form in Oblique Seas (χ = 30°) 84

Figure 20: Phase Angles of Exciting Forces for a Series 60, C_B = .70 Hull Form in Oblique Waves (χ = 30°) . 85

Figure B1: Contour of Integration in the k-Plane 98

Figure C1: Contour of Integration for $k>\nu+\kappa$ 105

Figure C2: Contour Around the Branch Cut in the ℓ-plane and $\sqrt{(\nu-\kappa)^2+\ell^2}$ plane 107

Figure C3: Contour of Integration for $\nu-\kappa<k<\nu+\kappa$ 108

Figure C4: Contour of Integration on the Real Axis for $k>k_1$ 113

Figure C5: Contour of Integration on the Real Axis for $k<k_1$ 114

Chapter I

INTRODUCTION

The scattering of waves by an object has always been of interest to the theoretical hydrodynamist. However, except for a few simple shapes, the complexity of the problem has prevented analytical solutions from being found. In ship motions theory the force due to the diffraction of waves is of primary interest, and consequently, methods for finding the total exciting forces have been derived. In the more mathematically correct methods (see Khaskind (1957) and Newman (1965)) the diffraction problem has been replaced by a forced oscillation one. As a result, the sectional force distribution due to an incident wave has been lost even though the total force on the ship is found.

With the advent of larger, longer ships, such as supertankers and Great Lakes ore carriers, the maximum stresses due to wave induced loads have become important design considerations. Since bending moments and shear stresses are functions of the longitudinal force distribution, an accurate method of determining the sectional force is desirable. The wave-excited main vibration of the ship's hull, commonly called "springing", has been investigated by numerous authors, e.g. Goodman (1971), where the usual strip theory is used for calculating wave-excitation forces. Springing is basically a short wave phenomena that occurs at different heading angles and different ship speeds. The use of the current strip theory in finding bending moments and springing stresses in short waves is not mathematically correct, yet there have been no investigations into the amount of error introduced by using it.

Newman (1970) showed that for zero forward speed, the determination of the sectional forces due to incident waves should have involved solving a Helmholtz equation in the cross plane instead of Laplace's equation as the usual strip theory did.

He stated that the integration of the solution to those two problems should have yielded the same total forces in an asymptotic sense. However, since those total forces are only mathematically equivalent as the wave length goes to zero, it is not obvious for non-zero wave lengths that the two will give equivalent total forces.

Ogilvie (1974) arrived at the same formula for the sectional force as Newman. He differed from Newman in that his derivation used a three dimensional approach whereas Newman simply used Green's theorem in two dimensions. Ogilvie also hypothesized that in assuming a short wave length theory, the result may not be asymptotically consistent but should be numerically consistent. In other words, as long as the assumptions involving the longitudinal behavior of the sectional forces are correct, the short wave approximation will give the proper numerical answers for longer waves.

The diffraction of waves by a ship for the special case of head seas has been investigated by Faltinsen (1971). He considered both the zero speed and forward speed cases and calculated the actual diffraction pressures rather than just the sectional exciting forces. The theory was based on a short wave assumption and compared well with experiments indicating that Ogilvie's hypothesis may be true. However, Faltinsen found only the results for a circular cylinder and did not indicate how the theory would produce answers for ship-shapes in waves from oblique headings.

The intention of this thesis is to solve the diffraction problem for a slender ship with zero and forward speed in oblique waves. Certain assumptions will be made in order to make the problem tractable. The validity of these assumptions will be shown through comparisons of theory and experiments.

As mentioned previously, Newman (1970) and Ogilvie (1974) have shown that the sectional force may be found by defining an auxiliary problem that can be physically interpreted as a forced oscillation potential that satisfies a Helmholtz equation in the fluid domain. The objection to this sort of

reciprocity relation is that the diffraction pressures have been lost through the use of Green's theorem. This thesis solves the total diffraction problem, consistent with the assumptions made. Once the diffraction potential is known, the pressures can be found and then integrated to give the sectional forces and moments.

Four restrictions are applied to the theory as follows:

(1) The ship hull should represent a slender body, i.e., the beam and draft must be small in comparison with the length, and the transverse sections must vary slowly along the length.

(2) The wave length is small, comparable with the beam of the ship. This restriction is applied for both the zero and non-zero speed cases.

(3) When considering speed effects, the forward speed is of order one.

(4) The heading angle is for oblique seas. For example, if ε is a slenderness parameter, $\kappa = 2\pi/\lambda$ the wave number, and $\nu=\kappa \cos \chi$ the wave number in the longitudinal direction where χ is the heading angle, then $\kappa = O(\varepsilon^{-1})$, $\nu = O(\varepsilon^{-1})$ and $\sqrt{\kappa^2 - \nu^2} = O(\varepsilon^{-1})$ as $\varepsilon \to 0$.

The second restriction is worth noting. In a work which justified the use of strip theory, Ogilvie & Tuck (1969) assumed a short wave theory of $\kappa = O(\varepsilon^{-1})$ for zero speed, but maintained the same order for the frequency of oscillation for forward speed which resulted in longer waves, i.e. $\kappa = O(\varepsilon^{-1/2})$. Faltinsen (1971) used the same restriction on wave length as used in this thesis which resulted in a theory that compared well with experiments. In addition, his forward speed solution was just a function of speed times the zero speed potential. We will see that this simple correction for forward speed does not extend to oblique

seas. We will also see that the results of this thesis may be correct for wave lengths larger than the second restriction implies.

The formulation of the zero speed problem is very similar to that found by Newman (1970) and Ogilvie (1974). The diffraction potential must satisfy a two-dimensional Helmholtz equation in the cross plane and a body boundary condition that requires its normal derivative to be equal to the negative of the normal derivative of the incident wave potential. An integral equation is derived and solved numerically by assuming the hull to be represented by circular arc segments.

The forward speed problem is solved by a perturbation analysis. The first term in the expansion is just the zero speed problem. The second term has some similarities with the results found in Ogilvie & Tuck (1969); however the governing differential equation is always a Helmholtz equation rather than Laplace's. The inner expansion of the second order problem requires in part, that there be linearly growing waves as the inner variables become large. This is a result of the inclusion of a non-homogenous boundary condition on the free surface. The solution to the second order problem is then written as the sum of three potentials, each satisfying different parts of the boundary conditions.

Chapter II

FORMULATION OF THE PROBLEM

The ship is assumed to be fixed in an incident stream of velocity U. The coordinate system, as shown in Figure 1, has the z-axis in the upwards direction, the y-axis positive to starboard and the x-axis parallel to and in the same direction as the incident stream. The incident waves make an angle χ with the x-axis, where $\chi = 0$ represents head seas.

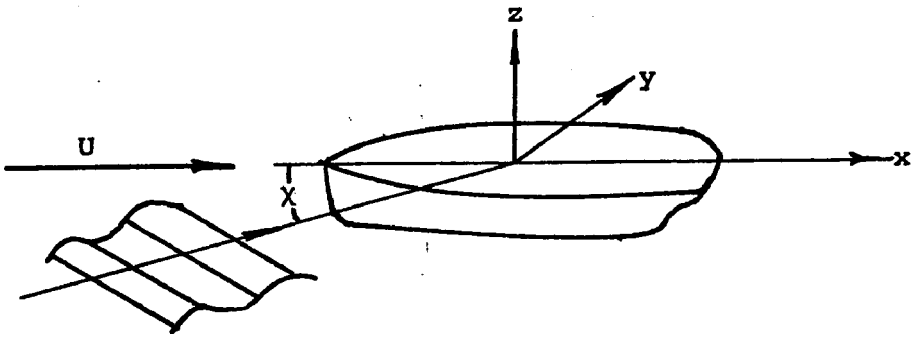

Figure 1: The Coordinate System.

The equation of the hull is given as:

$$y = h(x,z), \tag{1}$$

and the free surface is given as:

$$z = \zeta(x,y,t) \tag{2}$$

The usual assumptions are made about the fluid being inviscid, incompressible and irrotational. There exists a velocity potential $\Phi(x,y,z,t)$ that satisfies:

i) the Laplace equation in the fluid domain,

$$\frac{\partial^2\Phi}{\partial x^2} + \frac{\partial^2\Phi}{\partial y^2} + \frac{\partial^2\Phi}{\partial y^2} = 0; \tag{3}$$

ii) the dynamic boundary condition which states that the pressure is zero on the free surface,

$$g\zeta + \Phi_t + \frac{1}{2}\left\{\Phi_x^2 + \Phi_y^2 + \Phi_z^2\right\} = \frac{1}{2}U^2 \text{ , on } z = \zeta(x,y,t) \tag{4}$$

iii) the kinematic boundary condition which states that particles on the free surface remain there,

$$\Phi_x\zeta_x + \Phi_y\zeta_y - \Phi_z + \zeta_t = 0, \text{ on } z = \zeta(x,y,t); \tag{5}$$

iv) and the hull boundary condition which states that particles do not penetrate the hull,

$$\frac{\partial\Phi}{\partial n} = 0, \text{ on } y = h(x,z). \tag{6}$$

The ship is assumed to be a slender body characterized by a slenderness parameter ε. This parameter is considered to be small and indicative of the fact that the ship changes shape slowly along its length.

In the near field this assumption has a profound effect on differentiation. It can be stated as:

> "Derivatives of flow variables in the transverse direction are larger than longitudinal derivatives by an order of magnitude with respect to the slenderness parameter."

This implies the following:

$$\frac{\partial}{\partial x} = O(1); \quad \frac{\partial}{\partial y} = O(\varepsilon^{-1}); \quad \frac{\partial}{\partial z} = O(\varepsilon^{-1}) \tag{7a}$$

The characteristics of the hull can be interpreted as follows:

$$y = h(x,z) = \varepsilon H(x,z), \text{ where } H(x,z) = O(1);$$

and the inward normal $\underline{n}(x,y,z) = (n_1,n_2,n_3)$ has components

$$n_1 = O(\varepsilon), \quad n_2 = O(1), \quad n_3 = O(1) \tag{7b}$$

The wave length, λ, of the incident waves is assumed to be of the same order as the beam. The wave number, κ, is written as

$$\kappa = 2\pi/\lambda = O(\varepsilon^{-1})$$

This results in a wave number in the y direction of

$$\kappa \sin \chi = \sqrt{\kappa^2 - \nu^2} = O(\varepsilon^{-1})$$

The dispersion relation, relating the frequency to wave length, is

$$\omega_0^2 = \kappa g$$

where ω_0 is the frequency and g is the gravitational constant.

In the chapters that follow, these assumptions based on the slenderness parameter ε are applied to the governing equations to produce solvable problems.

For a more complete discussion on perturbation analysis in hydrodynamics, see Van Dyke (1964) or Ogilvie (1970). The latter has a detailed description of slender body theory.

Chapter III

THE ZERO SPEED PROBLEM

The method of matched asymptotic expansions is really not necessary to determine the solution for the zero speed case. We could make a very reasonable guess, just as Ogilvie (1974) and Newman (1970) did, to find the first approximation. However, in solving the zero speed problem formally, we lay the groundwork for solving the more difficult forward speed problem where reasonable guesses are not adequate.

We start the analysis by assuming the total potential is equal to the sum of the incident wave potential, Φ_I, and the diffraction potential, Φ_D. Φ_I is given as

$$\Phi_I(x,y,z,t) = \frac{g\zeta_0}{\omega_0} e^{i(\omega_o t - \nu x)} e^{\kappa z - iy\sqrt{\kappa^2 - \nu^2}}$$

$$\equiv e^{i(\omega_o t - \nu x)} \phi_o(y,z).$$

Setting U equal to zero, eliminating ζ, and dropping the higher order terms in equations (4) and (5) yield the usual linearized free surface boundary condition of

$$-\kappa\Phi + \Phi_z = 0, \text{ on } z = 0. \tag{8}$$

Since Φ is written as

$$\Phi = \Phi_I + \Phi_D,$$

and Φ_I satisfies (3) and (8), we get the following conditions on Φ :

$$\frac{\partial^2\Phi_D}{\partial x^2} + \frac{\partial^2\Phi_D}{\partial y^2} + \frac{\partial^2\Phi_D}{\partial z^2} = 0 \qquad \text{in the fluid domain,} \tag{9}$$

$$-\kappa\Phi_D + \Phi_{D_z} = 0 \qquad \text{on } z = 0 \tag{10}$$

and

$$\frac{\partial \Phi_D}{\partial n} = -\frac{\partial \Phi_I}{\partial n} \qquad \text{on} \quad y = h(x,z). \tag{11}$$

The Near Field Problem

Since the incident wave has the factor $e^{i(\omega_o t - \nu x)}$, and the ship is slender and the waves are short, it seems reasonable to expect the diffraction wave also to have this oscillatory behavior. This assumption is not valid near the ends, but then the assumptions implied by (7), i.e., things change slowly in the x direction, is not valid there either. It is for these reasons we assume that

$$\Phi_D(x,y,z,t) = e^{i(\omega_o t - \nu x)} \phi_7(x,y,z) \tag{12}$$

where $\Phi_7(x,y,z)$ is some slowly varying function of x.

Putting (12) into (9), (10) and (11) gives, respectively

$$\frac{\partial^2 \phi_7}{\partial y^2} + \frac{\partial^2 \phi_7}{\partial z^2} - \nu^2 \phi_7 - i\nu \frac{\partial \phi_7}{\partial x} + \frac{\partial^2 \phi_7}{\partial x^2} = 0 \tag{13}$$

$$-\kappa \phi_7 + \phi_{7_z} = 0 \qquad \text{on} \quad z = 0, \tag{14}$$

and

$$\frac{\partial \phi_7}{\partial n} = -\frac{\partial \phi_o}{\partial n} \qquad \text{on} \quad y = h(x,z). \tag{15}$$

We will now assume that ϕ_7 can be expanded in an asymptotic series of the form

$$\phi_7(x,y,z) \sim \sum_{i=1}^{N} \psi_i(x,y,z,\varepsilon). \tag{16}$$

As usual ψ_n satisfies $\psi_{n+1} = o(\psi_n)$ as $\varepsilon \to 0$ for fixed x,y,z.

Substituting (16) into (13), (14) and (15) and recalling the ordering of the derivatives given in (7a) and (7b), the governing equations for the first order problem, ψ_1, are:

$$\frac{\partial^2\psi_1}{\partial y^2} + \frac{\partial^2\psi_1}{\partial y^2} - \nu^2\psi_1 = 0 \qquad \text{in the fluid domain,} \qquad (17)$$

$$-\kappa\psi_1 + \psi_{1_z} = 0 \qquad \text{on } z = 0 \qquad (18)$$

and

$$\frac{\partial\psi_1}{\partial N} = -\frac{\partial\phi_o}{\partial N} \qquad \text{on } y = h(x,z). \qquad (19)$$

Here N is the two dimensional normal with components only in the transverse plane. Equation (19) was found by realizing that

$$\frac{\partial}{\partial n} = \underline{n} \cdot \nabla_{3\text{-D}} = \underline{N} \cdot \nabla_{2\text{-D}} + O(\varepsilon).$$

There are two noteworthy observations of the ψ_1 problem:

i) ψ_1 is dependent upon x only in a parametric sense. That is, once a section of the hull is given for a value of x, ψ_1 becomes a problem involving only the transverse dimensions, y and z. As a result, ψ_1 will now be written as $\psi_1(y,z;x)$.

ii) There is no radiation condition for ψ_1 as $\sqrt{y^2 + z^2} \to \infty$ and without it, ψ_1 is indeterminate. The radiation condition will come from matching the expansion of the inner region with that of the outer region. Though we might guess that ψ_1 will represent outgoing waves at large distances from the body, there is no formal justification for this. And while this guess would be correct for zero speed, it will be incomplete in the forward speed case ultimately leading to incorrect results. For this reason we will find the far

field expansion for the zero speed problem thus gaining valuable insight into the forward speed problem.

The Far Field Problem

In the far field, we expect the ship to appear as a line distribution of pulsating sources and horizontal dipoles on the free surface. The dipoles are needed since the body boundary condition given in (19) has both a symmetric and an asymmetric part to it. The symmetric term will generate even waves which will be represented by the sources and the asymmetric term will generate odd waves which will be represented by the dipoles.

On the free surface in the far field we expect waves to exist. Yet, if the formal rules of slender-body theory are applied, there are no gravity waves. To explain this contradiction we follow a rationale outlined in Ogilvie & Tuck (1969). "We include (inconsistently) all terms which could possibly be of importance in the far field and we obtain the solution to this more general problem. The real difficulty is that the far-field includes several regions in which there are different behaviors of the solutions. Thus our initial solution covers all of these regions." When we find the inner expansion of the outer, we will then only keep terms that are consistent with our level of approximation.

Let $\psi_s(x,y,z)e^{i\omega_o t}$ be the far field source potential.

Then $\psi_s(x,y,z)$ satisfies

$$\frac{\partial^2\psi_s}{\partial x^2} + \frac{\partial^2\psi_s}{\partial y^2} + \frac{\partial^2\psi_s}{\partial z^2} = \lim_{\substack{\xi\to 0\\ \eta\to 0}} \sum(x)e^{-i\nu x}\delta(y-\xi)\delta(z-\eta) \qquad (20a)$$

and

$$(i\omega_o + \mu)^2 \psi_s + g\psi_{s_z} = 0, \qquad \text{on} \quad z = 0 \tag{21}$$

Here $\sum(x)$ is a slowly varying source distribution and μ is the artificial Rayleigh viscosity that will be allowed to go to zero to give the proper radiation condition.

The solution for $\psi_s(x,y,z)$ can be found by taking the double Fourier transforms* of (20a) and (21), solving the resulting ordinary differential equation with variable coefficients by, say, the method of variation of parameters, and finally taking its inverse. Then with $\xi = 0$ and $\eta = 0$, $\psi_s(x,y,z)$ takes the form of

$$\psi_s(x,y,z) = \lim_{\mu\to 0}\left\{-\frac{1}{4\pi^2}\int_{-\infty}^{\infty} dk\, \sum{}^*(k+\nu)e^{ikx}\int_{-\infty}^{\infty} dl\, \frac{e^{ily+\sqrt{k^2+l^2}\,z}}{\sqrt{k^2+l^2}-\frac{1}{g}(\omega_o - i\mu)^2}\right\}$$

$$= -\frac{1}{4\pi^2}\int_{-\infty}^{\infty} dk\, \sum{}^*(k+\nu)e^{ikx}I_s(k) \tag{22a}$$

where $\sum^*(k+\nu)$ is the Fourier transform of $e^{-i\nu x}\sum(x)$ and

$$I_s(k) = \lim_{\mu\to 0}\int_{-\infty}^{\infty} dl\, \frac{e^{ily+\sqrt{k^2+l^2}\,z}}{\sqrt{k^2+l^2}-\frac{1}{g}(\omega_o - i\mu)^2} \quad . \tag{23a}$$

If we set $\nu = 0$ in (22a), we find that our result is equivalent to the potential for a line of pulsating sources given in Ogilvie & Tuck (1969).

Now let $\psi_D(x,y,z)e^{i\omega_o t}$ be the far field dipole potential. Then $\psi_D(x,y,z)$ satisfies

---

*The definitions of the Fourier Transform and its inverse as used in this work are

$$f^*(k) = \int_{-\infty}^{\infty} dx e^{-ikx} f(x) \quad ; \quad f(x) = \frac{1}{2\pi}\int_{-\infty}^{\infty} dk\, e^{ikx} f^*(k) \; .$$

$$\frac{\partial^2\psi_D}{\partial x^2} + \frac{\partial^2\psi_D}{\partial y^2} + \frac{\partial^2\psi_D}{\partial z^2} = \lim_{\substack{\xi\to 0\\ \eta\to 0}} \beta(x) e^{-i\nu x}\delta'(y-\xi)\delta(z-\eta) \tag{20b}$$

and the same free surface condition as $\psi_s(x,y,z)$. Only horizontal dipoles are needed to give the necessary asymmetry. Here $\beta(x)$ is a slowly varying dipole distribution, and the differentiation of the delta function is with respect to the singularity point, ξ. Then, in the same manner that $\psi_s(x,y,z)$ was found, $\psi_D(x,y,z)$ has the form

$$\psi_D(x,y,z) = \lim_{\mu\to 0}\left\{-\frac{i}{4\pi^2}\int_{-\infty}^{\infty} dk\beta^*(k+\nu)e^{ikx}\int_{-\infty}^{\infty} dl\,\frac{le^{ily+\sqrt{k^2+l^2}\,z}}{\sqrt{k^2+l^2}-\frac{1}{g}(\omega_o-i\mu)^2}\right\}$$

$$= -\frac{1}{4\pi^2}\int_{-\infty}^{\infty} dk\,\beta^*(k+\nu)e^{ikx}I_D(k), \tag{22b}$$

where $\beta^*(k+\nu)$ is the Fourier transform of $\beta(x)e^{-i\nu x}$ and

$$I_D(k) = \lim_{\mu\to 0} i\int_{-\infty}^{\infty} dl\,\frac{le^{ily+\sqrt{k^2+l^2}\,z}}{\sqrt{k^2+l^2}-\frac{1}{g}(\omega_o-i\mu)^2} \tag{23b}$$

Kellogg (1929), in his classic work on potential theory, shows that differentiation of a source with respect to its source point yields a dipole. We can see from (20a) that differentiation with respect to ξ is the same as differentiation with respect to $-y$. This is also true for (21). If the negative sign is included in the definition of β, then differentiation with respect to y will give (22b). This will be the method that we will use to find the expansion of the dipole potential in the rest of this work.

From Appendix C we can write down the approximate values for $I_s(k)$ and $I_D(k)$ if the assumption of short waves from oblique headings is made. These results are contained in Table 1 and Table 2, where a substitution of $k=k'-\nu$ was made, and then the primes were subsequently dropped.

Table 1

Values of $I_s(k)$ for Different Ranges of k with U Equal to Zero.

	$k>\nu+\kappa$ or $k<\nu-\kappa$	$\nu-\kappa<k<\nu+\kappa$
$I_s(k)$	$\dfrac{2\pi\kappa e^{-\lvert y\rvert\sqrt{(\nu-k)^2-\kappa^2}+z\kappa}}{\sqrt{(\nu-k)^2-\kappa^2}}$	$\dfrac{-2\pi i\kappa e^{-i\lvert y\rvert\sqrt{\kappa^2-(\nu-k)^2}+z\kappa}}{\sqrt{\kappa^2-(\nu-k)^2}}$

Table 2

Value of $I_D(k)$ for Different Ranges of k with U Equal to Zero.

	$k>\nu+\kappa$ or $k<\nu-\kappa$	$\nu-\kappa<k<\nu+\kappa$
$I_D(k)$	$-\mathrm{sgn}(y)\,2\pi\kappa e^{-\lvert y\rvert\sqrt{(\nu-k)^2-\kappa^2}+z\kappa}$	$-\mathrm{sgn}(y)\,2\pi\kappa e^{-i\lvert y\rvert\sqrt{\kappa^2-(\nu-k)^2}+z\kappa}$

The Inner Expansion of the Outer Expansion

Using the results found in Table 1 and Table 2, along with expressions (22a) and (22b), the following expressions are approximations to the potentials for line sources and dipoles:

$$\psi_s(x,y,z) \simeq -\frac{\kappa}{2\pi} e^{-i\nu x+\kappa z}\left[\int_{-\infty}^{\nu-\kappa} dk\, \sum^*(k)\, \frac{e^{ikx-\lvert y\rvert\sqrt{(\nu-k)^2-\kappa^2}}}{\sqrt{(\nu-k)^2-\kappa^2}}\right.$$

$$-i\int_{\nu-\kappa}^{\nu+\kappa} dk\, \sum^*(k)\, \frac{e^{i(kx-\lvert y\rvert\sqrt{\kappa^2-(\nu-k)^2})}}{\sqrt{\kappa^2-(\nu-k)^2}}$$

$$\left.+\int_{\nu+\kappa}^{\infty} dk\, \sum^*(k)\, \frac{e^{ikx-\lvert y\rvert\sqrt{(\nu-k)^2-\kappa^2}}}{\sqrt{(\nu-k)^2-\kappa^2}}\right] \qquad (24a)$$

and

$$\psi_D(x,y,z)=\mathrm{sgn}(y)\frac{\kappa}{2\pi}e^{-i\nu x+\kappa z}\left[\int_{-\infty}^{\nu-\kappa}dk\,\beta^*(k)e^{ikx-|y|\sqrt{(\nu-k)^2-\kappa^2}}\right.$$

$$+\int_{\nu-\kappa}^{\nu+\kappa}dk\beta^*(k)e^{i(kx-|y|\sqrt{\kappa^2-(\nu-k)^2})}$$

$$\left.+\int_{\nu+\kappa}^{\infty}dk\beta^*(k)\,e^{ikx-|y|\sqrt{(\nu-k)^2-\kappa^2}}\right] \qquad (24b)$$

A substitution of $k = k' - \nu$ was used in expressions (22a) and (22b). The primes were then dropped in (24a) and (24b).

The expression given in (24a) can be checked by setting $\nu = 0$ and comparing it with the outer expansion for a line distribution of sources found in Ogilvie & Tuck (1969) or by setting $\nu = \kappa$ and comparing it with the outer expansion for a line distribution of sources found in Faltinsen (1971). The expressions are identical except for factors of $1/2\pi$ which is due to the different convention used by those authors. This is as it should be since (24a) represents the general case of waves incident for an arbitrary angle while the Ogilvie-Tuck potential represents beam seas and the Faltinsen potential represents head seas. In the inner expansions of (24a) Ogilvie & Tuck (1969) showed, in effect, that the first and last integrals were of higher order, while Faltinsen got contributions from all three. An essential assumption in their analyses was that the Fourier transform of the source strength behaved like $1/k^3$ for large values of k. We will also assume that $\zeta^*(k)$ and $\beta^*(k)$ have this behavior.

It is interesting to note that Faltinsen's final result showed an attenuation of the incident wave as it progressed down the length of the ship. This is a direct result of the

inclusion of the first and third integrals of (24a) into his theory. One would expect this behavior to be limited to a very small range of heading angles near head seas. For the oblique seas case, we suspect that (24a) and (24b) can be approximated by only the second integral, just as in the Ogilvie-Tuck potential. When we find an upper bound for the discarded integrals, we will be able to relate it to the heading angle χ, and thus indicate asymptotically how close to head seas the one term inner expansion of the source potential for oblique seas may be used before the effects of these terms must be included. The assumptions here are consistent with those made by Faltinsen (1971).

Consider the third integral in (24a). Since κ is of the order ε^{-1} and $\kappa + \nu$ is of the same order, the integral can be bounded as follows:

$$\left| \int_{\nu+\kappa}^{\infty} dk \, \zeta^*(k) \frac{e^{ikx - |y|\sqrt{(\nu-k)^2-\kappa^2}}}{\sqrt{(\nu-k)^2-\kappa^2}} \right| \leq \int_{\nu+\kappa}^{\infty} dk \, \frac{C}{k^3\sqrt{(\nu-k)^2-\kappa^2}}$$

This uses the same assumption that Ogilvie & Tuck (1969) used concerning the behavior of $\zeta^*(k)$ for large values of k. The constant of proportionality, C, was chosen so that the inequality is valid. For the range of k considered, the following inequality holds:

$$\frac{1}{k^3\sqrt{(\nu-k)^2-\kappa^2}} \leq \frac{1}{k^2\sqrt{k^2-(\nu+\kappa)^2}}$$

and it follows that

$$\int_{\nu+\kappa}^{\infty} dk \, \frac{1}{k^3\sqrt{(\nu-k)^2-\kappa^2}} \leq \int_{\nu+\kappa}^{\infty} dk \, \frac{1}{k^2\sqrt{k^2-(\nu+\kappa)^2}}$$

$$= \frac{\sqrt{k^2-(\nu+\kappa)^2}}{(\nu+\kappa)^2 k} \Bigg|_{\nu+\kappa}^{\infty}$$

$$= O(\varepsilon^2)$$

This will be of higher order than the rest of the terms, even for head seas. Faltinsen (1971) found that an integral of this type contributed to his second order expansion. We are just interested in the first order approximation and can therefore disregard any effect due to this term.

For the first integral in expression (24a), k is less than $\nu-\kappa$ and

$$\frac{1}{\sqrt{(\nu-k)^2-\kappa^2}} \leq \frac{1}{\sqrt{k^2-(\nu-\kappa)^2}}$$

Then the integral can be bounded as follows:

$$\left| \int_{\infty}^{\nu-\kappa} dk \; \frac{\zeta^*(k) e^{ikx-|y|\sqrt{(\nu-k)^2-\kappa^2}}}{\sqrt{(\nu-k)^2-\kappa^2}} \right| \leq \left| \int_{-\infty}^{\nu-\kappa} dk \frac{C}{k^3\sqrt{(\nu-k)^2-\kappa^2}} \right|$$

$$\leq \left| \int_{-\infty}^{\nu-\kappa} \frac{dk}{k^2\sqrt{k^2-(\nu-\kappa)^2}} \right| \cdot C$$

$$= C \cdot \left[\frac{\sqrt{k^2-(\nu-\kappa)^2}}{2(\nu-\kappa)^2 k^2} + \frac{1}{2(\nu-\kappa)^3} \cos^{-1}\left[\frac{1}{k}(\nu-\kappa)\right] \right]_{-\infty}^{\nu-\kappa}$$

$$= O\left[\frac{1}{(\nu-\kappa)^3}\right] \qquad (25)$$

The integral identities are found in Gradsteyn and Ryzhik (1957). The assumed behavior of $\zeta^*(k)$ was again proportional to $1/k^3$ for large values of k. We assume that $k<\nu-\kappa$ is large enough to satisfy this requirement.

For the oblique seas, we can see that (25) is $o(\varepsilon)$ since $\nu-\kappa$ is assumed to be of order:

$$\nu - \kappa = O[\kappa(1 - \cos \chi)] = O(\varepsilon^{-1}) \cdot O(1 - \cos \chi) \quad (26)$$

and $1 - \cos \chi$ is not asymptotically small there.

To examine the behavior of the term $\nu - \kappa$ as $\chi \to 0$, define

$$\nu - \kappa = O(\varepsilon^{-\alpha}) \quad (27)$$

where α takes on values of $-\infty < \alpha < 1$. Here $\alpha \to 1$ corresponds to oblique seas and $\alpha \to -\infty$ corresponds to head seas. From (27) one can see that (25) is $O(\varepsilon^{3\alpha})$. If we require that (25) be of higher order than the middle integral in (24a), then α must satisfy

$$O(\varepsilon^{3\alpha}) = o(\varepsilon)$$

or

$$\alpha > 1/3$$

This requirement implicitly states that if the integral in (25) is of order ε, it can no longer be ignored.

From (26) and (27), a value for χ can be found:

$$o[\varepsilon^{-1}(1 - \cos \chi)] = O(\varepsilon^{-1/3})$$

which implies

$$o(1 - \cos \chi) = O(\varepsilon^{2/3})$$

Expanding $\cos \chi$ as $1 - \frac{\chi^2}{2} + \ldots$ allows us to substitute

$$1 - \cos \chi \simeq \frac{\chi^2}{2}$$

or

$$o(\chi) = O(\varepsilon^{1/3}).$$

The result can be summarized in words:

If the above assumptions are true, then in the first order approximation for values of χ outside a small

neighborhood of $\chi = 0$, the potential for the line distribution of sources in oblique waves will not represent any of the longitudinal effects predicted by Faltinsen (1971) for the case of head seas. Thus we are able to relate the two theories and at least get a feel for the extent of their validity, even though we cannot attach a numerical value to the limiting value of χ.

It should be emphasized that the above conclusion depends upon a number of assumptions, some of which may not be very likely. To reiterate, the assumptions are the following:

i) The Fourier transform of the source strength, $\sigma^*(k)$, behaves like $1/k^3$ for large k. This requires that $\sigma(x)$ be zero at the bow. See, for example, Ogilvie & Tuck (1969).

ii) The minimum value of k in the first integral is large enough to use the first assumption, i). In other words, $\nu - \kappa = O(\varepsilon^{-\alpha})$ is large enough to approximate $\sigma^*(k)$ by $1/k^3$.

iii) We require that (25) be of higher order than the middle integral of (24a) without stating explicitly what this order must be. This implies that the analysis should be valid in the asymptotic limit as $\varepsilon \to 0$. However, since we are interested in hull forms that have non-zero values of ε, we may need a more stringent requirement.

To continue, equation (24a) can then be approximated as

$$\psi_s(x,y,z) \simeq \frac{i\kappa}{2\pi} e^{-i\nu x + \kappa z} \int_{\nu-\kappa}^{\nu+\kappa} dk\, \sigma^*(k)\, \frac{e^{i(kx - |y|\sqrt{\kappa^2-(\nu-k)^2})}}{\sqrt{\kappa^2-(\nu-k)^2}} \qquad (28)$$

Using an argument similar to that found in Ogilvie & Tuck (1969), assume that the major contribution to the integral in (28) comes from around $k = 0$. Then at the upper square

root singularity, $\sum^*(\nu+\kappa)$ is small enough that the contribution to the integral from the neighborhood of the singularity is of higher order. At the lower limit, $\nu - \kappa = \kappa(1 - \cos\chi)$, and again it is assumed that this is large enough that $\sum^*(k) \sim O(1/k^3)$ in the neighborhood of the singularity. The contribution to the integral there should be of $O(\varepsilon)$. We can then expand the radicals for small values of k as follows:

$$\sqrt{\kappa^2-(\nu-k)^2} = \sqrt{\kappa^2-\nu^2}\sqrt{1+\frac{2\nu k-k^2}{\kappa^2-\nu^2}}$$

$$= \sqrt{\kappa^2-\nu^2}\left[1+\frac{\nu k}{\kappa^2-\nu^2}+\ldots.\right]$$

$$\simeq \sqrt{\kappa^2-\nu^2}+\frac{\nu k}{\sqrt{\kappa^2-\nu^2}} \quad ,$$

and

$$\frac{1}{\sqrt{\kappa^2-(\nu-k)^2}} \simeq \frac{1}{\sqrt{\kappa^2-\nu^2}} \quad ,$$

and finally

$$e^{i|y|\sqrt{\kappa^2-(\nu-k)^2}} \simeq \left(e^{i|y|\sqrt{\kappa^2-\nu^2}}\right)\left(e^{i|y|\nu k/\sqrt{\kappa^2-\nu^2}}\right)$$

The reason for not neglecting the $i|y|\nu k/\sqrt{\kappa^2-\nu^2}$ term in the exponent is that the exponent can be of the same order as e^{ikx} and hence adds a major contribution. Using these expansions in (28) gives

$$\psi_s(x,y,z) \simeq \frac{i\kappa}{2\pi} e^{-i\nu x+\kappa z} \frac{e^{-i|y|\sqrt{\kappa^2-\nu^2}}\nu-\kappa}{\sqrt{\kappa^2-\nu^2}} \int_{\nu-\kappa} dk \sum^*(k) e^{i(kx-|y|\nu k/\sqrt{\kappa^2-\nu^2})}$$

Extending the limits of integration to $\pm\infty$ introduces an error of higher order and (28) can finally be written as

$$\psi_s(x,y,z) \simeq \frac{i\kappa e^{-i\nu x+\kappa z-i|y|\sqrt{\kappa^2-\nu^2}}}{\sqrt{\kappa^2-\nu^2}} \cdot \frac{1}{2\pi}\int_{-\infty}^{\infty} dk\, \zeta^*(k) e^{ik(x-|y|\nu/\sqrt{\kappa^2-\nu^2})}$$

$$= \frac{i\kappa}{\sqrt{\kappa^2-\nu^2}}\, \zeta(x-|y|\nu/\sqrt{\kappa^2-\nu^2})\, e^{\kappa z-i(\nu x+|y|\sqrt{\kappa^2-\nu^2})} \qquad (29)$$

Expression (29) corresponds to the velocity potential for a pulsating line distribution of sources with the $e^{-i\nu x}$ behavior found in Ogilvie (1974). The method used in that paper for finding the potential was based on stationary phase principles and hence different from the method for finding $\psi_s(x,y,z)$. As stated previously, our method of solution for the zero speed problem was selected as a means of getting information on the forward speed problem, and so the preceding derivation is more than mere redundancy.

Some caution has to be exercised in finding the inner expansion of (29). The $e^{-i\nu x}$ term should be factored out first, since the inner expansion of $\psi_s(x,y,z)$ should match with the even part of the outer expansion of $e^{-i\nu x}\phi_7(x,y,z)$. Letting $|y|=O(\varepsilon)$, the inner expansion of $e^{i\nu x}\psi_s(x,y,z)$ is

$$e^{i\nu x}\psi_s(x,y,z) \simeq \frac{i\kappa}{\sqrt{\kappa^2-\nu^2}}\, \zeta(x)\, e^{\kappa z-i|y|\sqrt{\kappa^2-\nu^2}} \qquad (30a)$$

Similarly, the inner expansion of the dipole potential, expression (24b) is given by

$$e^{i\nu x}\psi_D(x,y,z) \simeq \operatorname{sgn}(y)\,\kappa\beta(x)\, e^{\kappa z-i|y|\sqrt{\kappa^2-\nu^2}} \qquad (30b)$$

There are a number of things worth noting about expressions (30a) and (30b). First, both represent two dimensional outgoing waves whose amplitude is a function of x. Second, as $\nu \to \kappa$, i.e., head seas, the source potential becomes singular like $1/\sqrt{\kappa^2 - \nu^2}$ while the dipole potential remains bounded. In fact, since $\psi_D(x,y,z)$ is a measure of the asymmetry of the problem, $\beta(x)$ should go to zero as $\nu \to \kappa$ since for head seas the diffraction potential is an even function with respect to y. Third, as $\nu \to 0$, i.e. beam seas, $\psi_s(x,y,z)$ becomes the same expression as found in Ogilvie & Tuck (1969). The transition from oblique seas to beam seas is a continuous one, and as will be shown in the following chapters, the inner region potential will be valid for a range of heading angles from oblique to beam seas. And finally, fourth, since the body boundary condition has an odd and even component of the same order, the dipole and source must generate waves of the same order from which we conclude $\beta = O(\varepsilon\Sigma)$.

Matching the Expansions

We have the inner expansion of the far field given in expressions (30a) and (30b). We will now show that this matches with the outer expansion of the near field without stating explicitly the solution in the near field.

Ursell (1968) has shown that a solution satisfying a Helmholtz equation and free surface boundary condition, (17) and (18) respectively, and general hull boundary conditions valid outside some radius r, can be written as the sum of a wave source, a wave dipole, regular waves and wave-free potentials located on the free surface. Since (30a) and (30b) represent outgoing waves, the regular wave term can be dropped.

In the near field then, $\psi_1(y,z;x)$ is given as

$$\psi_1(y,z;x) = A_{s_1}(x)S(y,z) + A_{D_1}(x)D(y,z)$$

$$+ \sum_{m=1}^{\infty} A_m^{(e)}(x)O_m^{(e)}(y,z) + A_m^{(o)}(x)O_m^{(o)}(y,z) \qquad (31)$$

where $S(y,z)$ is a wave source given as

$$S(y,z) = \frac{1}{\pi} \int_0^\infty \frac{d\mu\, \nu \cosh \mu}{\nu \cosh\mu - \kappa} \exp(\nu z \cosh \mu)\cos(k y \sinh \mu),$$

$D(y,z)$ is a wave dipole given as

$$D(y,z) = \frac{-\nu}{\pi} \int_0^\infty d\mu \frac{\cosh \mu \sinh \mu}{\cosh \mu - \kappa/\nu} \exp(\nu z \cosh \mu)\sin(ky \sinh \mu),$$

and $O_m^{(o)}(y,z)$ and $O_m^{(e)}(y,z)$ are odd and even wave-free potentials given as

$$O_m^{(o)}(y,z) = K_{2m-1}(\nu r)\sin(2m-1)\theta + K_{2m+1}(\nu r)\sin(2m+1)\theta$$

$$+ (2\kappa/\nu) K_{2m}(\nu r)\sin 2m\theta ,$$

$$O_m^{(e)}(y,z) = K_{2m-2}(\nu r)\cos(2m-2)\theta + K_{2m}(\nu r)\cos 2m\theta$$

$$+ (2\kappa/\nu) K_{2m}(\nu r)\cos 2m\theta .$$

The $K_i(\nu r)$ term is the K Bessel function of order i and r and θ are just the cylindrical coordinates in the (y,z) plane, where θ is the angle between r and the -z axis. $\psi_1(y,z;x)$ then has the behavior for large r of

$$\psi_1(y,z;x) \to \left[\frac{i\kappa A_{S1}(x)}{\sqrt{\kappa^2-\nu^2}} + \mathrm{sgn}(y)\kappa A_{D1}(x)\right] e^{\kappa z - i|y|\sqrt{\kappa^2-\nu^2}} \qquad (32)$$

Clearly, the expansion will match if $A_{S1}(x) = \sum(x)$ and $A_{D1}(x) = \beta(x)$. The means of finding $A_{S1}(x)$ and $A_{D1}(x)$ will be given in later sections. What is important here is that the far field has provided a radiation condition that allows us to define the inner region problem.

Summary of the Zero Speed Problem

The diffraction potential near the ship, to the first order, is defined by

$$\frac{\partial^2 \psi_1}{\partial y^2} + \frac{\partial^2 \psi_1}{\partial z^2} - \nu^2 \psi_1 = 0, \quad \text{in the fluid domain;} \tag{17}$$

$$-\kappa \psi_1 + \psi_{1_z} = 0, \quad \text{on } z = 0; \tag{18}$$

$$\frac{\partial \psi_1}{\partial N} = - \frac{\partial \phi_0}{\partial N}, \quad \text{on } y = h(x,z); \tag{19}$$

and a radiation condition of

$$\psi_1(y,z;x) \to \left[\frac{i\kappa A_{S1}(x)}{\sqrt{\kappa^2 - \nu^2}} + \operatorname{sgn}(y) \kappa A_{D1}(x) \right] e^{\kappa z - i|y|\sqrt{\kappa^2 - \nu^2}}, \tag{32}$$

$$\text{as} \quad \sqrt{y^2 + z^2} \to \infty .$$

The multi-pole expansion given in (31) is valid outside some circular section and could be used to find $\psi_1(y,z;x)$ if we restricted our interest to circular cylinders. For ship shapes, however, the series may not converge everywhere in the fluid region if this method is used. In order to consider an arbitrary hull shape, we derive an integral equation and present a numerical scheme for solving it in the next chapter. This will allow us to find $\psi_1(y,z;x)$ for any given cross section.

Chapter IV

Method of Solution for the ψ_1 Problem

Formulation of an Integral Representation: $\psi_1 = \int d\ell \sigma G$

Classical potential theory has shown how bodies with known hull boundary conditions can be replaced with surface distributions of singularities; e.g., Kellogg (1929). Various papers have dealt with the problem of a body in the presence of a free surface and at least one, Frank (1967), developed a numerical scheme for actually solving the flow field around a two dimensional hull. One of the drawbacks of using an integral representation is the existence of certain "irregular" or eigen frequencies for which the fluid motions cannot be computed. These frequencies were first shown by John (1950), computed numerically by Frank (1967) and discussed thoroughly by Ohmatsu (1975). Fortunately, these frequencies usually occur beyond the range of practical interest.

The derivation of an integral representation for a Helmholtz equation without a free surface is done in Lamb (1932). It is a simple procedure to include the free surface and the details will be omitted. We can then write:

$$\psi_1(y,z;x) = \int_{C_H(x)} d\ell G(y,z;\xi,\eta)\sigma(\xi,\eta) \qquad (33)$$

when $\sigma(\xi,\eta)$ is the source strength of the singularity distribution over the hull, $C_H(x)$ is the section of interest, and $d\ell$ is a function of (ξ,η).

The form of $G(y,z;0,0)$ has already been given as the wave source $S(y,z)$ used in (31). Ursell (1962) has given a series expansion for $S(y,z)$ valid for small νr, where $r = \sqrt{y^2+z^2}$. Extending that expansion to include a general source point requires the addition of the source's basic singularity, the $K_0(\nu r)$ Bessel function, and subtraction of its image, $K_0(\nu r')$, times an appropriate factor. For small values of νr we have then

$$G(y,z;\xi,\eta) = K_o(\nu r) + K_o(\nu r')$$
$$- 2\gamma \coth\gamma \left[I_o(\nu r') + 2\sum_{m=1}^{\infty}(-1)^m \cosh m\gamma\, I_m(\nu r')\cos m\theta'\right]$$
$$- 4 \coth\gamma \sum_{m=1}^{\infty}(-1)^m \sinh\gamma m \left[\frac{\partial}{\partial m}\left(I_m(\nu r')\cos m\theta'\right)\right]$$
$$- 2\pi i \coth\gamma \left[I_o(\nu r') + 2\sum_{m=1}^{\infty}(-1)^m \cosh\gamma m\; I_m(\nu r')\cos m\theta'\right] \qquad (34a)$$

where $I_m(\nu r')$ is the I Bessel function of order m,

$$r = \sqrt{(y-\xi)^2 + (z-\eta)^2}$$

$$r' = \sqrt{(y-\xi)^2 + (z+\eta)^2} \quad ,$$

$$\cosh\gamma = \kappa/\nu \quad ,$$

and θ' is the angle between r' and the z axis where $\theta' = 0$ is directed towards $z \to -\infty$.

Another form of the same potential, valid for all νr, but especially easy to compute for moderate and large values of νr is given by Khaskind (1953). It has the following form:

$$G(y,z;\xi,\eta) = K_0(\nu r) + K_0(\nu r')$$
$$+ 2\kappa e^{\kappa z} \int_{\infty}^{z} d\alpha e^{-\kappa\alpha} K_0\left(\nu\sqrt{(y-\xi)^2 + (\alpha+\eta)^2}\right)$$
$$- 2\pi i \frac{\kappa}{\sqrt{\kappa^2-\nu^2}} e^{\kappa(z+\eta) - i|y-\xi|\sqrt{\kappa^2-\nu^2}} \quad . \qquad (34b)$$

The following items are of interest:

i) Since the imaginary components of (34a) and (34b) must be equal, the series representing the imaginary part of (34a) can be greatly simplified, i.e.,

$$e^{\kappa(z+\eta)}\cos\left(|y-\xi|\sqrt{\kappa^2-\nu^2}\right) = I_o(\nu r') +$$
$$2\sum_{m=1}^{\infty}(-1)^m \cosh m\gamma\, I_m(\nu r')\cos m\theta'$$

ii) Both forms can easily be shown to represent a logarithmic source as $\nu \to 0$ and both become singular in their imaginary part like $1/\sqrt{\kappa^2-\nu^2}$ as $\nu \to \kappa$.

iii) The integral term in (34b) is much more easily evaluated numerically than that given in $S(y,z)$ (see (31)) for moderate and large values of νr.

For a more thorough discussion of $G(y,z;\xi,\eta)$, see Appendix A.

Derivation of an Integral Equation

The integral representation given in (33) contains two unknowns, ψ_1 and σ. In order to find σ, we recall that $\partial\psi_1/\partial N$ is known on $C_H(x)$. Applying the operator $\partial/\partial N_{(y,z)}$ where $N_{(y,z)}$ is the two dimensional normal at the point (y,z) on the section, we have

$$\frac{\partial \psi_1(y,z)}{\partial N_{(y,z)}} = \frac{\partial}{\partial N_{(y,z)}} \int_{C_H(x)} d\ell G(y,z;\xi,\eta)\sigma(\xi,\eta) \qquad (35)$$

on $y = h(x,z)$, where the integration on $C_H(x)$ is done in a clockwise direction.

We proceed now as Kellogg (1929) did for the Laplacian potential and note that $G(y,z;\xi,\eta)$ is singular as $(\xi,\eta)\to(y,z)$. From equation (34b) for points not on the free surface, $G(y,z;\xi,\eta)$ is singular like $K_o(\nu r)$ where $r = \sqrt{(y-\xi)^2+(z-\eta)^2}$. Inspection of the rest of the terms in (34b) show that they are continuous as $(\xi,\eta)\to(y,z)$ and do not cause any difficulty in the limit.

The singular nature of $G(y,z;\xi,\eta)$ prevents us from interchanging differentiation with integration when (y,z) is on the hull. We will simplify our investigation by considering a shift of the axis that places a straight section of $C_H(x)$ at the origin and then consider the behavior of (35) as the hull is approached from the fluid. Taking a limiting process allows us to investigate the behavior of $\frac{\partial}{\partial N}\int d\ell G\sigma$ before G becomes singular. Consider a portion of $C_H(x)$ as shown in Figure 2, and the point $(0,z)_{\lim z\to 0^-}$ in the fluid domain.

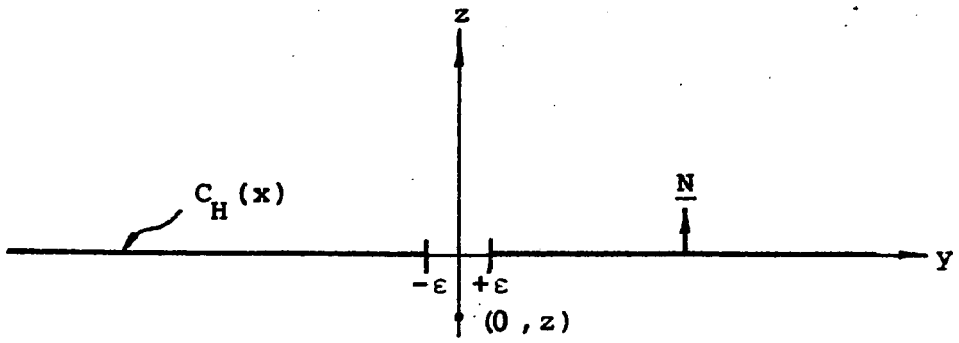

Figure 2: Hull Surface for Finding $\frac{\partial}{\partial N}\int d\ell G\sigma$

Here $\frac{\partial}{\partial N} = \frac{\partial}{\partial z}$ and (35) becomes

$$\lim_{z\to 0} \tfrac{1}{2}\frac{\partial \psi_1}{\partial z}(0,z;x) = \lim_{z\to 0}\frac{\partial}{\partial z}\int_{C_H(x)} d\ell G(o,z;\xi,\eta)\sigma(\xi,\eta)$$

$$= \int_{C_H(x)} d\ell\, \frac{\partial}{\partial z} G(0,0;\xi,\eta)\sigma(\xi,\eta)$$

$$+ \lim_{z\to o}\int_{\varepsilon}^{-\varepsilon} d\xi\, \frac{\partial}{\partial z} K_o(\nu r)\sigma(\xi,0). \qquad (36)$$

As the limit is approached, the first integral in (36) is understood to exclude the hull segment of $-\varepsilon<y<\varepsilon$.

The last integral comes from looking at that small increment deleted in the first where now the only contribution comes from the singular $K_o(\nu r)$ term. Since for small arguments, $K_o(\nu r) \simeq -\log(\nu r)$ (see Abramowitz and Stegun, 1974), the last integral becomes the following.

$$\lim_{z\to 0}\int_{+\varepsilon}^{-\varepsilon} d\xi\, \frac{\partial}{\partial z} K_o(\nu r)\sigma(\xi,0) \simeq -\sigma(o,o)\lim_{z\to o}\int_{+\varepsilon}^{-\varepsilon} d\xi\, \frac{\partial}{\partial z}\log\left(\nu\sqrt{\xi^2+z^2}\right)$$

$$= -\sigma(o,o) \lim_{z\to o^-} \int_{+\varepsilon}^{-\varepsilon} d\xi \frac{z}{\xi^2 + z^2}$$

$$= -\sigma(o,o) \lim_{z\to o^-} \tan^{-1}\frac{\xi}{z} \Big|_{+\varepsilon}^{-\varepsilon}$$

$$= -\pi\sigma(o,o)$$

Now expressing the results found above for any general axis system, we find the following integral equation:

$$\frac{\partial \psi_1}{\partial N}(y,z;x) = -\pi\sigma(y,z) + \int_{C_H(x)} d\ell \, \frac{\partial}{\partial N} G(y,z;\xi,\eta)\sigma(\xi,\eta) \qquad (37)$$

for $y = h(x,z)$. The left hand side of (37) is known from the boundary conditions leaving only σ unknown.

The above derivation was not meant to be rigorous. Rather, it was intended to indicate the method commonly used in potential theory by which an integral equation is formulated from an integral representation.

Solution of the Integral Equation

As mentioned earlier, Frank (1967) has solved the two dimensional problem where logarithmic sources were distributed over the hull section. He solved an integral equation similar to (37) and his method will be reviewed here for comparison.

There are two basic assumptions used in Frank's analysis. Given a hull section described by n offsets, consider the points surrounding the ith point, as in Figure 3, where $d\ell_i$ is the actual arclength between the i-1 and i points and ds_i is the straight line arclength between the i-1 and i points. Frank's first assumption was that the source strength $\sigma(\ell)$, varied slowly enough to be considered as constant over a given arc. Here the value of $\sigma(\ell)$ at the midpoint of each arc was used. Next, he assumed that the ship's hull could be represented by straight lines. These assumptions were used

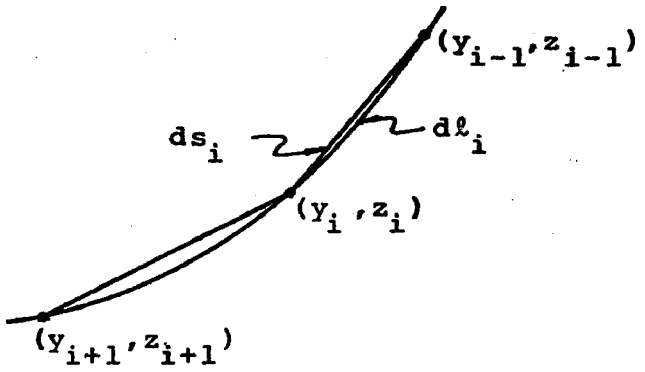

Figure 3: A Section of the Hull

to simplify (37) in the following manner:

$$\frac{\partial \psi_1}{\partial N}(\bar{y}_i, \bar{z}_i; x) = -\pi\sigma(\bar{y}_i, \bar{z}_i) + \int_{C_H(x)} d\ell \, \frac{\partial}{\partial N} G(\bar{y}_i, \bar{z}_i; \xi, \eta)\sigma(\xi, \eta)$$

$$= -\pi\sigma(\bar{y}_i, \bar{z}_i) + \sum_{j=1}^{n-1} \int_{d\ell_j} d\ell \, \frac{\partial}{\partial N} G(\bar{y}_i, \bar{z}_i; \xi, \eta)\sigma(\xi, \eta)$$

$$\tilde{=} -\pi\sigma(\bar{y}_i, \bar{z}_i) + \sum_{j=1}^{n-1} \sigma(\bar{y}_i, \bar{z}_i) \int_{d\ell_j} d\ell \, \frac{\partial}{\partial N} G(\bar{y}_i, \bar{z}_i; \xi, \eta)$$

$$\cong -\pi\sigma(\bar{y}_i, \bar{z}_i) + \sum_{j=1}^{n-1} \sigma(\bar{y}_i, \bar{z}_i) \int_{ds_j} ds \, \frac{\partial}{\partial N} G(\bar{y}_i, \bar{z}_i; \xi, \eta),$$

$$i=1, \ldots n-1 \qquad (38)$$

where $(\bar{y}_i, \bar{z}_i)$ is the midpoint of the ith line segment. The utility of (38) is that the integral term, $\int_{ds_i} ds \, \frac{\partial}{\partial N} G$, is a known integral that can be found in closed form for sources that satisfy Laplace's equation.

A question one might ask of Frank's solution is, "How dependent is the solution on the assumption that the source strength is constant over a given arc?" For an infinite number of arcs, this approximation becomes exact. However, for a finite number, say on the order of ten to twenty, (38) implies that same number of jumps in σ. In other words, σ

is not a continuous function over the given station in question, though a major assumption in the theory of surface singularities (see Kellogg (1929)) states that it is. In this thesis, we will show an alternate method of solution that will avoid having to answer this question.

The method used in this thesis utilizes a fact mentioned by Tricomi (1957) and Wehausen and Laitone (1960). They show that if one distributes logarithmic singularities over a section, then a term corresponding to the integral in (37), i.e. $\int d\ell \frac{\partial}{\partial N} \log (\sqrt{(y-\xi)^2+(z-\eta)^2})\sigma(\xi,\eta)$, does not have a singular integrand as $(\xi,\eta)\to(y,z)$ but in fact approaches a limit that is proportional to the curvature at the point (y,z). Indeed, that some limit exists as $(\xi,\eta)\to(y,z)$ can be implied from physical considerations. Stated in words, the kernel of the integral represents the velocity induced in the direction of the normal at (y,z) on the point (y,z) by a source located at (ξ,η). As $(\xi,\eta)\to(y,z)$ the magnitude of the velocity becomes very large; however, most of the velocity is in the tangential direction and in the limit, the velocity in the normal direction appears to be bounded. For example, if the point (y,z) lies on a straight section of the hull, as $(\xi,\eta)\to(y,z)$ all of the induced velocity is tangential and the normal component is zero. Of course, the above is based on the assumption that the hull is a smooth arc whose second derivative exists.

Since our basic singularity is the $K_o(\nu r)$ Bessel function which behaves like $-\log(\nu r)$ for small values of νr, we expect the same statement concerning the nature of the integrand in (37) to be true. In order to show this, consider Figure 4:

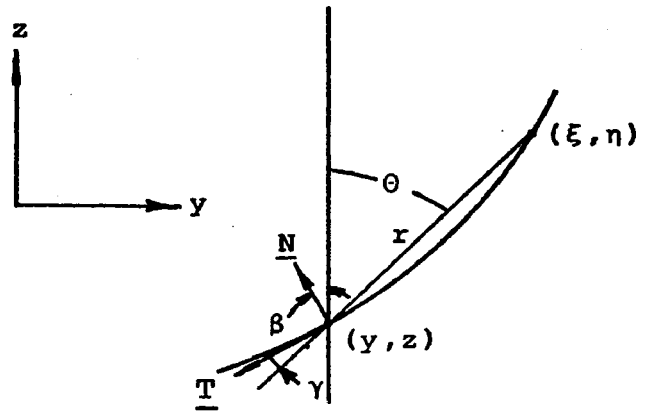

Figure 4: The Behavior of $\frac{\partial}{\partial N} K_o(\nu r)$ as $(\xi,\eta) \to (y,z)$

where $\underline{N}$ is the normal to the curve $C_H(x)$ at (y,z) with components (n_2,n_3),

$\underline{T}$ is the tangent to the curve $C_H(x)$ at (y,z),

β is the angle $\underline{N}$ makes with the z axis,

γ is the angle between $\underline{T}$ and r,

Θ is the angle r makes with the z axis,

and $r = \sqrt{(y-\xi)^2 + (z-\eta)^2}$. From Figure 4, we see that $\Theta = \pi/2-\gamma-\beta$, $n_2 = -\sin\beta$, and $n_3 = \cos\beta$.

Using the relations $\frac{\partial}{\partial N} = \nabla_{2-D} \cdot \underline{N}$ where ∇_{2-D} is the gradient operator defined as $\nabla_{2-D} = \frac{\partial}{\partial z}\underline{j} + \frac{\partial}{\partial z}\underline{k}$, $K_o'(z) = -K_1(z)$ (see Abramowitz and Stegun, 1964) and $(y-\xi) = -r \sin\Theta$, $(z-\eta) = -r\cos\Theta$, we find

$$\frac{\partial}{\partial N} K_o(\nu r) = -\nu\left[n_2 K_1(\nu r)\frac{(y-\xi)}{r} + n_3 K_1(\nu r)\frac{(z-\eta)}{r}\right]$$

$$= -\nu K_1(\nu r)\left[\sin\beta\sin\Theta - \cos\beta\cos\Theta\right]$$

$$= \nu K_1(\nu r)\sin\gamma$$

and as $\nu r \to 0$, $K_1(\nu r) \to \frac{1}{\nu r}$, then

$$\frac{\partial}{\partial N} K_o(\nu r) \to \frac{\sin\gamma}{r} \to \frac{\Gamma(y,z)}{2} \qquad (39)$$

Where $\Gamma(y,z)$ is the curvature at the point (y,z). The details in expression (39) can be found in Tricomi (1957) and will not be reproduced here. Equation (39) has the

desired behavior in that, as $(\xi,\eta)\to(y,z)$, r and γ both go to zero.

There is one point that may need some clarification. In the discussion that followed (35), we stated that the Green's function had a singular nature associated with it and hence we had to exclude a small element of arc length to examine this singular behavior. That investigation led directly to the $-\pi\sigma(y,z)$ contribution in the right hand side of (37). Now we have just proceded to show that the integrand in (37) is not really singular at all, but rather one that is nice and continuous. One may ask why we did not use the fact of the continuity of $\frac{\partial}{\partial N} K_o(\nu r)$ in the analysis following (35). The resolution of this apparent contradiction is that to arrive at (37), we realized that bringing the differential operator $\frac{\partial}{\partial N}$ inside the integral could not be done until a limiting process such as that in (36) was used. Once this was done, the integral could be interpreted as it was.

Now, using the fact that the integral in (37) can be evaluated at the point $(y=\xi,\ z=\eta)$, we have as a numerical solution for $\sigma(y,z)$ the following:

$$\frac{\partial\psi_I(y_i,z_i;x)}{\partial N} = -\pi\sigma(y_i,z_i) + \int_{C_H(x)} d\ell\ \frac{\partial}{\partial N} G(y_i,z_i;\xi,\eta)\sigma(\xi,\eta)$$

$$\cong -\pi\sigma(y_i,z_i) + \sum_{j=1}^{n} \frac{\partial}{\partial N} G(y_i,z_i;\xi_j,\eta_j)\sigma(\xi_j,\eta_j)\omega_j \qquad (40)$$

for $i=1, \ldots n$. Here ω_j is just an integrating factor based upon the integration quadrature selected. For example, if the trapezoidal rule is used, then

$$\omega_j = d\ell_j/2 \qquad j = 1, n$$

$$\omega_j = (d\ell_{i-1}+d\ell_i)/2 \qquad j = 2, \ldots n-1$$

where $d\ell_i$ is the arc length as given in Figure 3. While equation (40) is a simpler relation than (38); its accuracy can be improved by merely selecting different weighting

functions, i.e. ω_j's . The source strength σ can now be found through any of the routines that solve simultaneous linear equations.

In this thesis, the weighting function used is based on the trapezoidal rule. While it is not possible to state explicitly how the source strength varies over a given arc, it is possible to say that $\sigma(y,z)$ is at least a continuous function and the product of $\sigma(\xi,\eta)\frac{\partial}{\partial N} G(y,z;\xi,\eta)$ is assumed to vary linearly between points.

The arc length, $d\ell$, is approximated by a circular arc. That is, given three points, a circular arc is fitted through them and the normal and radius of curvature are then found for the middle point. The arc length is divided evenly between the angles formed by the three points and the center of the calculated circle.

The exception to this approximation occurs when the point is designated at a chine. Then straight line segments are used between points, the normal is just the average of the normals to the two line segments and the curvature is arbitrarily set equal to zero.

The advantages of this sort of procedure over a method similar to that used by Frank are the simplicity of computation and the assumed continuity of the source strength. These advantages should mean a substantial saving in computer time.

The disadvantages are choosing the proper integration quadrature that satisfactorily approximates the integrand and handling the source strength correctly when it gets very large. Consider the following as an example of the first: if different hull shapes required different quadratures, then the utility of any program using (40) would be limited. It was found that the trapezoidal rule gave high levels of accuracy for full ship sections with a minimum number of input points. As the sections became finer, such as the bow sections of ships with bulbous bows, more offsets were needed, indicating the advantage (40) enjoyed over (38) had diminished somewhat.

The second disadvantage can be illustrated by considering the problem of a rectangle in forced vertical oscillation governed by Laplace's equation. See Figure 5, where the imaginary part of $\sigma(y,z)$ is plotted as a function of position along the hull section. The real part of the source strength has the same behavior. We know that the source strength is singular at the corner, yet if we put in the points so that they describe a rectangle, we must return the value of the source strength at that singular point. The solid line, which represents the rectangle, has a near-zero value at the chine, indicating that it represents some sort of average between two very large numbers, one negative, the other positive. The dashed line represents rounding the corner off with a bilge radius of .05 times the draft. As can be seen from Table 3, the added mass and damping coefficients compare quite well with those given in Frank (1967) for the same problem. Obviously, the singularity in $\sigma(y,z)$ is an integrable one, and from Table 3 it appears that

TABLE 3.

Heaving Rectangular Cylinder

$B/T=2.5$, $2\pi/\lambda \cdot B = 2.0$	Added Mass	Damping
Rectangular Cylinder (Frank (1967))	1.08	.20
Rounded corners (Figure 5)	1.06	.20
Chine (Figure 5)	1.08	.19

it does not make much difference whether one takes the precaution of rounding the corner or not.

For numerical examples of (40), see Chapter VI.

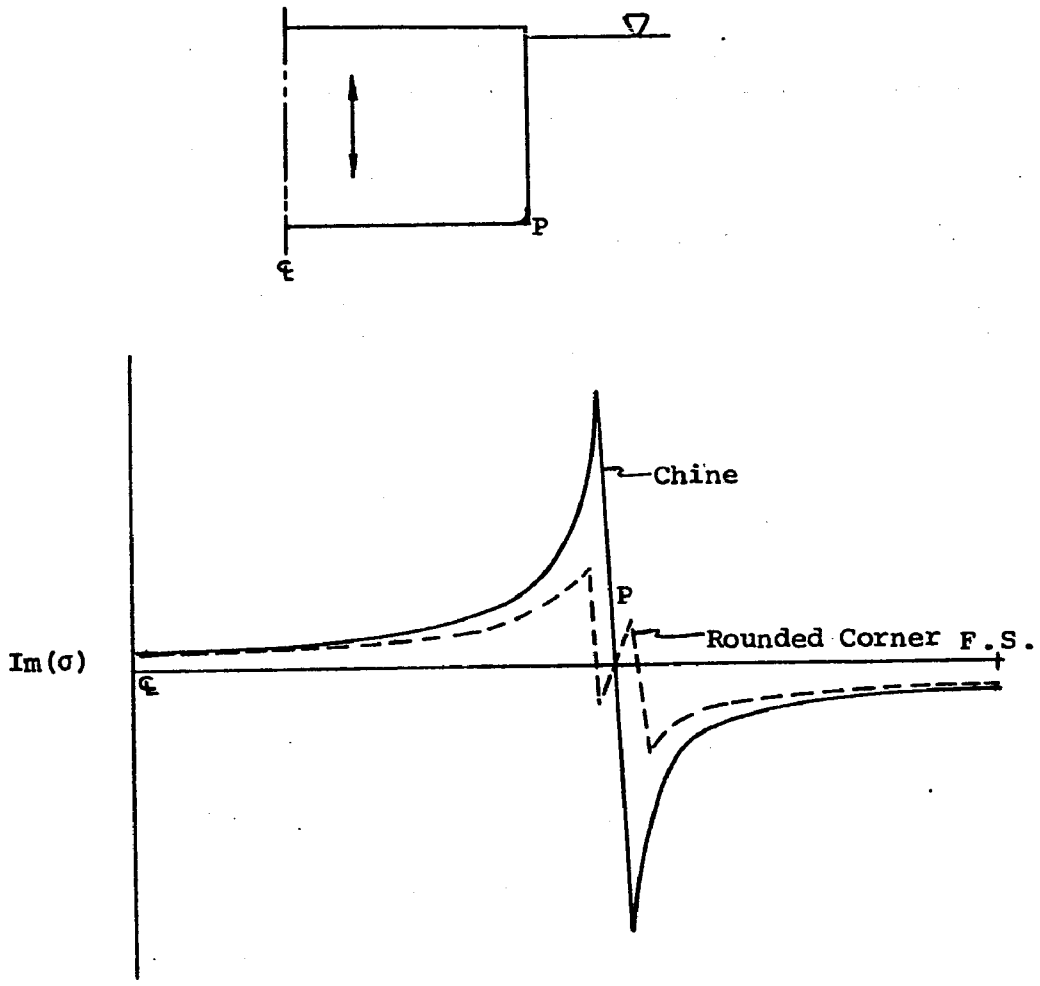

Figure 5: The Behavior of the Source Strength for a Heaving Rectangular Cylinder.

The Determination of the Potential

As described in Appendix A, it is an easy matter to find both $G(y,z;\xi,\eta)$ and $\frac{\partial}{\partial N}G(y,z;\xi,\eta)$ at the same time. For every input point where σ is found, G is given also. The

potential, $\psi_1(y,z;x)$, could then be found through the integral representation given in (33). There is one source of difficulty though. While we have shown that $\frac{\partial G}{\partial N}$ is continuous as $(\xi,\eta)\to(y,z)$, the integrand of (33) has an integrable singularity there. As a result, we have to modify our numerical scheme slightly to find $\psi_1(y,z;x)$.

Briefly, we use the same integration quadrature over the entire section for all of the non-singular terms in G and for the $K_o(\nu r)$ terms where $(y\neq\xi)$ and $(z\neq\eta)$. For the point $(y,z)=(\xi,\eta)$, we assume that the source is a linear function between that point and the surrounding points, and that ds could be approximated by dr where $r = \sqrt{(y-\xi)^2 + (z-\eta)^2}$. This means we have to evaluate integrals of the form

$$a \int_0^{dr_i} dr\ K_o(\nu r) \qquad \text{and} \qquad b \int_0^{dr_i} dr\ r\ K_o(\nu r) \quad . \qquad (41)$$

Here a and b are functions of the source distribution, σ , and known. See Figure 6 for a description of dr_i.

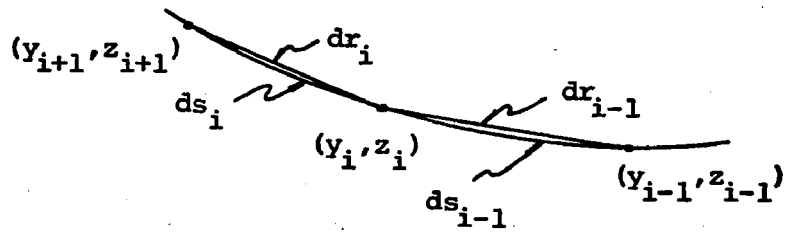

Figure 6: Description of dr_i.

For the arc length dr_i, the constants a and b in (41) are given as

$$a = \sigma(y_i,z_i) \quad \text{and} \quad b = [\sigma(y_{i+1},z_{i+1}) - \sigma(y_i,z_i)]/dr_i \ ,$$

and can be represented in a similar manner for dr_{i-1}. For methods of finding these integrals, see Abramowitz and Stegun (1964).

In order to simplify the notation when writing the algorithm for (33), define $g(y,z;\xi,\eta)$ as

$$G(y,z;\xi,\eta) = K_o(\nu r) + g(y,z;\xi,\eta) \tag{42}$$

where, from (34a) it is clear that

$$g(y,z;\xi,\eta) = K_o(\nu r') + 2\kappa e^{\kappa z} \int_{\infty}^{z} d\alpha e^{-\kappa\alpha} K_o(\nu\sqrt{(y-\xi)^2+(\alpha+\eta)^2})$$

$$- 2\pi i \frac{\kappa}{\sqrt{\kappa^2-\nu^2}} e^{\kappa(z+\eta) - i|y-\xi|\sqrt{\kappa^2-\nu^2}} \tag{43}$$

For points not on the free surface, $g(y,z;\xi,\eta)$ contains all of the non-singular terms of $G(y,z;\xi,\eta)$. For values of $\psi_1(y,z;x)$ on the hull, expression (33) can then be written as

$$\begin{aligned}
\psi_1(y_i,z_i;x) &= \int_{C_H(x)} d\ell G(y_i,z_i;\xi,\eta)\sigma(\xi,\eta) \\
&\simeq \sum_{j=1}^{i-1} G(y_i,z_i;\xi_j,\eta_j)\sigma(\xi_j,\eta_j)\omega_j \\
&+ \sum_{j=i+1}^{n} G(y_i,z_i;\xi_j,\eta_j)\sigma(\xi_j,\eta_j)\omega_j \\
&+ \sum_{j=i-1}^{i+1} g(y_i,z_i;\xi_j,\eta_j)\sigma(\xi_j,\eta_j)\omega_j \\
&+ \int_{dr_{i-1}}^{dr_i} dr\ (a+br)\ K_o(\nu r) \quad .
\end{aligned} \tag{44}$$

where $\sigma(\xi_i,\eta_i)$ is the known source strength, ω_i , is an integrating factor like the ω_j used in (40), $g(y_i,z_i;\xi_j,\eta_j)$ is given in (43) and the integral term is composed of such integrals as those in (41).

Now that we can calculate $\psi_1(y,z;x)$ on the hull, we can use Bernoulli's equation to find the pressure. See the section on numerical results for calculations of ψ_1 and

comparisons with experiments.

A Frank-type program was not at our disposal and so we could only compare our results with those published by Frank (1967). As a comparison between the two methods, the results given by him for the pressure distribution on a heaving circular cylinder represented by 21 input points on a half circle have been duplicated to the same accuracy using only 8 input points. Both of these methods reproduce the results of Porter (1960), who used a multipole expansion.

While we agree that most people familiar with Frank's program would use only 5 to 7 input points on a half section to get what is considered reasonable results for added mass and damping coefficients, we would like to point out the following:

i) Getting an acceptable accuracy in forces does not necessarily mean that the margin of error in the calculated pressures is the same. For example, if one is interested in the heave force, the pressure near the free surface could be wrong and still not effect the force.

ii) What we considered to be good comparisons were results that did not vary from Porter (1960) or Frank (1967) by more than a fraction of a per cent.

Chapter V

The Forward Speed Problem

In this section we will examine the effects of forward speed on the diffraction problem. The coordinate system is shown in Figure 1 and the governing equations are Laplace's equation, the free surface boundary conditions, and the hull boundary conditions given in (3), (4), (5) and (6), respectively. Recall that the ship is fixed in space.

Assume that the total potential $\Phi(x,y,z,t)$ is the sum of four potentials, Ux, $\Phi_S(x,y,z)$, $\Phi_I(x,y,z,t)$ and $\Phi_D(x,y,z,t)$ where Ux represents the steady stream, Φ_S the steady state potential, Φ_I the incident wave potential and Φ_D the diffracted wave potential. Φ can then be written as

$$\Phi(x,y,z,t) = Ux + \Phi_S(x,y,z) + \Phi_I(x,y,z,t) + \Phi_D(x,y,z,t) \tag{45}$$

where

$$\Phi_I = \frac{g\zeta_O}{\omega_O} \; e^{i(\omega t - \nu x)} \; e^{\kappa z - iy\sqrt{\kappa^2-\nu^2}}$$

$$\equiv e^{i(\omega t - \nu x)} \; \phi_O(y,z) \; . \tag{46}$$

As stated in the initial assumptions, ω , the frequency of encounter, is

$$\omega = \omega_O + \nu U = O(\varepsilon^{-1}) \tag{47}$$

and the dispersion relation is

$$\omega_O^2 = \kappa g = O(\varepsilon^{-1}) \quad .$$

Also, the speed U is assumed to be O(1).

The solution for the steady motion problem, Φ_S , is already known and only pertinent facts will be presented here. For details, see Tuck (1965). A brief summary of the problem is stated in the following:

In the near field, a first term expansion of $\Phi_s(x,y,z)$ satisfies

$$\Phi_{s_{yy}} + \Phi_{s_{zz}} = 0 \quad , \quad \text{in the fluid domain;}$$

$$\frac{g\eta_s}{U^2} = -\Phi_{s_x} - \frac{1}{2}\Phi_{s_y}^2 \quad , \quad \text{on } z = 0;$$

$$\Phi_{s_z} = 0 \quad , \quad \text{on } z = 0;$$

and

$$\frac{\partial \Phi_s}{\partial N} = \frac{h_x}{\sqrt{1+h_z^2}} \quad , \quad \text{on } y = h(x,z) \ .$$

$\eta_s(x,y,z)$ is the wave amplitude due to a steadily moving ship.

Far from the body, the inner expansion behaves like $a(x)\log r$ plus some function of x. Here $a(x)$ is proportional to the longitudinal rate of change of the sectional area and $r=\sqrt{y^2+z^2}$. In the near field Φ_s and its derivatives have the following order of magnitudes:

$$O(\Phi_s) = O(\Phi_{s_x}) = O(\eta_s) = O(\varepsilon^2) \ ,$$

$$O(\Phi_{s_y}) = O(\Phi_{s_z}) = O(\varepsilon) \ .$$

Also, $\Phi_{s_y}(x,y\ (x),0)=y_0'(x)$ where $y_0(x)$ is the half-beam at the waterline.

The Near Field Problem

Since there is no reason to expect the steady-speed wave amplitude to be dependent upon the incident wave amplitude, two small parameters will be defined. Given the assumption on the forward speed, the steady speed potential is related to the slenderness parameter ε which characterizes the hull geometry. The diffraction potential is a function of both the incident wave and the hull shape, and hence will be based on both the slenderness parameter ε and an incident wave parameter δ. Specifically, the incident wave amplitude ζ_o will be of the following order:

$$\zeta_o = O(\varepsilon\delta) \tag{48}$$

This insures that the wave amplitude will always be smaller than the beam even as $\varepsilon \to 0$. The explicit relations between the hull geometry and ε are given in (7a) and (7b).

Putting (47) and (48) in (4), (45), and (46) we find that the incident wave potential is of the following order:

$$\phi_o(y,z) = O(\varepsilon^{3/2}\delta)$$

Our purpose is now to expand the diffraction potential in a perturbation series. We will see in the following pages that the first term in the near field expansion is just the zero speed potential while the second term includes the forward speed effects. The first term will be shown to be of the same order as the incident wave potential while the second term will be $O(\varepsilon^{1/2})$ higher.

The governing equations will now be found to an order consistent with the above statement. We will define the following quantities:

$$\zeta(x,y,t) = \eta_s(x,y) + e^{i(\omega t - \nu x)}[\eta_o(y) + \eta_7(x,y)]$$

and

$$\Phi_D(x,y,z,t) = e^{i(\omega t - \nu x)}\phi_7(x,y,z) \ .$$

Here ζ is the total wave amplitude composed of the steady wave amplitude η_s, the incident wave amplitude η_o and the diffraction wave amplitude, η_7. It can easily be shown from (46) and Bernoulli's equation that

$$\eta_o(y) = -i\zeta_o e^{-iy\sqrt{\kappa^2-\nu^2}}$$

Using the above relations and discarding terms of higher order, the dynamic boundary condition on the free surface given in (4) is

$$\underset{[\varepsilon\delta]}{g\eta_7 + i\omega_o\phi_7} \simeq \underset{[\varepsilon^{3/2}\delta]}{-U\phi_{7_x} - U(\phi_{7_y} + \phi_{o_y})\Phi_{s_y}} \tag{49}$$

on $z = 0$,

and the kinematic boundary condition on the free surface given in (5) is

$$\underset{[\varepsilon^{1/2}\delta]}{\phi_{7_z}} - i\omega_o\eta_7 = U\eta_{7_x} + \underset{[\varepsilon\delta]}{U\Phi_{s_y}(\eta_{o_y}+\eta_{7_y})} + \underset{[\varepsilon\delta]}{U\Phi_{s_{yy}}(\eta_o+\eta_7)} \qquad (50)$$

on $z = 0$. The orders of magnitude are given under each of the equations. We take the liberty to state them here even though they are not known until the end of this section. The derivation of (49) and (50) is similar to that used in Ogilvie & Tuck (1969) to derive the free surface boundary conditions for the forced oscillation problem and the details are omitted.

Using the fact that $\eta_o=-i\omega_o\phi_o$ when combining (49) and (50) yields

$$\underset{[\varepsilon^{1/2}\delta]}{-\omega_o^2\,\phi_7+g\phi_{7_z}} = -2i\omega_o U\phi_{7_x} \underset{[\varepsilon\delta]}{-2i\omega_o U(\phi_{o_y}+\phi_{7_y})\Phi_{s_y}} - i\omega_o U\Phi_{s_{yy}}(\phi_o+\phi_7) \qquad (51)$$

on $z = 0$.

Since $\frac{\partial\Phi_s}{\partial N} = 0$ on $y=h(x,y)$, the body boundary condition, (6), for the first two terms in the diffraction problem is

$$\frac{\partial\phi_7}{\partial N} = -\frac{\partial\phi_o}{\partial N} \qquad \text{on} \quad y = h(x,y)\ , \qquad (52)$$

where N is the two dimensional normal in the transverse plane.

The equation of continuity, Laplace's equation for three dimensions, becomes a Helmholtz equation in two dimensions of the form:

$$\frac{\partial^2\phi_7}{\partial y^2} + \frac{\partial^2\phi_7}{\partial z^2} - \nu^2\phi_7 = 0\ , \qquad (53)$$

valid in the fluid region.

As in the zero speed problem, assume that ϕ_7 can be expanded in a series expansion of the form

$$\phi_7(x,y,z) \sim \sum_{i=1}^{N} \psi_n(x,y,z;\epsilon\delta) \ . \tag{54}$$

Then the first two terms of the series expansion satisfy the following equations:
The ψ_1 problem is

$$\nabla^2_{2-D}\psi_1 - \nu^2\psi_1 = 0 \ , \quad \text{in the fluid region;} \tag{55}$$

$$-\omega_o^2\psi_1 + g\psi_{1_z} = 0 \ , \quad \text{on } z = 0; \tag{56}$$

and

$$\frac{\partial\psi_1}{\partial N} = -\frac{\partial\phi_o}{\partial N} \ , \quad \text{on } y = h(x,z) \ . \tag{57}$$

The ψ_2 problem is

$$\nabla^2_{2-D}\psi - \nu^2\psi_2 = 0 \ , \quad \text{in the fluid region;} \tag{58}$$

$$-\omega_o^2\psi_2+g\psi_{2_z} = -2i\omega_o U\psi_{1_x}-2i\omega_o U\Phi_{s_y}(\phi_{o_y}+\psi_{1_y})-i\omega_o\Phi_{s_{yy}}U(\phi_o+\psi_1), \tag{59}$$

on $z = 0$;
and

$$\frac{\partial\psi_2}{\partial N} = 0 \ , \quad \text{on } y = h(x,z) \ . \tag{60}$$

Comparing equations (55), (56) and (57) with (17), (18), (19) shows that the ψ_1 problem for the forward speed case corresponds to the first order in the zero speed case. This problem has already been discussed in the previous chapter and only its solution will be presented here:

$$\psi_1(y,z;x) = \int_{C_H(x)} d\ell\sigma(\xi,\eta)G(y,z;\xi,\eta) \ . \tag{33}$$

The ψ_2 term appears to be quite a bit more complex. It satisfies a homogeneous differential equation and a homogeneous body boundary condition but a non-homogeneous free surface

condition. The terms on the right hand side of equation (59) can be grouped into two parts: one, which can be considered as local effects, and the other which extends to infinity. (That is, infinity in the sense of the near field. Remember that infinity in the inner variables corresponds to the outer variables approaching zero). The term which extends to infinity has an oscillatory nature to it, characteristic of the wave-like behavior of ψ_1 at large distances from the body.

If we were to apply an oscillating pressure distribution on the free surface of the form

$$e^{i\omega t}p(y) = e^{i\omega t}[-2i\omega_o U\psi_{1_x} - 2i\omega_o U(\phi_{o_y}+\psi_{1_y})\Phi s_y - i\omega_o \Phi_{syy} U(\phi_o+\psi_1)] , \tag{61}$$

on $z = 0$, the resulting problem would have precisely the same free surface condition as that given for ψ_2 in (59). Also, this pressure distribution is forcing the free surface at the same wave number and "natural" frequency that occurs in the free wave solution of (58) satisfying

$$-\omega_o^2\psi_2 + g\psi_{2_z} = 0 \qquad \text{on } z=0.$$

This sort of resonance phenomena is similar to the applied pressure problem found in Ogilvie & Tuck (1969), but differs in that the differential equation is a Helmholtz one, instead of the Laplace equation in two dimensions. The solution to this applied pressure problem is given in Appendix B.

It should be emphasized that without solving the ψ_1 and ψ_2 problems, stating equations (58), (59) and (60) in the form given is little more than speculation. These are only correct if $\psi_2 = O(\varepsilon^{1/2}\psi_1)$, which we will presently show. The usefulness of the far field expansion is that it will provide us with a radiation condition, indicating the proper relationship between ψ_2 and ψ_1. In (58), (59) and (60), we take the liberty of stating the equations in their correct form, using information not yet derived.

We will conclude this part by stating the outer expansion of the near field. If we let y and z get large and use the behavior of the inner expansion of Φ_s for large distances from the body, we see that (59) becomes

$$-\kappa\psi_2 + \psi_{2_z} \simeq -2\frac{\omega_o}{g} U\psi_{1_x}$$

We know the behavior of ψ_1 for large values of y and z from the zero speed problem. From (32) we see that

$$\psi_{1_x} \simeq \left[\frac{i\kappa A'_{S1}(x)}{\sqrt{\kappa^2-\nu^2}} + \operatorname{sgn}(y)\kappa A'_{D1}(x)\right] e^{\kappa z - i|y|\sqrt{\kappa^2-\nu^2}}$$

as $\sqrt{y^2+z^2} \to \infty$.

If we want the behavior of ψ_2 for large $\sqrt{y^2+z^2}$, we can see from (61) that it can be obtained by applying the following pressure on the free surface:

$$p(y) = -2\frac{i\omega_o}{g} Ue^{-i|y|\sqrt{\kappa^2-\nu^2}} \left[\frac{i\kappa A'_{S1}(x)}{\sqrt{\kappa^2-\nu^2}} + \operatorname{sgn}(y)\kappa A'_{D1}(x)\right]$$

In Appendix B we show that the outer expansion for a problem with this pressure distribution, and consequently the outer expansion of ψ_2 , is the following:

$$\psi_2 \simeq -2\frac{i\omega_o}{g} Ue^{-i|y|\sqrt{\kappa^2-\nu^2}} \left[\frac{i\kappa A'_{S1}(x)}{\sqrt{\kappa^2-\nu^2}} + \operatorname{sgn}(y)\kappa A'_{D1}(x)\right]\left[z - i|y|\frac{\kappa}{\sqrt{\kappa^2-\nu^2}}\right]$$

Using this result and the outer expansion of ψ_1, given in (32), we find that the two term outer expansion of a two term inner expansion is

$$\psi_1+\psi_2 \simeq e^{\kappa z - i|y|\sqrt{\kappa^2-\nu^2}} \left[\frac{i\kappa A_{S1}(x)}{\sqrt{\kappa^2-\nu^2}} + \operatorname{sgn}(y)\kappa A_{D1}(x)\right.$$

$$\left. -2\frac{i\omega_o}{g} U\left[\frac{i\kappa A'_{S1}(x)}{\sqrt{\kappa^2-\nu^2}} + \operatorname{sgn}(y)\kappa A'_{D1}(x)\right]\left[z - \frac{i|y|\kappa}{\sqrt{\kappa^2-\nu^2}}\right]\right] \quad (62)$$

Recall that $A_{D1}=O(\varepsilon A_{S1})$ (See the discussion following (30b)). We will have to match this with the two term inner expansion of the two term outer expansion.

From (59) we see that there is a local pressure distribution on the free surface and as a result, the ψ_2 problem will include outgoing waves. However, in the outer expansion these waves are of higher order and hence dropped from (62).

The Far Field Problem

The derivation of the zero speed problem has given us the necessary background to proceed with the forward speed case. Since many of the details are similar and at times redundant, only the major points will be presented.

As in the zero speed case, we expect an odd and even part to the potential, indicating that both sources and horizontal dipoles will be needed. The dipole potential will be found by differentiating the source potential with respect to its source point. Also, as explained for the zero speed case, we have a free surface condition that allows for the existence of surface waves, even though this will mean including higher order terms in the far field. When we find the inner expansion, we will only keep terms that are consistent with our level of approximation.

For a line distribution of pulsating sources in an incident stream, let the velocity potential Φ be the sum of an incident stream potential and a source potential. That is, let

$$\Phi(x,y,z,t) = Ux + e^{i\omega t}\,\psi_S(x,y,z) \tag{63}$$

Then the governing differential equation is

$$\nabla^2_{3-D}\psi_S(x,y,z) \doteq \lim_{\substack{\xi\to 0\\ \eta\to 0}} \sum(x)\; e^{-i\nu x}\,\delta(y-\xi)\,\delta(z-\eta) \tag{64}$$

and the free surface boundary condition is

$$\lim_{\mu\to 0}\left(i\omega+U\frac{\partial}{\partial x}+\mu\right)^2\psi_S+g\psi_{Sz}=0\ , \qquad \text{on } z=0 \tag{64}$$

Here $\omega=\omega_o+\nu U$, $\omega_o^2/g=\kappa$ and μ is a fictitious viscosity that insures outgoing waves. Solving (64) subject to (65) by the method of Fourier Transforms yields

$$\psi_s(x,y,z) = \lim_{\mu\to 0} \frac{-1}{4\pi^2} \int_{-\infty}^{\infty} dk e^{ikx} \sum^*(k+\nu) \int_{-\infty}^{\infty} d\ell \frac{e^{i\ell y+\sqrt{k^2+\ell^2}\ z}}{\sqrt{k^2+\ell^2} - \frac{1}{g}(\omega+kU-i\mu)^2}$$

$$= \frac{-1}{4\pi^2} \int_{-\infty}^{\infty} dk\ e^{ikx}\ \sum^*\ (k+\nu)\ I_s\ (k) \quad , \tag{66}$$

where $\sum^*(k+\nu)$ is the Fourier Transform of $e^{-i\nu x}\ \sum^*(x)$ and

$$I_s(k) = \lim_{\mu\to 0} \int_{-\infty}^{\infty} d\ell\ \frac{e^{i\ell y+\sqrt{k^2+\ell^2}\ z}}{\sqrt{k^2+\ell^2} - \frac{1}{g}(\omega+kU-i\mu)^2} \tag{67}$$

If $U=0$, then $\omega=\omega_o$ and (67) corresponds to (23a). As in the zero speed case, the details for the simplification of $I_s(k)$ are given in Appendix C and the results are shown in Table 4. The values for k_1 and k_2 are also given in Appendix C.

TABLE 4

$I_s(k)$ for different values of k and U not equal to zero.

	$I_s(k)$
$k>k_1$	$\dfrac{-2\pi i e^{-iy\sqrt{\frac{1}{g^2}(\omega_o+kU)^4-(\nu-k)^2}} \cdot e^{\frac{1}{g}(\omega_o+kU)^2 z} \cdot \frac{1}{g}(\omega_o+kU)^2}{\sqrt{\frac{1}{g^2}(\omega_o+kU)^4-(\nu-k)^2}}$
$k_2<k<k_1$	$\dfrac{2\pi\ e^{-y\sqrt{(\nu-k)^2-\frac{1}{g^2}(\omega_o+kU)^4}} \cdot e^{\frac{1}{g}(\omega_o+kU)^2 z} \cdot \frac{1}{g}(\omega_o+kU)^2}{\sqrt{(\nu-k)^2-\frac{1}{g^2}(\omega_o+kU)^4}}$
$k<k_2$	$\dfrac{2\pi i e^{iy\sqrt{\frac{1}{g^2}(\omega_o+kU)^4-(\nu-k)^2}} \cdot e^{\frac{1}{g}(\omega_o+kU)^2 z} \cdot \frac{1}{g}(\omega_o+kU)^2}{\sqrt{\frac{1}{g^2}(\omega_o+kU)^4-(\nu-k)^2}}$

The potential $\psi_s(x,y,z)$ given in (66) can now be approximated. First, make the substitution $k=k'-\nu$ in (66), then use the results of Table 4 to find

$$\psi_s(x,y,z) \simeq \frac{-1}{4\pi^2} e^{-i\nu x}\left[-\int_{k_1}^{\infty} dk\, e^{ikx} \sum^*(k) 2\pi i e^{-iy\sqrt{\frac{1}{g^2}(\omega_o+kU)^4-(\nu-k)^2}} \right.$$

$$\cdot e^{\frac{1}{g}(\omega_o+kU)^2 z} \cdot \frac{1}{g}(\omega_o+kU)^2 \Big/ \sqrt{\frac{1}{g^2}(\omega_o+kU)^4-(\nu-k)^2}$$

$$+ \int_{k_2}^{k_1} dk\, e^{ikx} \sum^*(k)\, 2\pi e^{-y\sqrt{(\nu-k)^2-\frac{1}{g^2}(\omega_o+kU)^4}}$$

$$\cdot e^{\frac{1}{g}(\omega_o+kU)^2 z} \cdot \frac{1}{g}(\omega_o+kU)^2 \Big/ \sqrt{\frac{1}{g^2}(\nu-k)^2-(\omega_o+kU)^4}$$

$$+ \int_{-\infty}^{k_2} dk\, e^{ikx} \sum^*(k)\, 2\pi i\, e^{iy\sqrt{\frac{1}{g^2}(\omega_o+kU)^4-(\nu-k)^2}}$$

$$\left. \cdot e^{\frac{1}{g}(\omega_o+kU)^2 z} \cdot \frac{1}{g}(\omega_o+kU)^2 \Big/ \sqrt{\frac{1}{g^2}(\omega_o+kU)^4-(\nu-k)^2} \right] \quad (68)$$

Remember that (68) is valid for $y>0$ and the range of integration in the first integral includes the value $k=0$. Then, in an analysis similar to the zero speed problem, the Fourier Transform of the source strength is assumed to behave like $1/k^3$ for large values of k and hence the last two integrals can be shown to be $O(\varepsilon)$. The details are similar to that leading to (25) and are omitted here. Also, extending the lower limit of the first integral to $-\infty$ does not effect the accuracy of the potential to the order considered, as can easily be verified. The potential, $\psi_s(x,y,z)$, can then be written as

$$\psi_s(x,y,z) \simeq \frac{i}{2\pi} e^{-i\nu x} \int_{-\infty}^{\infty} dk\, e^{ikx} \sum^*(k)\, e^{-iy\sqrt{\frac{1}{g^2}(\omega_o+kU)^4-(\nu-k)^2}}$$

$$\cdot e^{\frac{1}{g}(\omega_o+k)^2 z} \cdot \frac{1}{g}(\omega_o+kU)^2 \Big/ \sqrt{\frac{1}{g^2}(\omega_o+kU)^4-(\nu-k)^2} \quad . \quad (69)$$

Following the argument used for the zero speed problem (see the discussion following (28)), assume that the major part of the integral in (69) comes from values of k near to zero. Then we can show that the square root singularities have only a higher order effect on the integral and consequently the terms in (69) can then be expanded about k=0. For example, define

$$f(k) \equiv \sqrt{\frac{1}{g^2}(\omega_o+kU)^4 - (\nu-k)^2}$$

$$= \sqrt{k^2-\nu^2}\left[1 + \frac{k}{(k^2-\nu^2)}\left(2\frac{U\kappa^2}{\omega_o}+\nu\right) + k^2 \quad \ldots\right]$$

$$\simeq \sqrt{k^2-\nu^2}\left[1 + \frac{k}{(k^2-\nu^2)} \quad 2\frac{U\kappa^2}{\omega_o}\right] \tag{70}$$

and

$$h(k) \equiv \frac{1}{g}(\omega_o+kU)^2$$

$$\simeq \kappa\left(1 + 2\frac{kU}{\omega_o}\right) \tag{71}$$

Dividing h by f gives the following:

$$h(k)/f(k) \simeq \frac{\kappa}{\sqrt{\kappa^2-\nu^2}}\left[1 + k\left(\frac{2U}{\omega_o} - \frac{2U\kappa^2}{\omega_o(\kappa^2-\nu^2)}\right)\right] \tag{72}$$

We will now put the approximations of (70), (71) and (72) into (69). These are small k approximations but the limits of integration, which are $-\infty$ to ∞, are retained producing only higher order errors. The potential ψ_s can then be written in the following manner:

$$\psi_s(x,y,z) \simeq \frac{i}{2\pi} e^{-i\nu x}\int_{-\infty}^{\infty} dk\, e^{ikx}\, \zeta^*(k)\, e^{-iy\sqrt{\kappa^2-\nu^2}}\left[1 + \frac{k}{(\kappa^2-\nu^2)}\frac{2U\kappa^2}{\omega_o}\right]$$

$$\cdot\, e^{\kappa\left(1+\frac{2kU}{\omega_o}\right)z} \cdot \frac{\kappa}{\sqrt{\kappa^2-\nu^2}}\left[1 + k\left(\frac{2U}{\omega_o} - \frac{2U\kappa^2}{\omega_o(\kappa^2-\nu^2)}\right)\right] \tag{73}$$

This is the two term far field expansion. We can check (73) against the potential given in Ogilvie & Tuck (1969) representing a line of pulsating sources without the $e^{-i\nu x}$ dependence. If we set $\nu=0$, and add a higher order term of no consequence, i.e. $e^{\kappa(z-iy)U^2k^2/\omega_o^2}$, we find that (73) can be written as

$$\psi_s(x,y,z) \simeq \frac{i}{2\pi} \int_{-\infty}^{\infty} dk e^{ikx} \zeta^*(k) \; e^{\kappa(z-iy)(1+\frac{Uk}{\omega_o})^2} \quad .$$

Except for a factor $\frac{1}{4\pi}$, which is the difference in definition of source strength used in (64), the two are equivalent. Thus, the relation give in (73) is valid for modeling the far field diffraction behavior of both beam seas and oblique seas. We will now proceed to determine the behavior of (73) in the inner region of the far-field.

The Inner Expansion of the Far-Field Expansion

To find the two term inner expansion of (73), let $y=O(\varepsilon)$ and $z=O(\varepsilon)$. Then the exponetials can be approximated by

$$e^{-iy\sqrt{\kappa^2-\nu^2}} \left[1 + \frac{k}{(\kappa^2-\nu^2)} \frac{2U\kappa^2}{\omega_o}\right] \sim e^{-iy\sqrt{\kappa^2-\nu^2}} \left[1 - \frac{iyk2U\kappa^2}{\omega_o\sqrt{\kappa^2-\nu^2}}\right]$$

and

$$e^{\kappa(1+\frac{2kU}{\omega_o})z} \sim e^{\kappa z} \left[1 + kz \frac{\omega_o 2U}{g}\right] \quad .$$

Now, noting the Fourier-transform properties of

$$\zeta(x) = \frac{1}{2\pi} \int_{-\infty}^{\infty} dk \; e^{ikx} \zeta^*(k)$$

and

$$\zeta'(x) = \frac{i}{2\pi} \int_{-\infty}^{\infty} dk \; e^{ikx} \, k\zeta^*(k)$$

and dropping k^2 and higher terms in (73), we obtain the

following:

$$\psi_s(x,y,z) \simeq \frac{i}{2\pi} e^{-i\nu x - iy\sqrt{\kappa^2-\nu^2}+\kappa z} \cdot \frac{\kappa}{\sqrt{\kappa^2-\nu^2}} \left[\int_{-\infty}^{\infty} dk\, e^{ikx} \sum^*(k) \right.$$

$$\left. + \left[\frac{2U}{\omega_o} - \frac{2U\kappa^2}{\omega_o(\kappa^2-\nu^2)} + \frac{2U\omega_o}{g} \left(z - \frac{iy\kappa}{\sqrt{\kappa^2-\nu^2}}\right) \right] \int_{-\infty}^{\infty} dk\, e^{ikx} k \sum^*(k) \right]$$

$$= \frac{\kappa i}{\sqrt{\kappa^2-\nu^2}} e^{-i\nu x - iy\sqrt{\kappa^2-\nu^2}+\kappa z} \left[\sum(x) \right.$$

$$\left. - i \sum'(x) \left[\frac{2U}{\omega_o} - \frac{2U\kappa^2}{\omega_o(\kappa^2-\nu^2)} + \frac{2U\omega_o}{g} \left(z - \frac{iy\kappa}{\sqrt{\kappa^2-\nu^2}}\right) \right] \right] .$$

The first term is just the zero speed potential (see (30a)) and the second term, which is of order $\epsilon^{1/2}$ higher, has a regular wave term and a wave-like term that grows linearly in the y and z coordinates. This is not the total inner expansion since $\sum(x)$ should also be expanded in an asymptotic series like

$$\sum(x;\epsilon) \sim \sum_1(x;\epsilon) + \sum_2(x;\epsilon) + \ldots$$

where $\sum_2 = o(\sum_1)$. This will add another regular wave term at the second order. Thus, the final form of the two term inner expansion is

$$e^{i\nu x}\, \psi_s(x,y,z) \simeq \frac{\kappa i}{\sqrt{\kappa^2-\nu^2}} e^{\kappa z - i|y|\sqrt{\kappa^2-\nu^2}} \left[\sum_1(x) + \sum_2(x) \right.$$

$$\left. - i \sum_1'(x) \left[\frac{2U}{\omega_o} - \frac{2U\kappa^2}{\omega_o(\kappa^2-\nu^2)} + \frac{2U\omega_o}{g} \left(z - \frac{i|y|\kappa}{\sqrt{\kappa^2-\nu^2}}\right) \right] \right] \qquad (74a)$$

Note that y has been replaced by $|y|$. We can do this, since the source potential is an even function in y.

To find the horizontal dipole potential, we just differentiate (74a) with respect to its source point, ξ. We see from (64) that differentiation with respect to ξ is equivalent

to differentiation with respect to -y. Consequently, we can immediately write down the two term inner expansion of the dipole potential $\psi_D(x,y,z)$ as

$$e^{i\nu x}\,\psi_D(x,y,z) \simeq \operatorname{sgn}(y)\kappa\, e^{\kappa z - i|y|\sqrt{\kappa^2-\nu^2}} \left[\beta_1(x) + \beta_2(x) - i\beta_1'(x)\left[\frac{2U}{\omega_o} + \frac{2U\omega_o}{g}\left(z - \frac{i|y|\kappa}{\sqrt{\kappa^2-\nu^2}}\right)\right]\right]. \qquad (74b)$$

Note that the minus sign has been absorbed into the dipole constant $\beta(x)$. We will now match these expansions with the outer expansion of the near field.

Matching the Expansions

The difficult work is now done and it is just a matter of comparing expressions to see if they are equal. The two-term outer expansion of the two-term inner expansion is given in (62) and it should match the two-term inner expansion of the two-term outer given in (74a) plus (74b). We see that if we set:

$$\sum_1(x) = A_{S1}(x) \quad ,$$

$$\beta_1(x) = A_{D1}(x) \quad ,$$

$$\sum_2(x) = i\sum_1'(x)\left[\frac{2U}{\omega_o} - \frac{2U\kappa^2}{\omega_o(\kappa^2-\nu^2)}\right] ,$$

and

$$\beta_2(x) = i\beta_1'(x)\,\frac{2U}{\omega_o} \quad ,$$

all the terms will match. It is important to note that in setting $\sum_1(x)=A_{S1}(x)$ and $\beta_1(x)=A_{D1}(x)$ both the first order terms and the linearly growing second order term match identically.

Up to this point, no mention has been made as to the method of determining $A_{S1}(x)$ and $A_{D1}(x)$. We will address ourselves to that problem now.

If we have the solution to ψ_1 on the hull given in the form of (33), then we can use the asymptotic nature of $G(y,z;\xi,\eta)$ to find A_{s1} and A_{D1}. Specifically, from (32) and (34b), where we use the nature of G for large values of y^2+z^2, we write:

$$e^{\kappa z - i|y|\sqrt{\kappa^2-\nu^2}} \left[A_{s1} \frac{i\kappa}{\sqrt{\kappa^2-\nu^2}} + A_{D1}\, \mathrm{sgn}(y)\kappa \right] \sim \int_{C_H(x)} d\ell\sigma(\xi,\eta) G(x,y;\xi,\eta)$$

$$\sqrt{y^2+z^2} \to \infty$$

$$= -\int_{C_H(x)} d\ell\sigma(\xi,\eta) \frac{i\kappa}{\sqrt{\kappa^2-\nu^2}} e^{\kappa(z+\eta) - i|y-\xi|\sqrt{\kappa^2-\nu^2}} \qquad (75)$$

Since $\frac{\partial\psi_1}{\partial N}$ on the hull is composed of an even plus an odd function, ψ_1 can be written as $\psi_1 = \psi_1^{(e)} + \psi_1^{(o)} = \int_C d\ell\sigma^{(e)} G + \int d\ell\sigma^{(o)} G$ or $\sigma = \sigma^{(e)} + \sigma^{(o)}$. It follows that:

$$\sigma^{(e)}(\xi,\eta) = \frac{1}{2}\left[\sigma(\xi,\eta) + \sigma(-\xi,\eta)\right]$$

and

$$\sigma^{(o)}(\xi,\eta) = \frac{1}{2}\left[\sigma(\xi,\eta) - \sigma(-\xi,\eta)\right] .$$

Then from (75), it is clear that

$$A_{s1}(x) = -\int_{C_H(x)} d\ell\sigma^{(e)}(\xi,\eta)\, e^{\kappa\eta + i\xi\sqrt{\kappa^2-\nu^2}} \qquad (76a)$$

and

$$A_{D1}(x) = \frac{-i}{\sqrt{\kappa^2-\nu^2}} \int_{C_H(x)} d\ell\sigma^{(o)}(\xi,\eta)\, e^{\kappa\eta + i\xi\sqrt{\kappa^2-\nu^2}} \qquad (76b)$$

These relations give us the values of A_{s1} and A_{D1} so that the second order problem ψ_2 can be determined.

We are through with the far field expansion. Its usefulness has been in verifying the representation of the second order term in the near field given by equations (58), (59)

and (60). We can now state that the forward speed effects, represented by the second order term, are of an order $\varepsilon^{1/2}$ higher than the zero speed term, represented by the lowest order approximation.

Summary of the Forward Speed Problem and Its Solution

The preceding material in addition to the applied pressure problem with its solution described in Appendix B, gives us the necessary information to write down the solution to the forward speed potential. The near field potential can be approximated as follows:

The first term, ψ_1 , in the asymptotic series (54), satisfies

$$\nabla^2_{2-D}\psi_1 - \nu^2\psi_1 = 0 , \qquad \text{in the fluid region} \qquad (55)$$

$$-\omega_o^2\psi_1 + g\psi_{1z} = 0 , \qquad \text{on } z = 0 \qquad (56)$$

and

$$\frac{\partial\psi_1}{\partial N} = -\frac{\partial\phi_o}{\partial N} , \qquad \text{on } y = h(x,z) \qquad (57)$$

The solution of ψ_1 is given by

$$\psi_1(y,z;x) = \int_{C_H(x)} d\ell\,\sigma(\xi,\eta)G(y,z;\xi,\eta) , \qquad (33)$$

and methods for solving this numerically have been discussed in Chapter IV.

The second term in (54) , ψ_2 , satisfies

$$\nabla^2_{2-D}\psi_2 - \nu^2\psi_2 = 0 , \qquad \text{in the fluid region;} \qquad (58)$$

$$-\omega_o^2\psi_2 + g\psi_{2_z} = -2i\omega_o U\psi_{1_x} - 2i\omega_o U(\phi_{oy}+\psi_{1_y})\Phi_{s_y} - i\omega_o U\Phi_{s_{yy}}(\phi_o+\psi_1) \qquad (59)$$

on $z = 0$;

and

$$\frac{\partial \psi_2}{\partial N} = 0 , \qquad \text{on } y = h(x,z) \quad . \tag{60}$$

Let ψ_2 be composed of three potentials Ψ_1 , Ψ_2, and Ψ_3. These auxiliary potentials will each satisfy a particular part of the boundary conditions with their sum satisfying (59) and (60).

For the Ψ_1 problem, consider an oscillating pressure on the free surface extending to infinity and in the absence of any body. In particular, let

$$\nabla^2_{2-D}\Psi_1 - \nu^2\Psi_1 = 0 \qquad \text{in the fluid region;}$$

and

$$-\kappa\Psi_1 + \Psi_{1z} = \frac{-2i\omega_o}{g} U \left[\frac{i\kappa A'_{S1}(x)}{\sqrt{\kappa^2-\nu^2}} + \text{sgn}(y)\kappa A'_{D1}(x)\right] e^{-i|y|\sqrt{\kappa^2-\nu^2}}$$

$$\equiv [p_1 + \text{sgn}(y)p_2]\, e^{-i|y|\sqrt{\kappa^2-\nu^2}} \qquad \text{on } z=0.$$

Here we define p_1 and p_2 which are functions of x only and thus can be considered as constants. The terms A_{S1} and A_{D1} , are given by (76a) and (76b), respectively. This free surface condition is just the behavior of (59) for large values of $\sqrt{y^2+z^2}$. From Appendix B, we can write down the solution for Ψ_1 as

$$\Psi_1(y,z;x) = [p_1+\text{sgn}(y)p_2]\left[e^{-i|y|\sqrt{\kappa^2-\nu^2}+\kappa z}\right]\left[z - \frac{i|y|\kappa}{\sqrt{\kappa^2-\nu^2}}\right] + i_1+i_2 \tag{77}$$

where

$$i_1 = \frac{-p_1}{\pi}\sqrt{\kappa^2-\nu^2}\int_\nu^\infty dk \frac{e^{-|y|k}}{(ik+\sqrt{\kappa^2-\nu^2})(ik-\sqrt{\kappa^2-\nu^2})}\left[\frac{e^{iz\sqrt{k^2-\nu^2}}}{-\kappa+i\sqrt{k^2-\nu^2}} + \frac{e^{-iz\sqrt{k^2-\nu^2}}}{\kappa+i\sqrt{k^2-\nu^2}}\right]$$

and

$$i_2 = \text{sgn}(y)\frac{p_2 i}{\pi}\int_\nu^\infty dk \frac{ke^{-|y|k}}{(ik+\sqrt{\kappa^2-\nu^2})(ik-\sqrt{\kappa^2-\nu^2})}\left[\frac{e^{iz\sqrt{k^2-\nu^2}}}{-\kappa+i\sqrt{k^2-\nu^2}} + \frac{e^{-iz\sqrt{k^2-\nu^2}}}{\kappa+i\sqrt{k^2-\nu^2}}\right].$$

Now consider Ψ_2 as a local pressure distribution on the free surface, also in the absence of a body. Since we know the asymptotic nature of Ψ_2 for large values of $\sqrt{y^2+z^2}$, we subtract this behavior from (59) and are left with strictly local effects. Let Ψ_2 satisfy

$$\nabla^2_{2-D}\Psi_2 - \nu^2\Psi_2 = 0 \qquad \text{in the fluid region;}$$

and

$$-\kappa\Psi_2+\Psi_{2z} = \frac{-2i\omega_o}{g} U\psi_{1x} - \frac{2i\omega_o}{g} U(\phi_{oy}+\psi_{1y})\Phi_{sy} - \frac{i\omega_o}{g} U\Phi_{syy}(\phi_o+\psi_1)$$
$$+ \frac{2i\omega_o}{g} U\left[\frac{i\kappa A'_{S1}(x)}{\sqrt{\kappa^2-\nu^2}} + \operatorname{sgn}(y)\kappa A'_{D1}(x)\right] e^{-i|y|\sqrt{\kappa^2-\nu^2}}$$
$$\equiv p_3(y;x) \qquad \text{on } z = 0 \ .$$

where $p_3(y)$ is a function of y and goes to zero as $|y|$ gets large. Then from Appendix B, we can write the solution for Ψ_2 as

$$\Psi_2(y,z;x) = \frac{1}{2\pi}\int_{-\infty}^{\infty} dk \frac{e^{iky+z\sqrt{\nu^2+k^2}}}{-\kappa+\sqrt{\nu^2+k^2}} \int_{-\infty}^{\infty} d\xi e^{-i\xi k} p_3(\xi;x) \qquad (78)$$

The integral has two poles and the path of integration is indented as shown.

Since the sum of Ψ_1 and Ψ_2 satisfy (59) on z=0, we can now consider Ψ_3 which will satisfy a homogenous free surface boundary condition and a given hull boundary condition. In particular, let

$$\nabla^2_{2-D}\Psi_3 - \nu^2\Psi_3 = 0 \qquad \text{in the fluid region;}$$

$$-\omega_o^2\Psi_3 + g\Psi_{3z} = 0 \qquad \text{on } z = 0 \ ;$$

and $$\frac{\partial\Psi_3}{\partial N} = -\left[\frac{\partial\Psi_1}{\partial N} + \frac{\partial\Psi_2}{\partial N}\right] \qquad \text{on } y = h(x,z).$$

Its solution can then be written in terms of a surface singularity distribution similar to (33). Thus, Ψ_3 is given by

$$\Psi_3(y,z;x) = \int_{C_H(x)} d\ell\alpha(\xi,\eta)G(y,z;\xi,\eta) \tag{79}$$

and methods for numerically solving this have been given in Chapter IV. It is easily verified that the sum of Ψ_1 , Ψ_2 and ψ_3 satisfy all the governing equations of the Ψ_1 problem given in (58), (59) and (60).

To summarize, the second order term, ψ_2 , is given as

$$\psi_2(y,z;x) = \Psi_1(y,z;x) + \Psi_2(y,z;x) + \Psi_3(y,z;x) \tag{80}$$

where Ψ_1 , Ψ_2 and Ψ_3 are given in (77), (78) and (79), respectively.

The Pressure and Force on the Hull

To find the pressure on the hull, we apply the Bernoulli equation as follows:

$$\frac{-p}{\rho} = gz + \Phi_t + \frac{1}{2}[\Phi_x^2 + \Phi_y^2 + \Phi_z^2] - U^2/2 \tag{81}$$

Where Φ has the assumed form given in (45). To find just the dynamic pressure, put (45) and (54) into (81) and retain terms of $O(\varepsilon^{3/2}\delta)$ and lower to find

$$\frac{-p_D}{\rho} \simeq e^{i(\omega t-\nu x)}[i\omega_o(\phi_o+\phi_7)+U\phi_{7_x}+U\phi_{s_y}(\phi_{o_y}+\phi_{7_y})+U\phi_{s_z}(\phi_{o_z}+\phi_{7_z})]$$

$$\simeq e^{i(\omega t-\nu x)}[\underbrace{i\omega_o(\phi_o+\psi_1)}_{[\varepsilon\delta]}+\underbrace{i\omega_o\psi_2}_{[\varepsilon^{3/2}\delta]}+U\psi_{1_x}+U\phi_{s_y}(\phi_{o_y}+\psi_{1_y})$$

$$+ U\phi_{s_z}(\phi_{o_z}+\psi_{1_z})] \tag{82}$$

$$[\varepsilon^{3/2}\delta]$$

The first term is $O(\varepsilon\delta)$ and represents the zero speed pres-

sure. Note that the Froude-Krylov pressure, i.e., the pressure due to the undisturbed wave, is the same order as the first term of the diffraction pressure represented by ψ_1. The speed dependent terms are $O(\varepsilon^{1/2})$ higher.

Some observations should be made here as to the ease of computing the dynamic pressure p_D given in (82). The lowest order terms are relatively easy to find as described in Chapter IV and as illustrated in Chapter VI. One $O(\varepsilon^{3/2}\delta)$ term invovles differentiating ψ_1 with respect to x. This can be done numerically and should not involve a lot of work since ψ_1 is assumed to vary slowly with respect to x. The term that causes considerable difficulty is the $i\omega_o\psi_2$ term whose solution is given in (80). In particular, note that the contribution from (78) involves a double integral of an integrand that is only known numerically. It seems that this is a tedious calculation to find only a higher order correction to the zero speed, lowest order term. If we are just interested in the sectional exciting forces we will see that by defining an auxillary problem, the forced oscillation potential, some of the tedium can be removed.

Only the longitudinal force distribution will be derived here. The roll moment can be found by using the same analysis. In the cross plane there are two force components, F_2, the sway force distribution and F_3, the longitudinal heave force distribution. The general dynamic force distribution can be written as

$$F_i(x,t) = -\int_{C_H(x)} d\ell\, p_D(x,\xi,\eta,t)\, n_i(\xi,\eta) \tag{83}$$

where p_D is given in (82). Then using (82) we find

$$F_i(x,t) = \rho e^{i(\omega t-\nu x)} \int_{C_H(x)} d\ell\, [i\omega_o(\phi_o+\psi_1)+i\omega_o\psi_2+U\psi_{1_x}$$

$$+ U\Phi_{s_y}(\phi_{o_y}+\psi_{1_y})+U\Phi_{s_z}(\phi_{o_z}+\psi_{1_z})]n_i \; ; i=2,3 \tag{84}$$

The terms ψ_{1_y} and ψ_{1_z} should be easy to find once ψ_1 is known. As noted earlier, ψ_{1_x} will have to be found numerically, though as shown in the numerical examples, this is not too difficult. The steady speed potential, Φ_s, and its derivatives are considered as known. This means the only term that makes the determination of the section force distribution difficult is the second order ψ_2 term. Let us examine a number of simplifications that can be made.

First, define a forced oscillation potential ϕ_i , i = 2,3, where ϕ_i satisfies the following:

$$\nabla^2_{2-D}\phi_i - \nu^2\phi_i = 0 \qquad \text{in the fluid domain;}$$

$$-\kappa\phi_i + \phi_{i_z} = 0 \qquad \text{on } z = 0;$$

and

$$\frac{\partial\phi_i}{\partial N} = n_i \qquad \text{on } y = h(x,z).$$

Also, if there are two functions A and B that satisfy a Helmholtz equation in two dimensions, then it can easily be shown that Green's Theorem takes a form

$$\int_C d\ell \left(A\frac{\partial B}{\partial N} - B\frac{\partial A}{\partial N}\right) = 0$$

where N is the normal to the closed curve C.

Using ϕ_i , Green's Theorem, and (60), (i.e. $\frac{\partial\psi_2}{\partial N} = 0$), the i-th sectional force due to ψ_2 can be written as follows:

$$\int_{C_H(x)} d\ell\, n_i\psi_2 = -\left[\int_{F.S.} + \int_{S_{|y|=\infty}} + \int_{S_{z=-\infty}}\right] d\ell \left[\frac{\partial\phi_i}{\partial N}\psi_2 - \phi_i\frac{\partial\psi_2}{\partial N}\right] \qquad (85)$$

where F.S. is the mean free surface represented by z = 0 , $S_{|y|=\infty}$ are the two vertical planes at $y=\pm\infty$ and $S_{z=-\infty}$ is a horizontal plane at $z=-\infty$.

Since ϕ_i will decay in the -z direction like $e^{\kappa z}$, it will dominate the linear growth of ψ_2 and hence the integral over the plane $S_{z=-\infty}$ will contribute nothing.

Now consider the behavior of ϕ_i and ψ_2 at the planes $S_{|y|=R}$ as $R\to\infty$. We know from the discussion of the outer expansion of ψ_1 that the behavior of ϕ_i as $\sqrt{y^2+z^2}\to\infty$ is

$$\phi_i \to C_i \frac{i\kappa}{\sqrt{\kappa^2-\nu^2}} e^{-i|y|\sqrt{\kappa^2-\nu^2}+\kappa z} \tag{86}$$

where C_3 is a constant and C_2 is a constant multiplied by sgn(y). As stated previously, ψ_2 behaves like

$$\psi_2 \sim \frac{-2i\omega_0}{g} Ue^{\kappa z - i|y|\sqrt{\kappa^2-\nu^2}} \left[\frac{i\kappa A'_{S1}}{\sqrt{\kappa^2-\nu^2}} + \mathrm{sgn}(y)\kappa A'_{D1}\right]\left[z - i|y|\frac{\kappa}{\sqrt{\kappa^2-\nu^2}}\right] \tag{87}$$

In the interst of brevity, we will only examine the heave sectional force. The sway sectional force is similar and its description is omitted.

For the heave sectional force then, the contribution to (85) from the planes $S_{|y|=R}$ as $R\to\infty$ can be found by using (86) and (87) and noting that $\frac{\partial}{\partial N} = \pm\frac{\partial}{\partial y}$ on these planes. It is the following:

$$\int_{S_{|y|=\infty}} d\ell \left[\frac{\partial\phi_3}{\partial N}\psi_2 - \phi_3\frac{\partial\psi_2}{\partial N}\right] = \lim_{R\to\infty} \frac{2C_3\kappa^2}{(\kappa^2-\nu^2)^{3/2}} A'_{S1}\frac{\omega_0}{g} Ue^{-i\frac{\pi}{2}|R|\sqrt{\kappa^2-\nu^2}} \tag{88}$$

Equation (88) has no meaning if we let R go to infinity. However, we expect to have the same trouble with the free surface integral in (85) and fortunately these two difficulties cancel each other.

On the free surface, $\frac{\partial}{\partial N}$ equals $\frac{\partial}{\partial z}$. Using this, and the free surface boundary conditions for ϕ_3 and ψ_2, we have for the free surface integral in (85)

$$\int_{F.S.} d\ell \left[\frac{\partial \phi_3}{\partial N}\,\psi_2 - \phi_3 \frac{\partial \psi_2}{\partial N}\right] = \int_{F.S.} dy \left[\frac{2i}{g}\omega U \psi_{1_x} \phi_3 + \frac{2i\omega}{g} U \Phi_{s_y} \phi_3 (\phi_{o_y} + \psi_{1_y}) \right.$$

$$\left. + \frac{i\omega}{g} U \Phi_{s_{yy}} \phi_3 (\phi_o + \psi_1)\right] \tag{89}$$

The terms involving the derivative of Φ_s go to zero for large values of y but the term containing $\psi_{1_x}\phi_3$ represents an outgoing wave of amplitude $\frac{iC_3\kappa}{\sqrt{\kappa^2-\nu^2}}\left[\frac{i\kappa A'_{s1}}{\sqrt{\kappa^2-\nu^2}} - \mathrm{sgn}(y)\kappa A'_{D1}\right]$.

It is precisely this sort of term that we wish to cancel in (88), and we can accomplish this by adding and subtracting an outgoing wave of this amplitude. If $y_o(x)$ is the half-beam at the waterline, then (89) can be re-written as

$$\int_{F.S.} d\ell \left[\frac{\partial \phi_3}{\partial N}\,\psi_2 - \phi_3 \frac{\partial \psi_2}{\partial N}\right] = \int_{\infty}^{y_o} + \int_{-y_o}^{-\infty} dy \left[\frac{2i\omega}{g}\omega U(\phi_{o_y} + \psi_{1_y}) \Phi_{s_y} \phi_3 \right.$$

$$+ \frac{i\omega}{g} U(\phi_o + \psi_1) \Phi_{s_{yy}} \phi_3 + \frac{2i\omega_o}{g} U\left[\phi_3 \psi_{1_x} \right.$$

$$\left. - \frac{iC_3\kappa}{\sqrt{\kappa^2-\nu^2}}\left[\frac{i\kappa A'_{D1}}{\sqrt{\kappa^2-\nu^2}} + \mathrm{sgn}(y)\kappa A'_{D1}\right] e^{-2i|y|\sqrt{\kappa^2-\nu^2}}\right]$$

$$\left. + \lim_{R\to\infty} \frac{2C_3\kappa^2}{(\kappa^2-\nu^2)^{3/2}} A'_{s1} \frac{\omega}{g} U\left[e^{-2iy_o\sqrt{\kappa^2-\nu^2}} - e^{-2iR\sqrt{\kappa^2-\nu^2}}\right]\right. \tag{90}$$

The last term contains one part that exactly cancels the oscillatory nature of (88) and another part that is easily found. The term containing $\Phi_{s_{yy}}$ can be integrated once by parts and then using the fact that $\Phi_{s_y}(x, y_o(x), o) = y'_o(x)$ we have

$$\int_{\infty}^{y_o} + \int_{-y_o}^{-\infty} dy (\phi_o + \psi_1) \Phi_{s_{yy}} \phi_3 = y'_o [\phi_3(\phi_o + \psi_1)\Big|_{y=-y_o} - \phi_3(\phi_o + \psi_1)\Big|_{y=y_o}]$$

$$- \int_{\infty}^{y_o} + \int_{-y_o}^{-\infty} dy \Phi_{s_y} [(\phi_{o_y} + \psi_{1_y})\phi_3 + (\phi_o + \psi_1)\phi_{3_y}]$$

Using this and (90) in (85), we have, finally, the following expression for the contribution by ψ_2:

$$\int_{C_H(x)} d\ell n_3 \psi_2 = -\left[\int_{\infty}^{y_o} + \int_{-y_o}^{-\infty}\right] dy \left[\frac{i\omega_o U}{g} \Phi_{sy}[\phi_3(\phi_{oy}+\psi_{1y}) - \phi_{3y}(\phi_o+\psi_1)]\right.$$

$$+ \frac{2i\omega_o}{g} U \left[\phi_3\psi_{1x} - \frac{iC_3\kappa}{\sqrt{\kappa^2-\nu^2}} \frac{(i\kappa A'_{s1} + \mathrm{sgn}(y)\kappa A'_{D1}) e^{-2i|y|\sqrt{\kappa^2-\nu^2}}}{\sqrt{\kappa^2-\nu^2}}\right]\Bigg|_{z=o}$$

$$- \frac{2C_3\kappa^2}{(\kappa^2-\nu^2)^{3/2}} A'_{s1} \frac{\omega_o}{g} U e^{-2iy_o\sqrt{\kappa^2-\nu^2}}$$

$$\left. - y'_o [\phi_3(\phi_o+\psi_1)|_{\substack{y=-y_o \\ z=o}} - \phi_3(\phi_o+\psi_1)|_{\substack{y=y_o \\ z=o}}]\right| \qquad (91)$$

The integrand is bounded by $e^{i|y|\sqrt{\kappa^2-\nu^2}}/y$ for large y and thus the integral exists.

The sectional heave force can now be found by putting (91) into (84). Using the sectional force in this form means that we do not have to evaluate the double integral in (78). However, the free surface integral is still not simple and its calculation may be of little use in actual design procedures. In Chapter VI we have attempted to show the relative order of the forward speed correction to the zero speed term by finding the value of $U\psi_{1x}$ on the hull. As will be shown for the case considered, this term did not appreciably affect the zero speed results.

Chapter VI

NUMERICAL RESULTS

In this chapter we will present numerical results that illustrate the material found in the preceding sections. The theory was derived for oblique seas but as beam seas are approached, i.e., as $\nu \to 0$, the Helmholtz equation reduces to the Laplace equation, and the results are uniformly valid as the transition is made. As head seas are approached, i.e., as $\nu \to \kappa$, the imaginary part of the Green's function (see (34b)) becomes singular like $1/\sqrt{\kappa^2-\nu^2}$. As a result, the analysis is not valid near head seas. The pressure distribution on an ore carrier for zero speed is found for oblique seas and the results are compared with experimental values and the theoretical predictions given by the Laplace equation. For forward speed, the total pressure is given by the terms in (82). Some of the higher order terms (in particular the ψ_2 term) will not be calculated in this work due to their complexity. However, one higher order term, the ψ_{1_x} term, will be found. This will indicate the effect the higher order terms have on the zero speed potential. It may also be considered as an "engineering approximation" of the forward speed problem, since for time-dependent functions, differentiation with respect to time in a coordinate system moving in the x-direction is accomplished by applying the operator $\frac{\partial}{\partial t} + U\frac{\partial}{\partial x}$ to the original function. (The pressure, to the first order, is proportional to the time derivative of the potential.) The sectional force on a ship for zero speed is found and compared with the integrand of the total force given by the Khaskind relations. This integrand has been wrongly interpreted as being equivalent to the sectional force. (See Ogilvie (1974).) And finally, the total exciting force on a fixed ship with zero speed will be found by both the Khaskind relations and the integrated pressure distribution of the diffraction problem.

Pressure Distribution

The pressure distribution for zero forward speed was found for the midship section of an ore carrier tested by Nakamura, et. al. (1973). Two different wave lengths were used. Figure 7 and Figure 8 show the magnitude of the pressure and its phase for $L/\lambda = 1.96$ and $L/\lambda = 1.44$ respectively.

The pressure is given by the lowest order terms in (82) and includes both the Froude-Krylov pressure plus the first order diffraction pressure. The pressure amplitude is nondimensionalized with respect to $\rho g \zeta_o$, where ρ is the water density, g is the acceleration of gravity and ζ_o is the incident wave amplitude. The solid line represents the solution using the Helmholtz equation for the diffraction pressure. The dashed line represents the solution of the same boundary value problem, but using Laplace's equation as the governing equation. This is the diffraction problem that would be solved if the usual assumptions in strip theory are used.

The experimental results published by Nakamura, et. al. (1973) are shown for the waves coming from both the bow ($\chi = 45°$) and the stern ($\chi = 135°$). There is only one theoretical line for both wave directions because the two dimensional problem is identical for both wave directions. The experiments show some difference in the pressures for the two directions which is probably due to experimental error and some slight interference between sections. The Helmholtz and Laplace solutions are in close agreement on the windward side of the ship but show some differences on the leeward side. The phase angles are approximately the same on the windward side but again there are differences on the leeward side. The variations in the pressure amplitude and phases, when combined, can cause substantial differences in the integrated sectional exciting forces as seen in Table 5.

$F_2(x)$ and $F_3(x)$ are the complex sectional exciting forces in the horizontal and vertical directions respectively. They

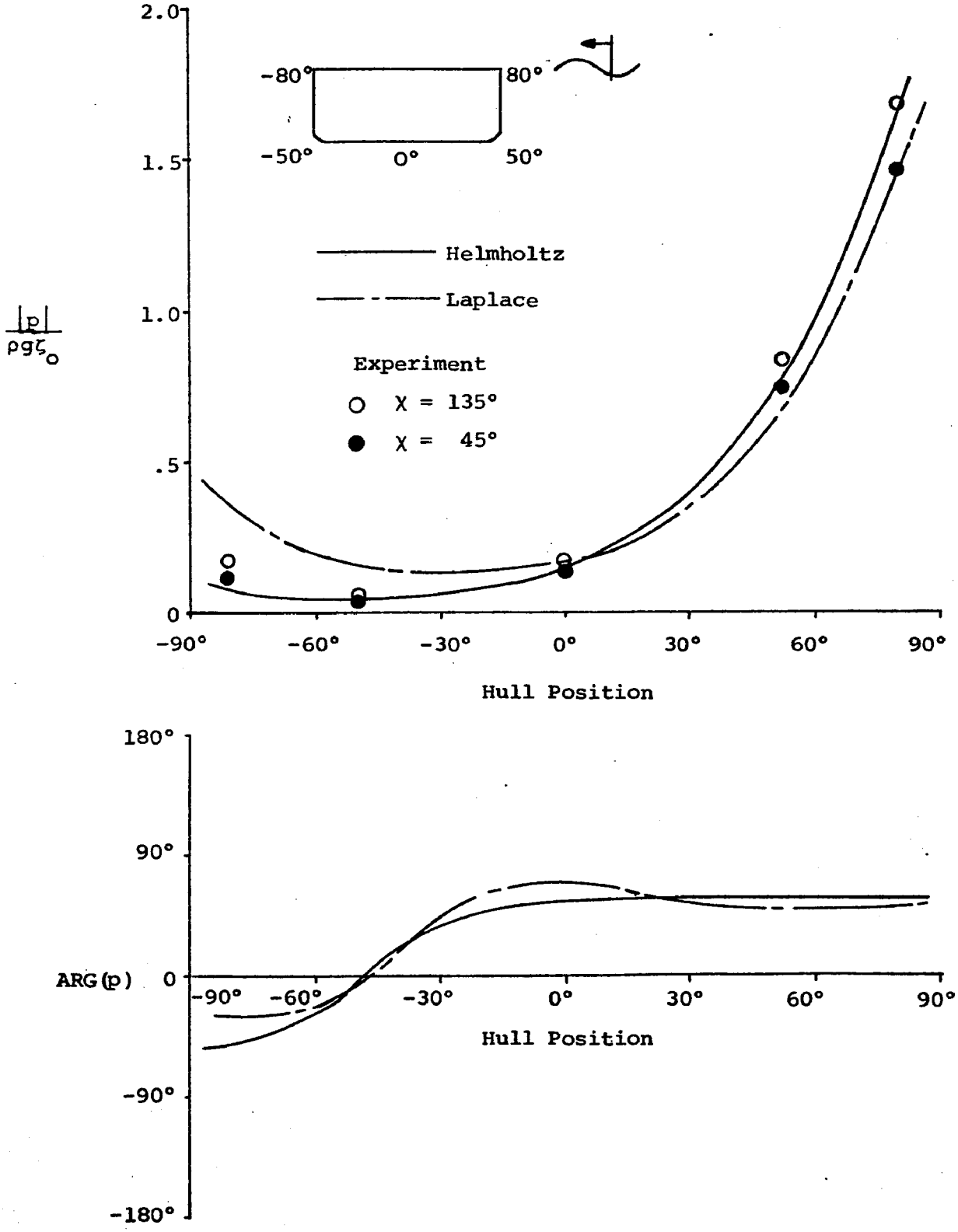

Figure 7: Girthwise Pressure Distribution for a Midship Section of an Ore Carrier in Oblique Seas. ($L/\lambda = 1.96$, $\chi = 45°$)

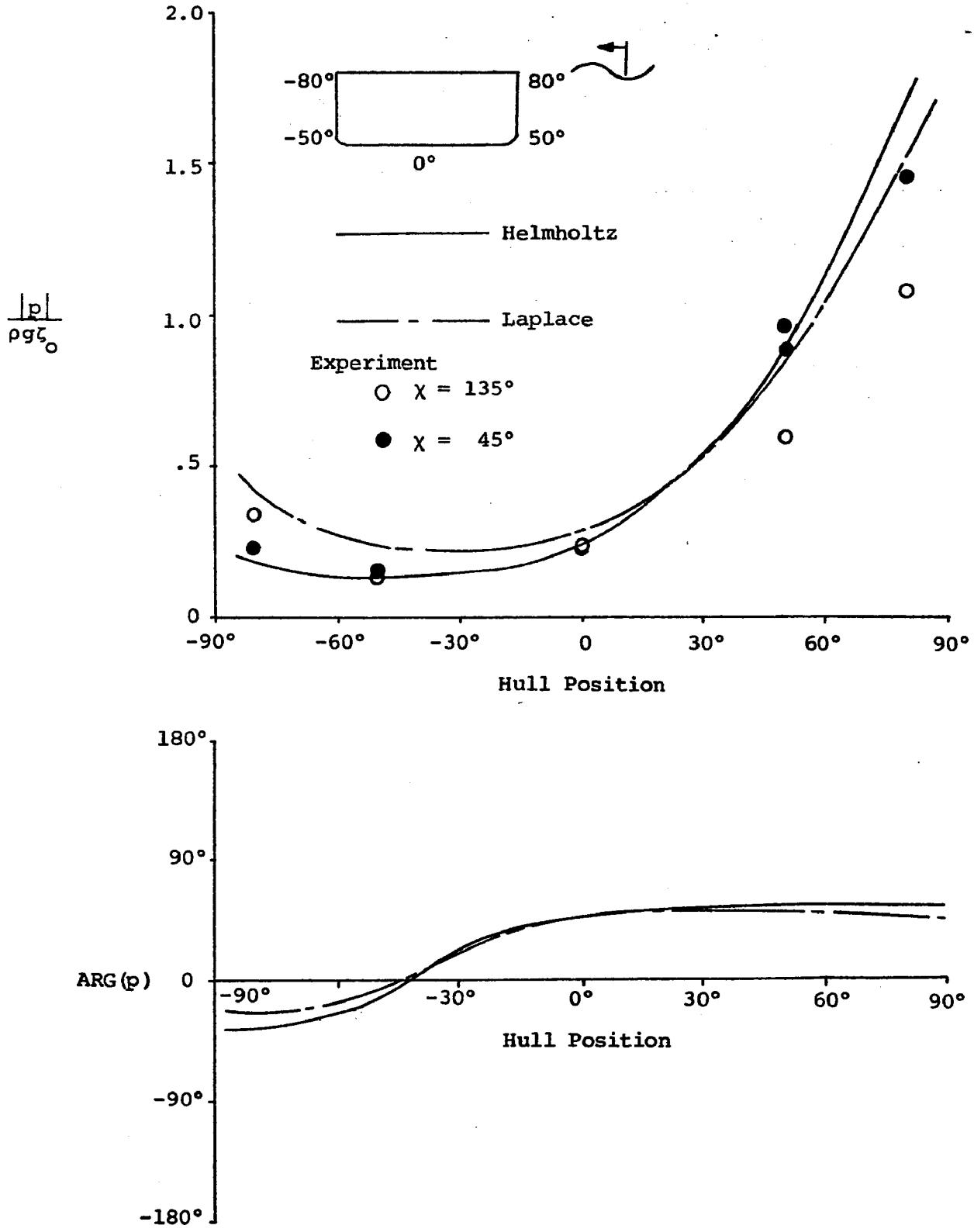

Figure 8: Girthwise Pressure Distribution for a Midship Section of an Ore Carrier in Oblique Seas. ($L/\lambda = 1.44$, $\chi = 45°$)

are nondimensionalized with respect to $\rho g \zeta_o B/2$ where B is the beam of the ship.

Nakamura, et. al. (1973) did not give phase angles, either theoretical or experimental in their work. The curves for the phase angles were calculated by the computer program that generated the pressure potential for the Helmholtz equation. This was accomplished by maintaining the same boundary condition but replacing the oblique seas Green's function by one that is correct for beam seas. The pressure amplitudes found this way agreed with those calculated by Nakamura, et. al. (1973).

Table 5

Sectional Exciting Force for a Midship Section of Ore Carrier (χ=45°)

	$L/\lambda = 1.96$				$L/\lambda = 1.44$			
	Helmholtz		Laplace		Helmholtz		Laplace	
	Mag.	Phase	Mag.	Phase	Mag.	Phase	Mag.	Phase
$\frac{F_2(x)}{\rho g \zeta_o B/2}$	1.11	120°	.95	115°	1.14	118°	.97	117°
$\frac{F_3(x)}{\rho g \zeta_o B/2}$	.49	-55°	.47	-57°	.71	-48°	.73	-41°

The relation used for the forward speed pressure is an abbreviated form of (82). It is the following:

$$\frac{-P_D}{\rho} \sim e^{i(\omega t - \nu x)} \left[i\omega_o (\phi_o + \psi_1) + U\psi_{1_x} \right]$$

The pressure distribution was found for the same hull form as before. Instead of the midship section, a forward station located 15% of the ship's length from the bow was used. The experimental values were taken from SSRJ (1974) and represent the pressure distribution for two wave headings and three Froude numbers.

We will digress for a moment and describe the manner in which ψ_{1_x} was found. If we are given ψ_{1_x} and the change of ψ_1 in the direction of the two dimensional normal to the hull, then ψ_1 can be found. Consider the following:

$$\Delta\psi_1(x_o,y_o,z_o) \equiv \psi_1(x_o+\Delta x, y_o+\Delta y, z_o+\Delta z) - \psi_1(x_o,y_o,z_o)$$

$$\simeq \psi_{1_x}\Delta x + \psi_{1_y}\Delta y + \psi_{1_y}\Delta z$$

under the constraint $\left[\Delta y\,\underline{j} + \Delta z\,\underline{k}\right] / \sqrt{(\Delta y)^2 + (\Delta z)^2} = \underline{N}$

where N is the normal in the transverse plane. Then

$$\frac{\psi_{1_y}\Delta y + \psi_{1_z}\Delta z}{\sqrt{(\Delta y)^2 + (\Delta z)^2}} = \underline{N} \cdot \nabla\psi_1 = \frac{\partial\psi_1}{\partial N} = -\frac{\partial\phi_o}{\partial N}$$

from equation (57) and it follows that

$$\psi_{1_x} \simeq \left[\Delta\psi_1 + \frac{\partial\phi_o}{\partial N}\sqrt{(\Delta y)^2 + (\Delta z)^2}\right] / \Delta x \qquad \text{on} \quad y = h(x,z).$$

The results are given in Figure 9 and Figure 10 for stern seas ($\chi = 135°$) and bow seas ($\chi = 45°$) respectively. The theoretical values for zero Froude number are the same in both plots. The addition of $U\psi_{1_x}$ for a Froude number of 0.2 ($F_n = 0.2$) did little more than thicken the lines for either heading.

We can see that for a midship section the Helmholtz equation is in rather good agreement with experiments (see Figures 7 and 8) for zero speed. For a forward section the Helmholtz equation still seems to be good for stern seas

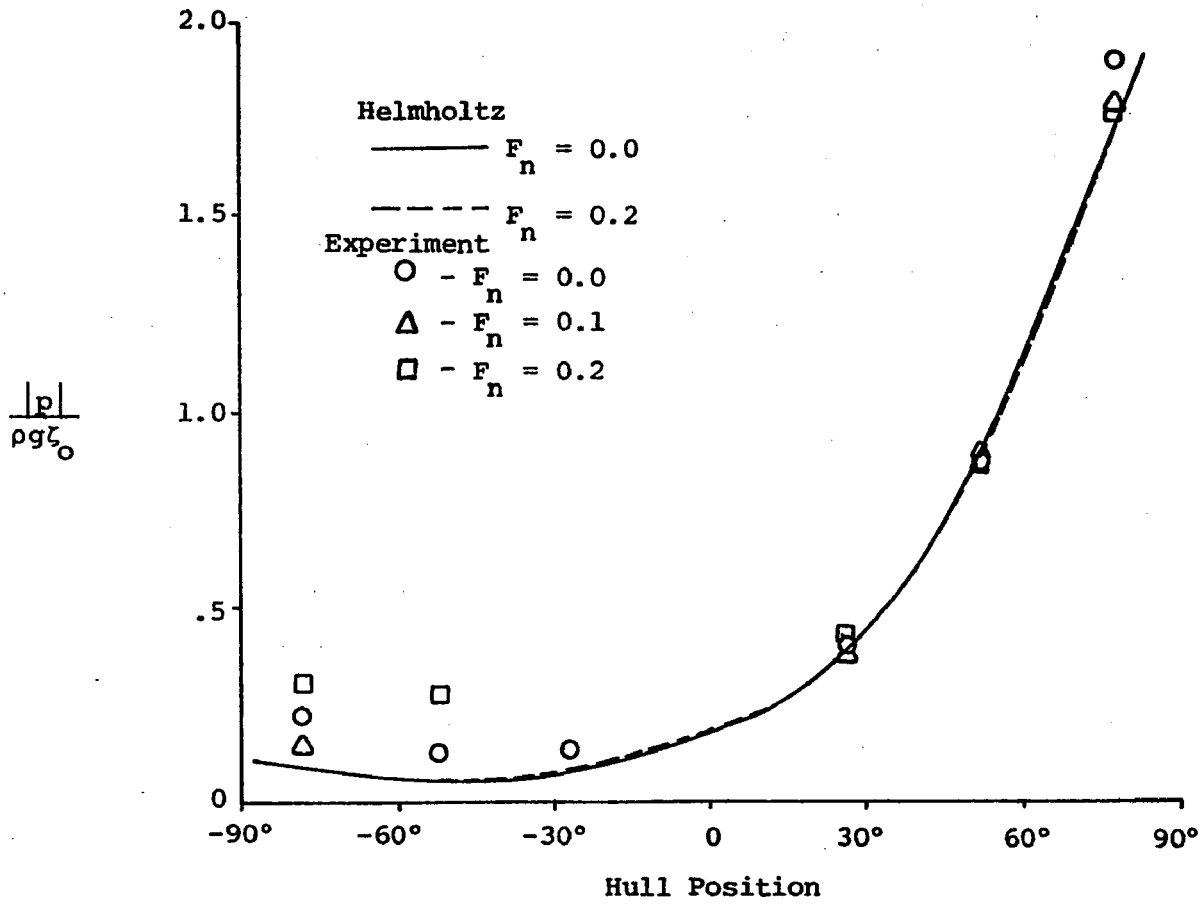

Figure 9: Girthwise Pressure Distribution for a Forward Station of an Ore Carrier in Oblique Seas. ($L/\lambda = 2.0$, $\chi = 135°$)

($\chi = 135°$) on both sides of the hull while the theory only agrees with experiments on the windward side for bow seas ($\chi = 45°$). The forward speed effect is more pronounced on the leeward side for bow seas than for stern seas. In fact, for stern seas, the forward speed effects do not differ enough from the zero speed effects to be considered as showing definite trends. In other words, the forward speed data occur within the range of experimental scatter of the

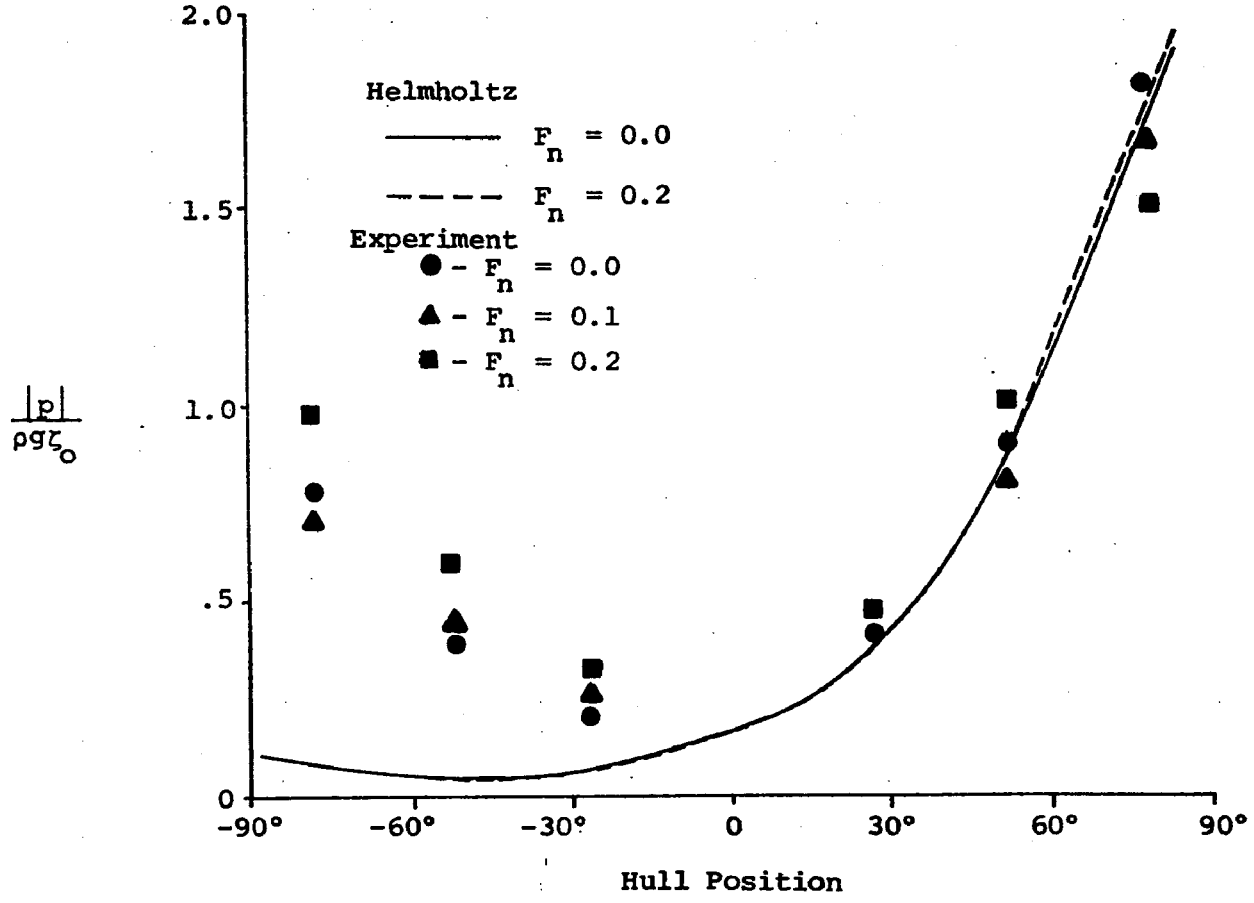

Figure 10: Girthwise Pressure Distribution for a Forward Station of an Ore Carrier in Oblique Seas. ($L/\lambda = 2.0$, $\chi = 45°$)

zero speed data. This does not appear to be the case for the bow seas.

We can speculate as to the reasons for the difference of the pressures in bow seas and stern seas for sections near the end of the hull. If we consider acoustical waves impinging on a symmetrical form as shown in Figure 11, then for short waves, there will be a shadow region on the leeward side of the body.

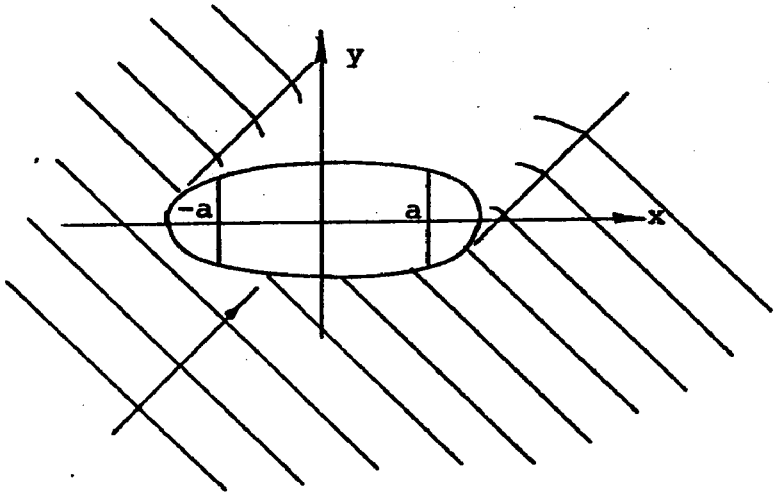

Figure 11: The Shadow Region of an Obstacle in Incident Waves.

For two values of x ($x = \pm a$), we expect that the potential will be nearly equivalent on the windward side. However, as a result of the close proximity of the leeward side of the section at x = -a to the edge of the shadow region, there will be a definite contribution to the potential from the incident waves while the section of x = a should see relatively little effect. We suggest that it is this sort of phenomena that causes the variations in bow and stern seas as shown in Figures 9 and 10. This is only speculation and a possible topic for further research.

Sectional Force Distribution

If the motion of a ship without forward speed in a seaway is to be known then the hull response characteristics, the added mass and damping, in addition to the exciting force must be found. Khaskind (1957) and later Newman (1965) showed how the forced oscillation potential used in the calculation of added mass and damping coefficients could also be used to find the exciting force due to the diffraction problem. These relations are referred to in the

literature as "Khaskind relations." The use of these relations meant that the diffraction problem did not have to be solved.

To illustrate the form of these Khaskind relations, consider the total vertical exciting force Z. The method is to define a new potential function Φ_3, such that $\partial\Phi_3/\partial n = n_3$ on the hull and then use Green's theorem on the integral of the diffraction pressure so that one can replace Φ_D with Φ_3, where Φ_D is the diffraction potential. Then Φ_3 is assumed to satisfy the two dimensional Laplace equation in the immediate vicinity of the hull which gives rise to the usual application of strip theory. This results in an expression for Z in the following form:

$$Z = -i\rho\omega \int_H ds\left(n_3\Phi_I - \Phi_3 \frac{\partial}{\partial n}\Phi_I\right) \quad , \tag{92}$$

where H is the ship's hull. The first term is the usual Froude-Krylov force, i.e., the force due to the undisturbed wave. The second term in the integrand in (92) is then approximated in the usual strip theory sense:

$$\int_H ds\ \Phi_3 \frac{\partial}{\partial n}\Phi_I \simeq \int_L dx \int_{C_H(x)} dl\ \Phi_3 \frac{\partial}{\partial N}\Phi_I \tag{93}$$

where N is the two dimensional normal in the transverse plane, L is the length of the ship and $C_H(x)$ is a given section in the y-z plane. Φ_3 is now assumed to satisfy the Laplace equation in two dimensions.

Newman (1970) and Ogilvie (1974) point out that the second integral in (93) cannot, in general, be identified with the sectional force on the hull. Since Green's theorem was used, any association with the diffraction pressure has been lost. They formulate the problem that can be associated with the sectional force distribution. It has the same form as

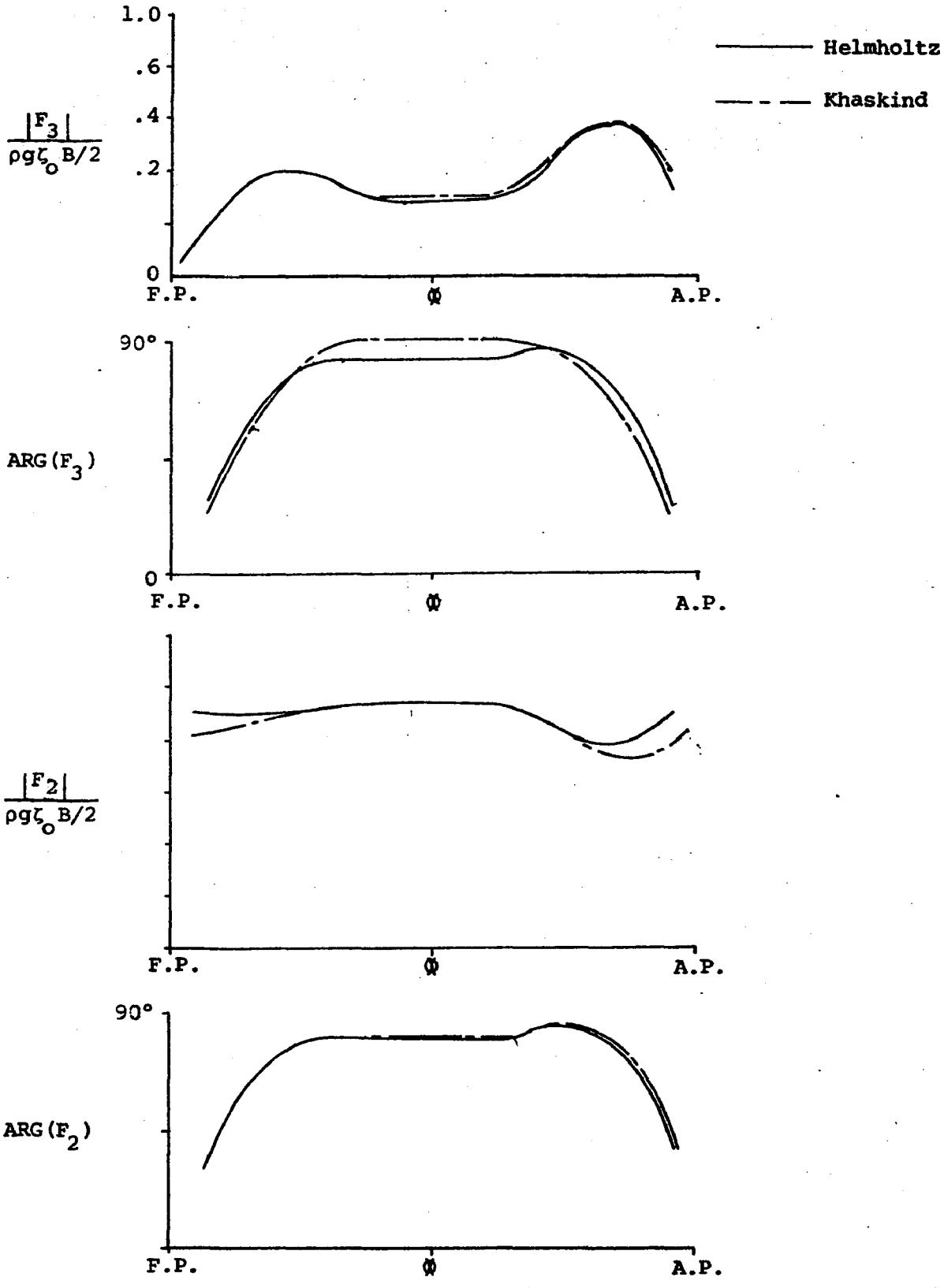

Figure 12: Sectional Force Distribution for a Series 60, C_B = .70 Hull Form (L/λ = 3.33, χ = 60°)

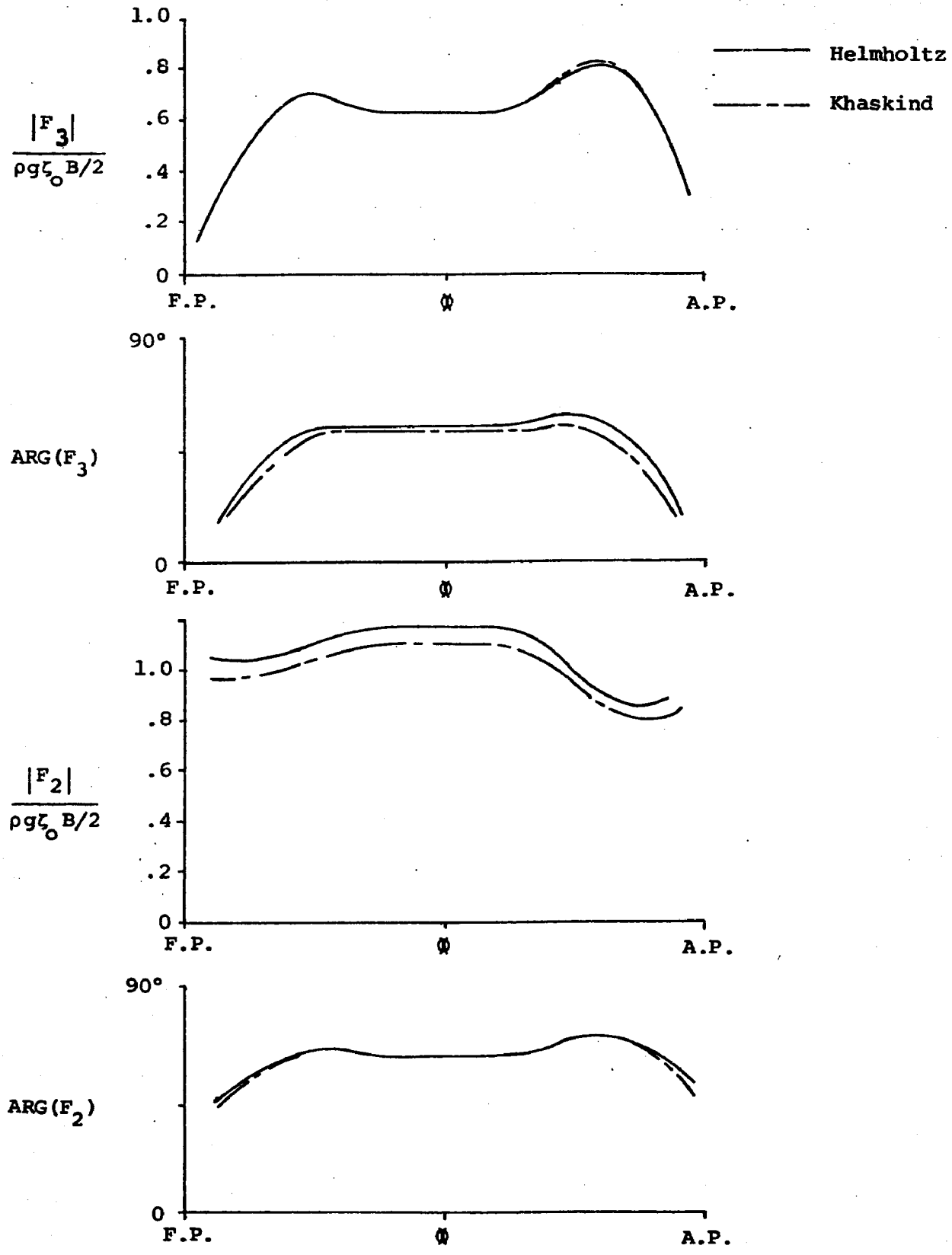

Figure 13: Sectional Force Distribution for a Series 60, C_B = .70 Hull Form (L/λ = 2.0, χ = 60°).

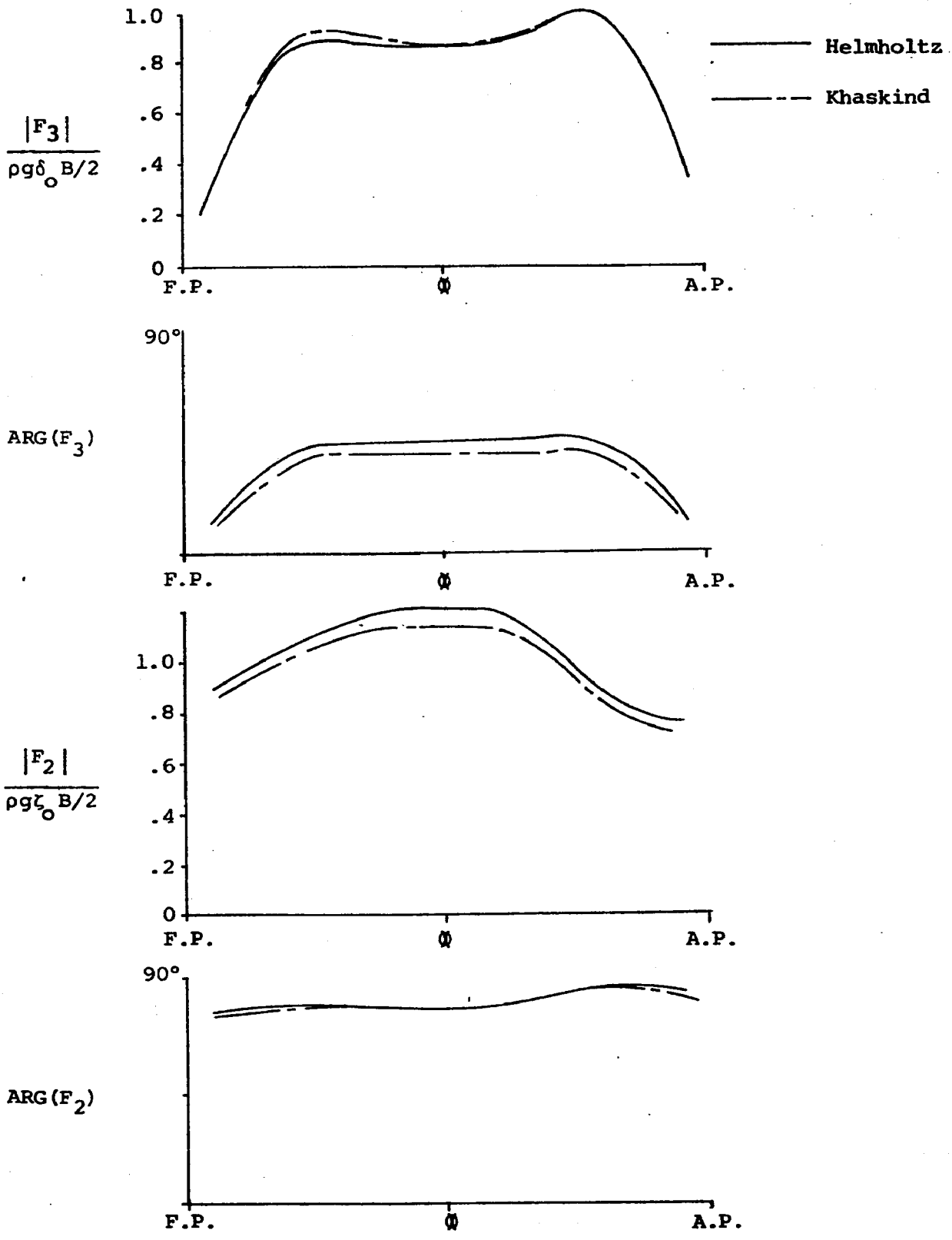

Figure 14: Sectional Force Distribution for a Series 60, C_B = .70 Hull Form (L/λ = 1.43, χ = 60°).

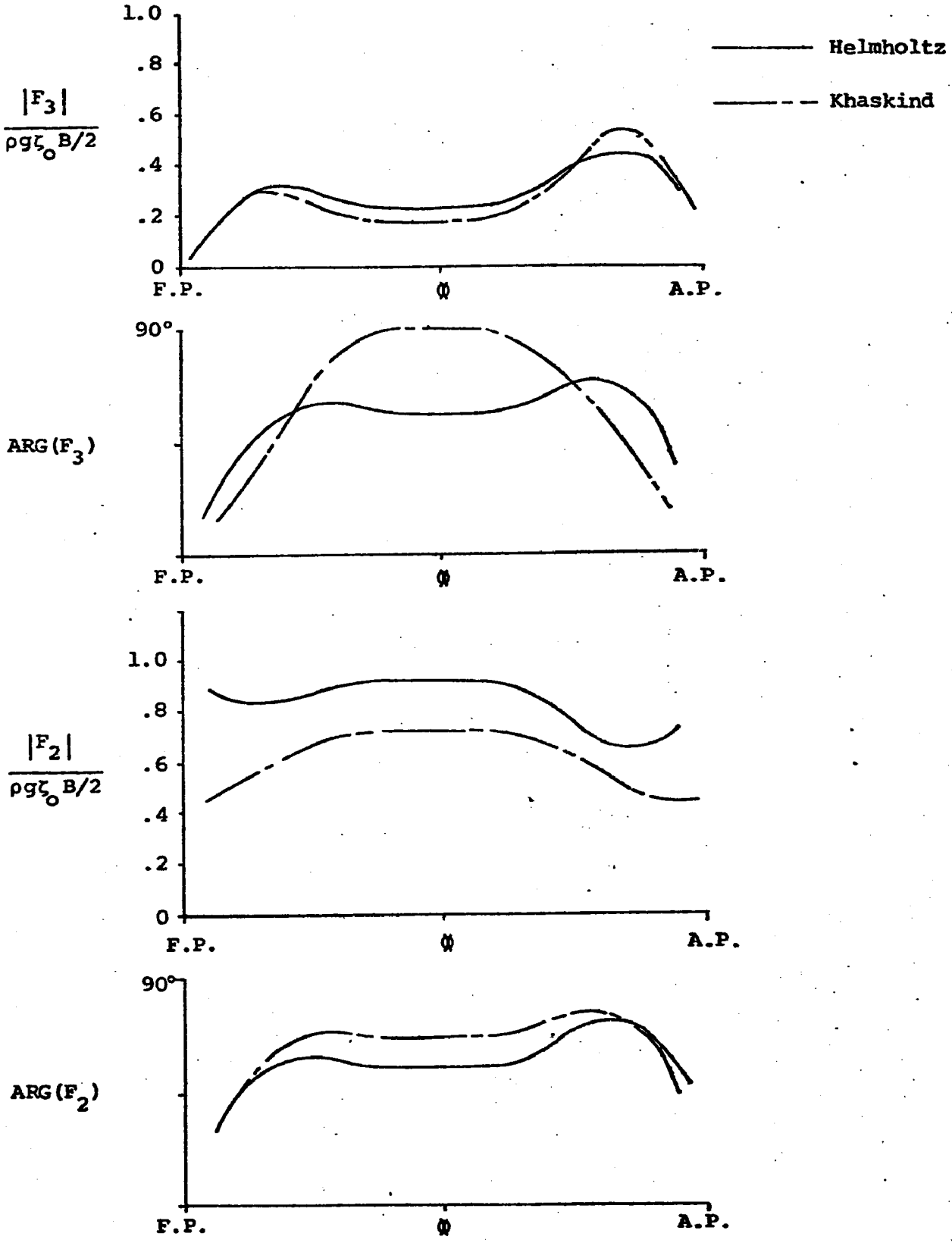

Figure 15: Sectional Force Distribution for a Series 60, C_B = .70 Hull Form (L/λ = 3.33, χ = 30°).

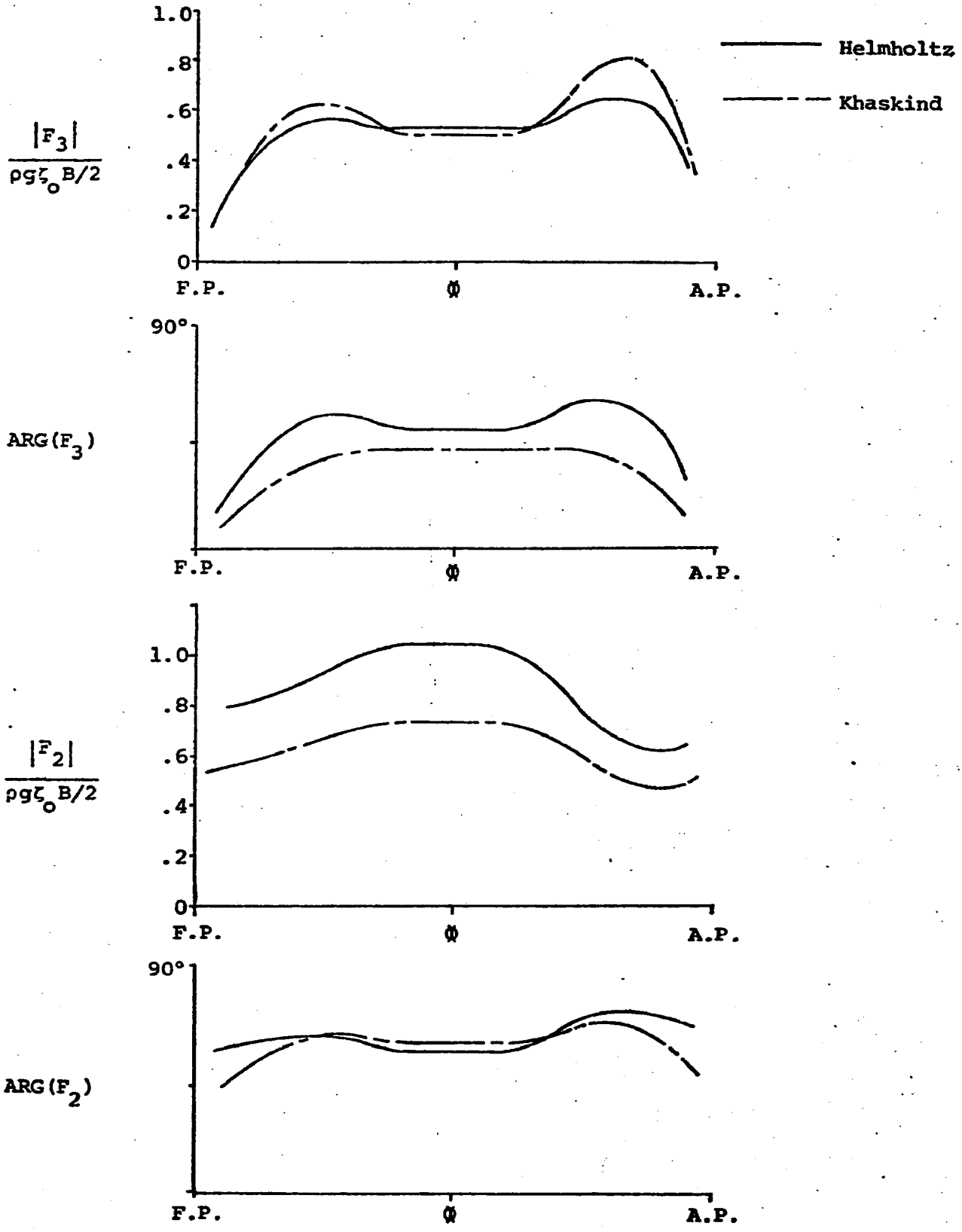

Figure 16: Sectional Force Distribution for a Series 60, C_B = .70 Hull Form (L/λ = 2.0, χ = 30°).

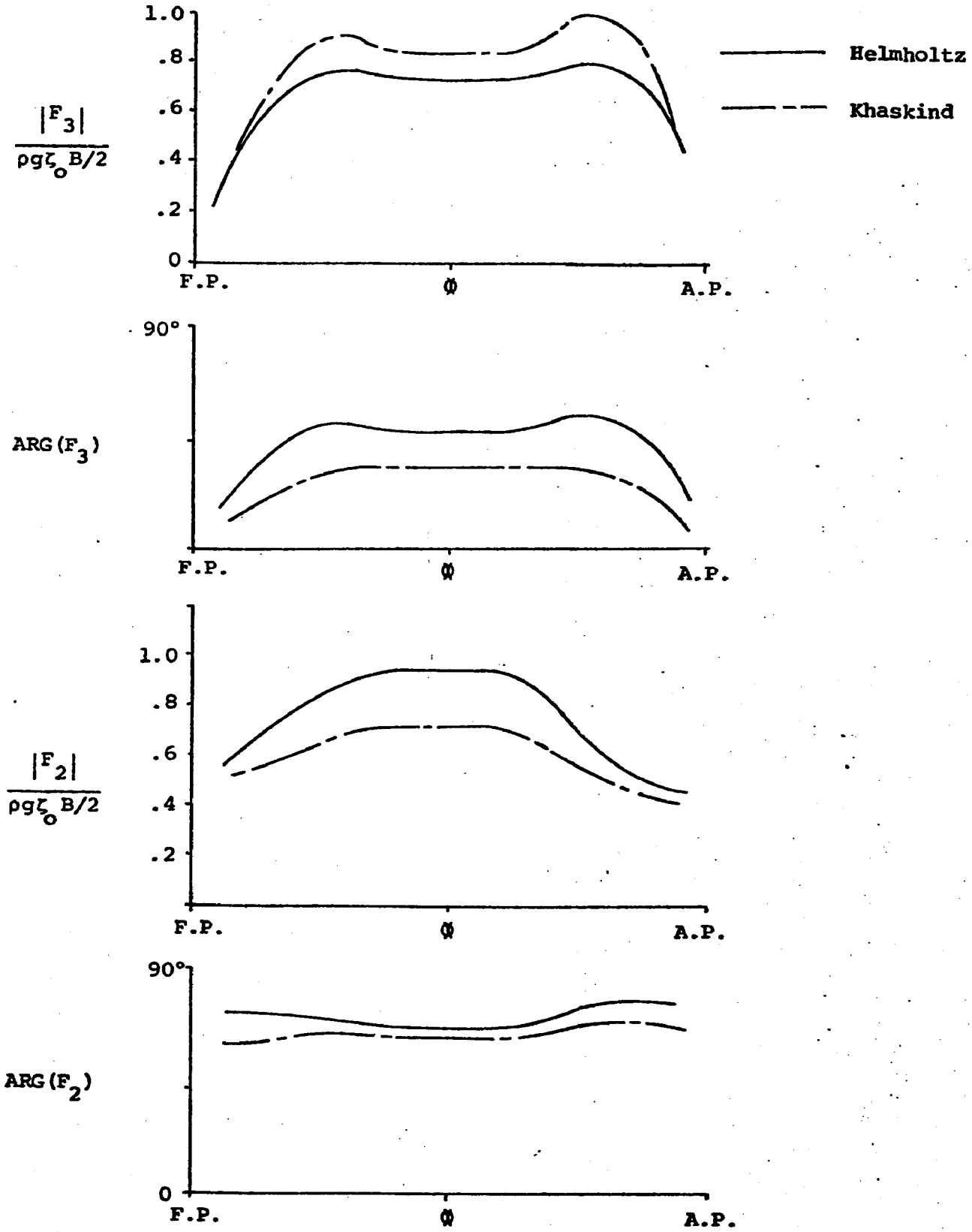

Figure 17: Sectional Force Distribution for a Series 60, C_B = .70 Hull Form (L/λ = 1.43, χ = 30°).

the second integral in (93), only now, the Φ_3 forced oscillation potential satisfies the Helmholtz equation in the cross plane instead of the Laplace equation. For example, see the description of ϕ_i following equation (84).

As beam seas are approached, the Helmholtz operator $(\nabla^2 - \nu^2)$ becomes the Laplace operator (∇^2) since $\nu \to 0$. Consequently, the second integral in (93) approaches the value of the sectional force as the seas go around to the beam.

In Figures 12-17, the magnitude and phase of both the vertical and horizontal sectional exciting force distributions along the length of a Series 60, $C_B = .70$ parent hull form are shown. The phase does not include the $e^{-i\nu x}$ dependence found in the x - direction. The forces, which include both the Froude-Krylov force plus the diffraction force, are non-dimensionalized by $\rho g \zeta_o B/2$ as in Table 5. There are two heading angles, $\chi = 60°$ and $\chi = 30°$, and three wave lengths $L/\lambda = 3.33, 2.0, 1.43$. The curves are not continued to the ends of the body because as with any slender body theory in which only two dimensional problems are solved, the results in this region are not valid.

The solid line shows the sectional force as found by integrating equation (82) with U equal to zero. This includes the solution of the Helmholtz equation, which is a mathematical statement of the problem. The dashed line contains the second integral in (93) which when integrated over the hull equals the total diffraction force. However, it is not to be considered as the sectional force unless the seas are from the beam. In most present day strip theory computations, though, the dashed curve is the sectional exciting force commonly used. Both curves include the same Froude-Krylov force.

For seas with a heading angle of $\chi = 60°$, the two curves are in close agreement. For seas with a heading angle of $\chi = 30°$, there are substantial differences. We can conclude that for the sectional exciting force, either the Laplace representation or the Helmholtz representation will give

reasonable results for seas from the beam or nearly from the beam. For oblique seas, i.e., $\chi = 45°$, there are major differences between the two results. And finally, as the seas become either head or following, we have seen that the Green's function, and hence our theory, becomes unbounded and one must use an analysis similar to Faltinsen's (1971). As we have tried to indicate in Chapter III, this Faltinsen effect should be restricted to a small region around head seas.

Total Force

Newman (1970 stated that the total force found by integrating the sectional force as derived from the Helmholtz equation should equal the force found from a Khaskind relation (i.e., equation (92)) in an asymptotic sense. This means as the small wave length-beam parameter ε goes to zero, the two forces are equivalent.

In an effort to see how small ε had to be in practical situations, the force distribution was found for the Series 60, $C_B = .70$ parent hull form (see Figures 12-17) and integrated over the hull. The wave lengths ranged from $L/\lambda = 3.33$, which can be considered as short and thereby encompassed by the theory, to $L/\lambda = 1.0$, which is relatively long and hence not really within the limits of a "small ε". The results are plotted in Figures 18 and 19 for heading angles of $\chi = 120°$ and $\chi = 30°$, respectively. Following Vughts (1970), the vertical force amplitude [Z], was nondimensionalized by $\rho g \zeta_o A_{WL}$, where A_{WL} is the area of the waterplane. The horizontal exciting force amplitude $|Y|$, was nondimensionalized by $\rho g \zeta_o \nabla \kappa$ where ∇ is the volume displacement of the ship. The results given by the dashed lines are from the Khaskind relations like equation (92) for the vertical mode and an equivalent one for the horizontal mode. These curves, along with the experiments,

were given by Vuguts (1970). The solid line represents the total exciting force found by integrating the zero speed part of the wave induced pressure given in equation (82).

The differences in the amplitudes of the total exciting forces as found by the two methods are slight. This may have been expected for $\chi = 120°$, since we have already seen from Figures 12-17 that there is little difference between the sectional force predicted by the Khaskind relations and that predicted by the mathematically correct Helmholtz equation for seas off the beam. This should be true for even long waves. However, the results for $\chi = 30°$ are more surprising. The two methods agree to the accuracy of the plot for both short and relatively long waves. Thus, the integration of the wave induced pressure as given by the lowest order of equation (82) over the hull yields a total exciting force that is comparable to that predicted by the use of the Khaskind relations. The phase angles plotted in Figure 20 for a heading angle of $\chi = 30°$ show similar agreement.

As the wave length gets large, the ν^2 term in the Helmholtz equation becomes of a higher order than the ∇^2 operator and consequently the governing equation is approximated by Laplace's equation to the first order. If the wave length is long relative to the beam, then there will be little difference between the results given by the Helmholtz equation and the Khashkind relations to the first order. This may explain the agreement between the two methods for the longer wave lengths in Figure 19.

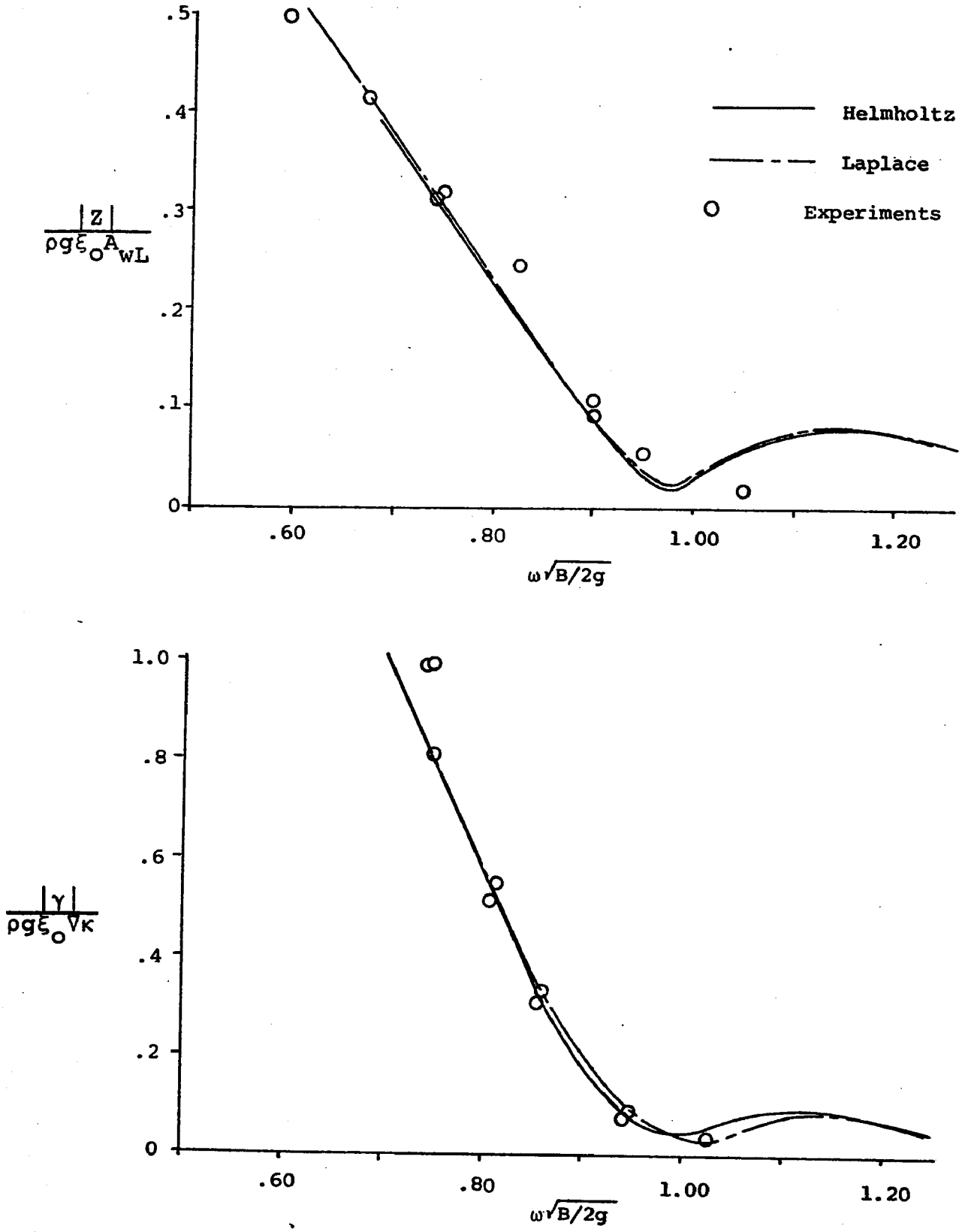

Figure 18: Total Force for a Series 60, C_B = .70 Hull Form in Oblique Waves (χ = 120°).

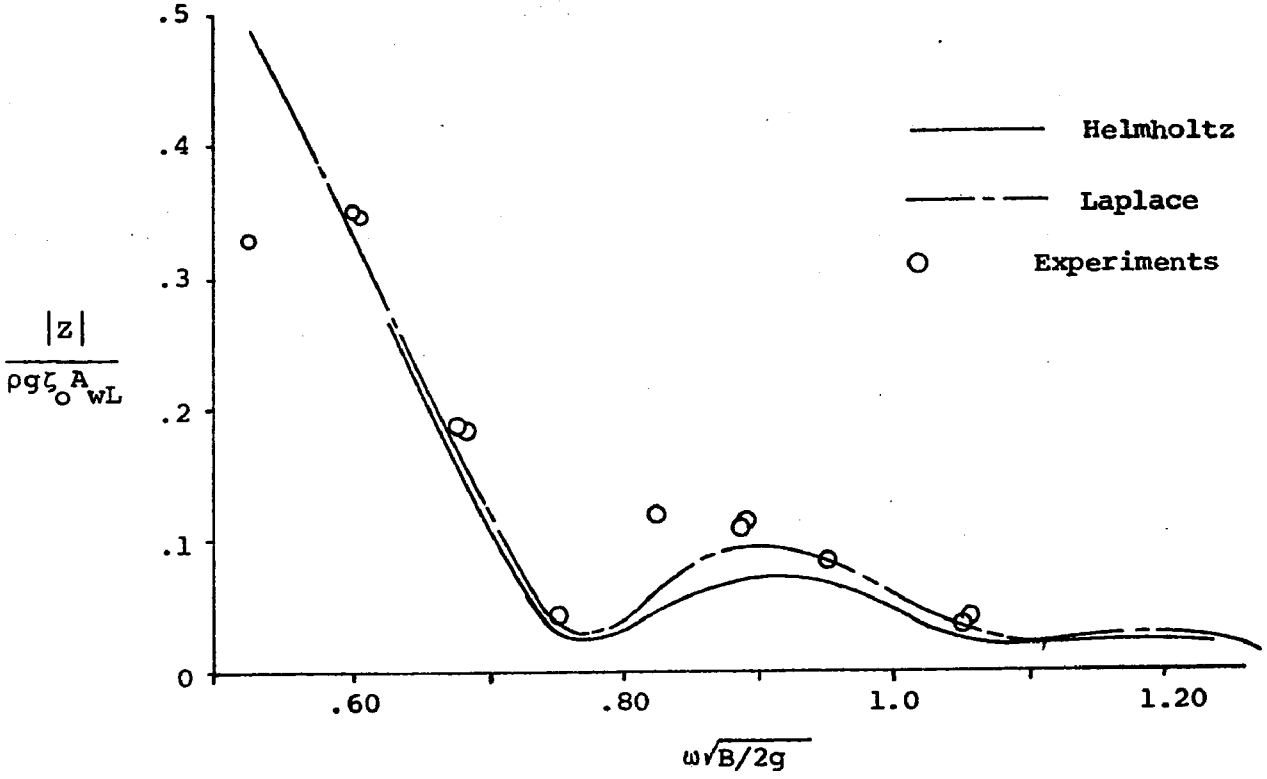

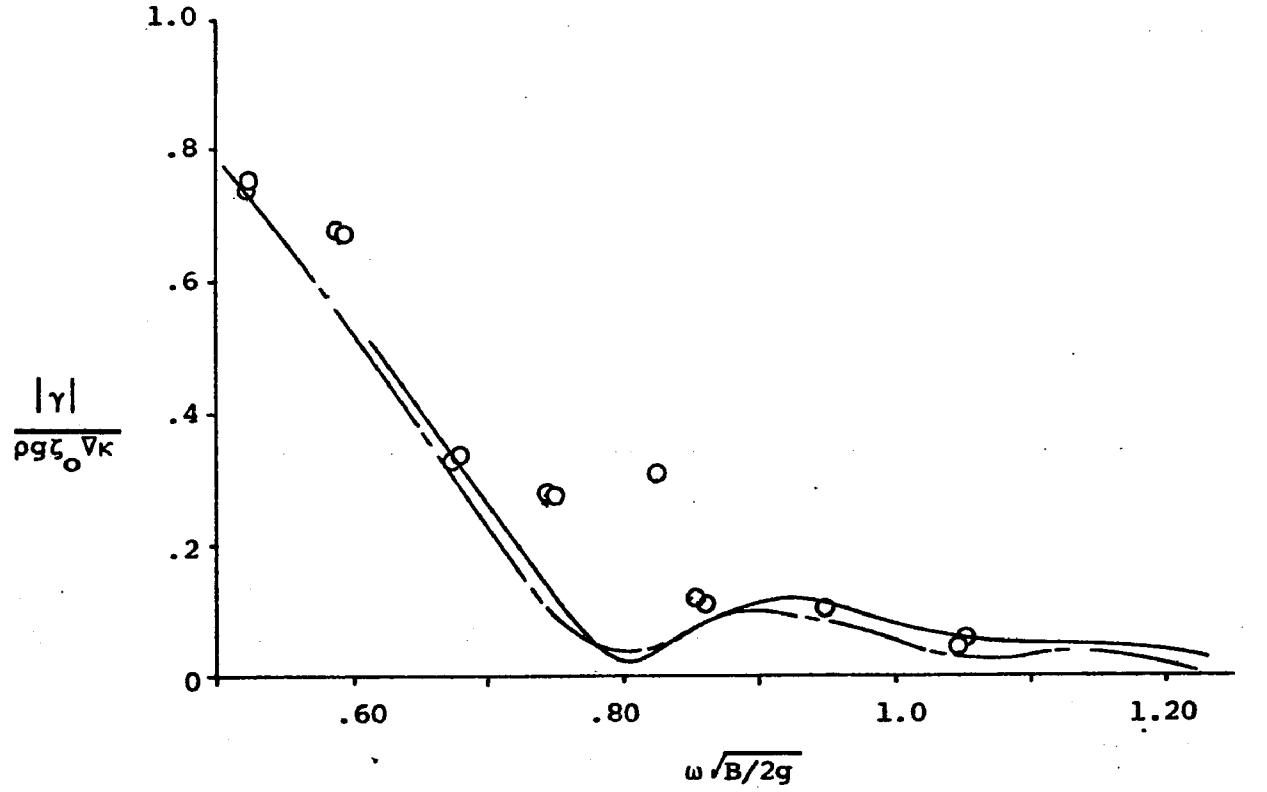

Figure 19: Total Force for a Series 60, C_B = .70 Hull Form in Oblique Waves (χ = 30°).

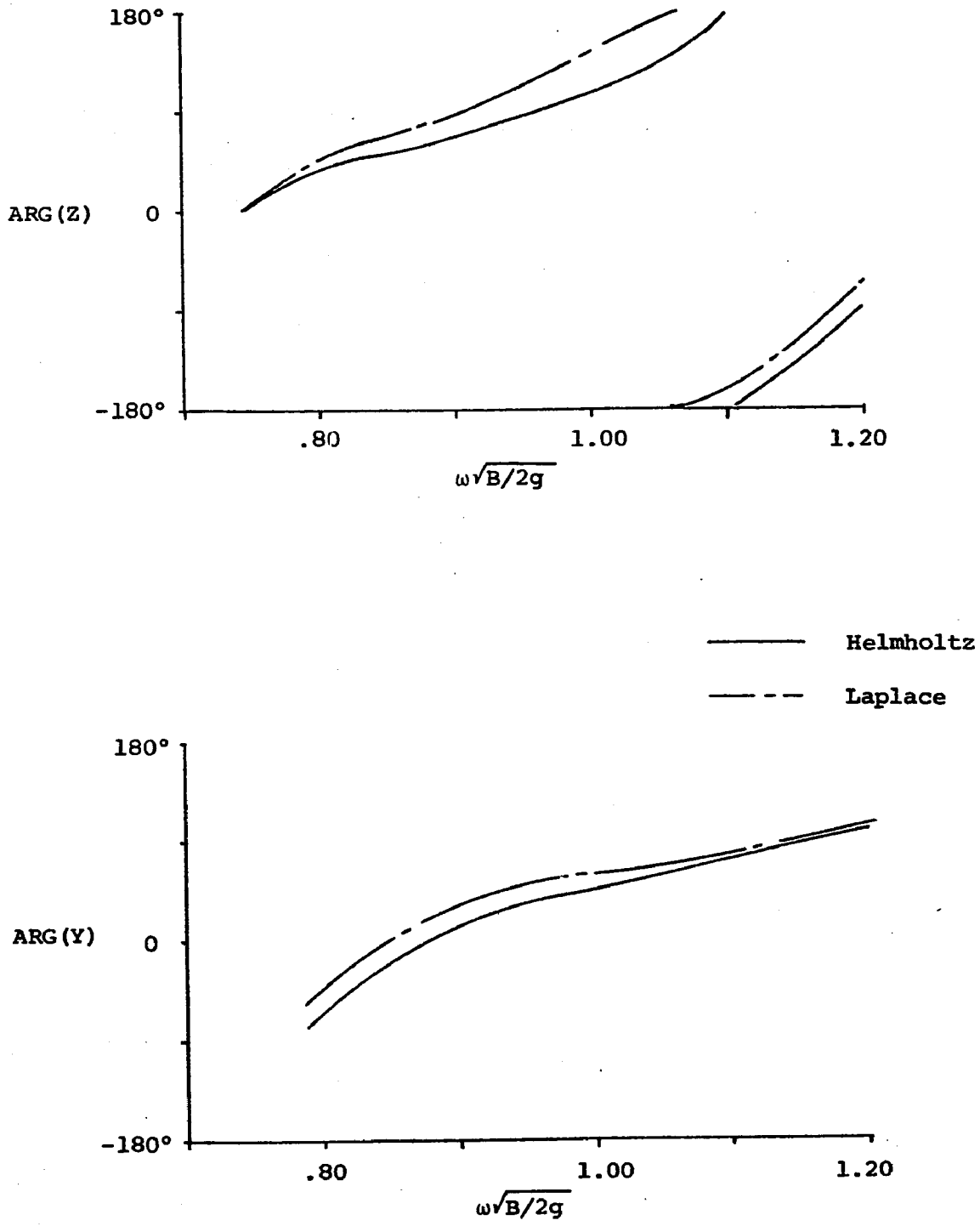

Figure 20: Phase Angles of Exciting Forces for a Series 60, C_B = .70 Hull Form in Oblique Waves (χ = 30°).

Chapter VII

SUMMARY AND CONCLUSIONS

In this work, we have found a potential that approximates the behavior of a diffracted wave of short wave length on a slender body at rest and moving forward at moderate speeds. The incident waves were considered to be from an oblique heading. The potential is expanded in an asymptotic series where one term is found for zero speed and two terms are found for forward speed. The two terms in the forward speed expansion include ψ_1, which is just the lowest order zero speed approximation and ψ_2, which includes the velocity effects. The potential ψ_1 satisfies the following:

$$\nabla^2_{2-D}\ \psi_1 - \nu^2 \psi_1 = 0 \qquad \text{in the fluid region;} \qquad (55)$$

$$-\kappa\psi_1 + \psi_{1_z} = 0 \qquad \text{on} \quad z = 0\ ; \qquad (56)$$

and

$$\frac{\partial\psi_1}{\partial N} = -\frac{\partial\phi_o}{\partial N} \qquad \text{on} \quad y = h(x,z)\,. \qquad (57)$$

The solution to the ψ_1 potential can be described as a distribution of surface singularities in the following manner:

$$\psi_1(y,z;x) = \int_{C_H(x)} d\,\ell\,\sigma(\xi,\eta)\,G(y,z;\xi,\eta)\quad . \qquad (33)$$

The second order potential, ψ_2, satisfies:

$$\nabla^2_{2-D}\ \psi_2 - \nu^2\psi_2 = 0 \qquad \text{in the fluid region;} \qquad (58)$$

$$-\omega_o^2 \psi_2 + \psi_{2_z} = -2i\omega_o U \psi_{1_x} - 2i\omega_o U(\phi_{o_y} + \psi_{1_y}) \Phi_{s_y} - i\omega_o U \Phi_{s_{yy}} (\phi_o + \psi_1) \quad \text{on} \quad z = 0 \tag{59}$$

and

$$\frac{\partial \psi_2}{\partial N} = 0 \qquad \text{on} \quad y = h(x,z). \tag{60}$$

The steady motion potential is given by Φ_s and the incident wave by ϕ_o. The solution to the ψ_2 problem is given by (80).

The evaluation of the source strength σ in (33) is found by forming an integral equation and solving for the value of σ at a number of discrete points. For an alternate method of solving (33), see Choo (1975). He assumes that σ is constant over finite line segments similar to the description given of Frank's method in Chapter IV. Once the source strength is known, it can be integrated over the hull to find the potential ψ_1.

The sectional force is given for both zero and forward speeds. We have shown that one does not have to solve the ψ_2 problem in order to determine the sectional force. By defining an auxiliary problem, the forced oscillation potential, we derive an equation in the form of (91) that eliminates the need to know ψ_2.

Included are numerical results for the zero speed pressure and an abbreviated form for the forward speed pressure. The theory shows good correlation with experiments except where end effects dominate. When these pressures are integrated over the hull to give a sectional force or a total force, we have found that for oblique seas, the Helmholtz equation gives different results than the commonly used Khaskind relations for the sectional exciting force, but similar results when the entire exciting force is found.

The theory as stated, is a short wave theory and hence there is no reason to integrate the diffraction pressures to find the total exciting forces. The Khaskind relations

are much better suited for finding them. In addition, as the wave-length gets short, the dynamic pressure over the length of the hull will tend to average out to zero with only the contribution from the ends being felt. Since this theory is a strip theory, it is not valid in that region as can be seen from Figure 10. The value of this theory is that it can predict the longitudinal variation of forces that produce bending moments and shear stresses.

Finally, there should be a comment on the selection of the order of magnitudes. Making the order of the wave length the same as the beam led to a Helmholtz problem in the transverse plane. For zero speed this assumption is the same as found in the head seas problem described by Faltinsen (1971) and the forced oscillation problem described by Ogilvie & Tuck (1969). For forward speed, this work, like Faltinsen (1971), maintains the same wave length assumption and changes the frequency of encounter. However, the Ogilvie-Tuck report kept the same frequency of oscillation, which means the exciting waves are longer. McCreight (1973), in considering the diffraction problem, has shown that the Ogilvie-Tuck ordering will lead to a first order potential that satisfies Laplace's equation and a second order potential that satisfies a Helmholtz equation. We have seen from Figures 7 and 8 that for the model and wave lengths tested, a Helmholtz equation gives better agreement with experiments than Laplace's equation for zero speed. For forward speed, we have also seen from Figure 9 that when end effects do not dominate, a Helmholtz equation still gives reasonable results. This would seem to indicate that if the diffraction pressures are desired, an assumption on the wave length that leads to a Helmholtz equation in the lowest order would be more appropriate than one that would lead to Laplace's equation. We note, however, that the stated purpose of the Ogilvie-Tuck report was to see what assumptions were necessary to arrive at a

mathematical justification for strip theory. McCreight (1973) extended the use of their oscillation potential to include a form of the Khaskind relations for the exciting forces. With this goal in mind, there would be no reason to complicate their analysis by insisting that the initial assumptions produce an accurate description of the diffraction pressures in addition to finding the total exciting forces. Hence, it is clear that while our short wave assumption may be necessary to find pressures, the utility of the assumptions made in the Ogilvie-Tuck report, which greatly simplify the calculations for total exciting forces, cannot be denied. We also should emphasize that strip theory has been in use for some time, and the comparison of theoretical values with experimental values (see Vugts (1970)) for ship motions is quite good.

The range of applicability should be included in this discussion on orders of magnitude. The stated assumption is that the wave length is the same magnitude as the beam and both are much shorter than the length of the hull. We have seen that the total exciting forces displayed in Figures 18 and 19 are effectively the same whether found by integrating the pressures given by the Helmholtz equation, or by using the Khaskind relations. This appears to be true for wave lengths much longer than the stated assumption implies. Also, from Figure 8, the pressure distribution for a wave three-quarters the length of the hull compares well with experiment. That the results compare well for wave lengths longer than expected seems to be in line with the conjecture made by Ogilvie (1975). He stated that in the region of transition between short waves and long waves, a short wave assumption may be asymptotically inconsistent but numerically correct. In the diffraction problem, it seems one ought to adopt a short-wave hypothesis except where waves longer than the ship are to be considered.

APPENDIX A

The Green's Function

In this appendix we investigate the behavior of the Green's function $G(y,z;\xi,\eta)$ given in (34a) and (34b). The two forms are necessary since we wish to evaluate G for a range of $\sqrt{(y-\xi)^2 + (z-\eta)^2}$ from near zero to large values and a range of ν/κ (recall $\nu = \kappa \cos\chi$) from near zero (i.e., beam seas) to a value near one (i.e., oblique seas). We will discuss the advantages and disadvantages of each form and then state our procedure for finding G and its normal derivative $\frac{\partial G}{\partial N}$.

Ursell (1962) gave a series expansion of $G(y,z;\xi,\eta)$ for small values of $\nu r = \nu\sqrt{(y-\xi)^2 + (z-\eta)^2}$ as shown in (34a). It will be repeated here for convenience:

$$G(y,z;\xi,\eta) = K_o(\nu r) + K_o(\nu r') - 2\gamma \coth\gamma \left[I_o(\nu r') + 2\sum_{m=1}^{\infty} (-1)^m \cosh m\gamma\, I_m(\nu r')\cos m\theta' \right]$$

$$- 4\coth\gamma \sum_{m=1}^{\infty} (-1)^m \sinh m\gamma \frac{\partial}{\partial m}\left(I_m(\nu r')\cos m\theta'\right)$$

$$- 2\pi i \coth\gamma \left[I_m(\nu r') + 2\sum_{m=1}^{\infty} (-1)^m \cosh m\gamma\, I_m(\nu r')\cos m\theta' \right] \qquad (34a)$$

where $I_m(\nu r)$ is the I Bessel function of order m (see Abramowitz and Stegen (1964)),

$$r' = \sqrt{(y-\xi)^2 + (z+\eta)^2} \ ,$$

$$\cosh\gamma = \kappa/\nu \ ,$$

and θ' is the angle r' makes with the z axis.

The advantages of this form of G is that it can easily be evaluated for small values of r by taking a limited number of terms. There are two prominent disadvantages. First, as $\nu \to 0$ (i.e., beam seas) the K_o Bessel functions have a $2 \log \nu$ singularity and the series requires the determination of terms like $\cosh m\gamma I_m(\nu r)$ where one term is getting very large and the other is getting very small. We want to emphasize that analytically this form of G is correct as beam seas are approached, but numerically it is very difficult to find. The second disadvantage is that for moderate values of νr, the series has a slow rate of convergence. The $I_m(\nu r)$ term grows exponentially and an efficient method increasing the convergence rate of the alternating terms was not found. This form of G was used for only small values of $\sqrt{(y-\xi)^2 + (z-\eta)^2}$ for seas from oblique headings.

The form of G given (34b) as derived by Khaskind (1953) will also be repeated here:

$$G(y,z;\xi,\eta) = K_o(\nu r) + K_o(\nu r') + 2\kappa e^{\kappa z} \int_{\infty}^{z} d\alpha e^{-\kappa\alpha} K_o\left(\nu\sqrt{(y-\xi)^2 + (\alpha+\eta)^2}\right) - 2\pi \frac{i\kappa}{\sqrt{\kappa^2-\nu^2}} e^{\kappa(z+\eta) - i|y-\xi|\sqrt{\kappa^2-\nu^2}} \qquad (34b)$$

The integral term of (34b) can be integrated once by parts to give the following form of G:

$$G(y,z;\xi,\eta) = K_o(\nu r) - K_o(\nu r') + 2\nu \int_{o}^{\infty} d\alpha \frac{e^{-\kappa\alpha}(\alpha+z+\eta) K_1\left(\nu\sqrt{(y-\xi)^2 + (\alpha+z+\eta)^2}\right)}{\sqrt{(y-\xi)^2 + (\alpha+z+\eta)^2}} - \frac{2\pi i\kappa}{\sqrt{\kappa^2-\nu^2}} e^{\kappa(z+\eta) - i|y-\xi|\sqrt{\kappa^2-\nu^2}} \qquad (A1)$$

One advantage of this form of G is that the integrand of the integral term is in a form similar to that needed to find $\frac{\partial G}{\partial N}$ and thus computation time is saved.

For large values of $\sqrt{(y-\xi)^2 + (z-\eta)^2}$ the integral can easily be approximated by a four or eight point Laguerre quadrature (see Abramowitz and Stegen (1964)). For moderate values of $\sqrt{(y-\xi)^2 + (z-\eta)^2}$, the integrand is not suited for the same treatment, since the $K_1(\nu\sqrt{(y-\xi)^2+(\alpha+z+\eta)^2})$ term begins to have a hump in it in the range of integration.

We add and subtract the behavior of K_1 for small values of $R \equiv \sqrt{(y-\xi)^2 + (\alpha+z+\eta)^2}$ and, the integral term becomes:

$$2\nu \int_0^\infty d\alpha e^{-\kappa\alpha} \frac{(\alpha+z+\eta)}{R} K_1(\nu R) = 2\nu \int_0^\infty d\alpha e^{-\kappa\alpha} \frac{(\alpha+z+\eta)}{R} \left[K_1(\nu R) - \frac{1}{\nu R}\right]$$

$$+ 2 \int_0^\infty d\alpha e^{-\kappa\alpha} \frac{(\alpha+z+\eta)}{R^2}$$

Using formula 5.1.44 from Abramowitz and Stegen, we find

$$2 \int_0^\infty d\alpha e^{-\kappa\alpha} \frac{(\alpha+z+\eta)}{R^2} = 2e^{\kappa(z+\eta)} \operatorname{Re}\left[e^{i\kappa|y-\xi|} E_1[\kappa(z+\eta)+i\kappa|y-\xi|]\right]$$

where $E_1(z)$ is the complex exponential integral. Combining all of this with (A1) yields the following form of G:

$$G(y,z;\xi,\eta) = \left[K_o(\nu r) - K_o(\nu r')\right] + 2\nu \int_o^\infty d\alpha e^{-\kappa\alpha} \frac{(\alpha+z+\eta)}{R}\left[K_1(\nu R) - \frac{1}{\nu R}\right]$$

$$+ \quad 2\, e^{\kappa(z+\eta)} \mathrm{Re}\left[e^{i\kappa|y-\xi|} E_1\left[\kappa(z+\eta)+i\kappa|y-\xi|\right]\right]$$

$$- 2\pi \frac{i\kappa}{\sqrt{\kappa^2-\nu^2}} e^{\kappa(z+\eta)-i|y-\xi|\sqrt{\kappa^2-\nu^2}} \quad . \qquad \text{(A2)}$$

Note that as $\nu \to 0$ (beam seas), the $K_o(\nu r) - K_o(\nu r')$ term goes to $-\log r + \log r'$ and the integral term goes to zero. G for beam seas is then

$$G(y,z;\xi,\eta) \to \quad (-\log r + \log r')$$

$$+ \quad 2\, e^{\kappa(z+\eta)} \mathrm{Re}\left[e^{i\kappa|y-\xi|} E_1\left[\kappa(z+\eta)+i\kappa|y-\xi|\right]\right]$$

$$- 2\pi i e^{\kappa(z+\eta)-i\kappa|y-\xi|} \qquad \text{as} \quad \nu \to 0 \quad .$$

This form represents a source oscillating with an $e^{i\omega t}$ time dependence. When multiplied by (-1) and corrected for an $e^{-i\omega t}$ time dependence, the above form of G is the same as used by Frank (1967) to solve arbitrary cylinder problems governed by Laplace's equation. Thus, equation (A2) can be used for all values of $\sqrt{(y-\xi)^2+(z-\eta)^2}$ as beam seas are approached with the only restriction being that ν can never equal zero exactly. Using this form of G, we were able to verify our computing scheme by checking its results against those published by Frank (1967) and Porter (1960).

In summary, then, for small values of r for seas from oblique headings, (34a) was used. For large values of r for seas from oblique headings (A1) was used. And finally, for

moderate values of r for oblique seas and all values of r for near beam seas, (A2) was used. The actual mechanics of the computer program were designed in such a manner as to minimize the computing time and the details will not be presented here.

We have already shown in Chapter IV that $\frac{\partial G}{\partial N}$ is continuous on the hull. This is also true as the free surface is approached by the field point if the ship is wall sided at its water line. Requiring the ship's hull to be orthogonal to the free surface at the point of intersection was suggested by John (1950) in his classic paper on the motions of floating bodies. It does not seem unreasonable to make the same restriction here.

APPENDIX B

The Applied-Pressure Problem

In order to match the near-field behavior with the far-field behavior of the forward speed potential, we need information on the following problem:

Given a two-dimensional pressure field applied on the free surface:

$$P(y,t) = p(y)e^{i\omega t}$$

where the governing equation for the velocity potential is a Helmholtz one, find the potential.

There is a strong similarity between this problem and the applied-pressure problem solved in Ogilvie & Tuck (1969). However, they had a potential that satisfied Laplace's equation and therefore could use complex analysis to solve for it. Since our two dimensional potential is not harmonic, we must select another method. In particular, we will use the method of Fourier transforms.

The undisturbed free surface is the y-axis and z is positive upwards. Since this problem is related to the near field potential, it must be valid for small $\sqrt{y^2+z^2}$. We will actually investigate three problems here. The first one will be a symmetric pressure distribution extending to infinity. The second will be an anti-symmetric pressure distribution extending to infinity and the third will be a local pressure distribution. The solution to the third type of problem (a local pressure distribution) for two dimensional flows in a domain governed by Laplace's equation can be found in Wehausen and Laitone (1960).

Consider the following problem:

$$\nabla^2_{2-D}\,\phi - \nu^2\phi = 0 \qquad \text{in the fluid region;} \qquad \text{(B1)}$$

and $\quad -\kappa\phi + \phi_z = p(y) \quad$ on $z=0.$ (B2)

The $e^{i\omega t}$ time dependence has been factored out and the usual dispersion relation is $\omega^2 = \kappa g$. Also, the relation between κ and ν is as before: $\nu = \kappa \cos\chi$ where χ is the heading angle. If $p(y)$ equaled zero (the homogenous free surface boundary condition) then the free wave potential, designated $\phi_{f.w.}$, is

$$\phi_{f.w.} \propto e^{\kappa z - iy\sqrt{\kappa^2-\nu^2}}$$

This is an indication that when $p(y) \propto e^{-i|y|\sqrt{\kappa^2-\nu^2}}$, we will be forcing the system at its resonant frequency. As a way around this difficulty, we will use a device suggested by Ogilvie & Tuck (1969). That is, we will define a preliminary problem of the following form:

$$p(y) = p_o e^{-\mu|y| - i|y|\sqrt{\gamma^2-\nu^2}} \tag{B3}$$

where μ is a small positive constant and $\gamma \neq \kappa$. After this problem is solved, we will let $\mu \to 0$ and $\gamma \to \kappa$. μ will have the same effect as a Rayleigh viscosity does in the usual water wave problems in that it insures outgoing waves.

A pressure of the form (B3) represents the first type of problem that we will consider. We define the Fourier transform and the inverse Fourier transform respectively as

$$\phi^*(k;z) = \int_{-\infty}^{\infty} dy\, e^{-iky}\, \phi(y,z)$$

and

$$\phi(y,z) = \frac{1}{2\pi} \int_{-\infty}^{\infty} dk\, e^{iky}\, \phi^*(k;z).$$

Then, after requiring that ϕ^* has less than exponential growth in the negative z direction, the solution to the transform of (B1) becomes,

$$\phi^*(k;z) = C(k)e^{\sqrt{\nu^2+\kappa^2}\ z}$$

Here C(k) is a constant determined from the transform of (B2):

$$-\kappa C + \sqrt{\nu^2+k^2}\ C = p^*(k) \qquad \text{on} \quad z = 0.$$

To find $p^*(k)$, the transform of p(y), we note from (B3) that p is an even function and hence use the cosine transform. From (B3) then, it follows:

$$p^*(k) = 2p_o \int_0^\infty dy\ \cos(ky)e^{-\mu y - iy\sqrt{\gamma^2-\nu^2}}$$

$$= -p_o\left[\frac{1}{-\mu+i(k-\sqrt{\gamma^2-\nu^2})} + \frac{1}{-\mu-i(k+\sqrt{\gamma^2-\nu^2})}\right]$$

Hence, C(k) can be written as

$$C(k) = -p_o\ \frac{-2\mu - 2i\sqrt{\gamma^2-\nu^2}}{[i(k-k_1)][-i(k-k_2)][-\kappa+\sqrt{\nu^2-k^2}}$$

where we have defined

$$k_1 = \sqrt{\gamma^2-\nu^2} - i\mu$$

$$k_2 = -\sqrt{\gamma^2-\nu^2} + i\mu$$

Using the definition of the inverse transform, the solution for the symmetric problem, $\phi_s(y,z)$, is

$$\phi_s(y,z) = \frac{p_o}{2\pi}\int_{-\infty}^{\infty} dk\ \frac{e^{iky+z\sqrt{\nu^2+k^2}}\ (2\mu + 2i\sqrt{\gamma^2-\nu^2})}{(k-k_1)(k-k_2)(-\kappa+\sqrt{\nu^2+k^2})} \qquad \text{(B4)}$$

To evaluate (B4) we will use the residue theorem. The integral has branch points at $\pm k_o$ and poles at $k_1,\ldots k_4$, where

$$k_o = i\nu$$

$$k_1 = \sqrt{\gamma^2 - \nu^2} - i\mu$$

$$k_2 = -\sqrt{\gamma^2 - \nu^2} + i\mu$$

$$k_3 = \sqrt{\kappa^2 - \nu^2}$$

$$k_4 = -\sqrt{\kappa^2 - \nu^2}$$

The branch cuts are taken on the imaginary axis.

Also, note that as $\mu \to 0$ and $\gamma \to \kappa$, $k_1 \to k_3$ and $k_2 \to k_4$.

If we restrict our attention to $y>0$, then we can apply the residue theorem to the curve shown in Figure B1.

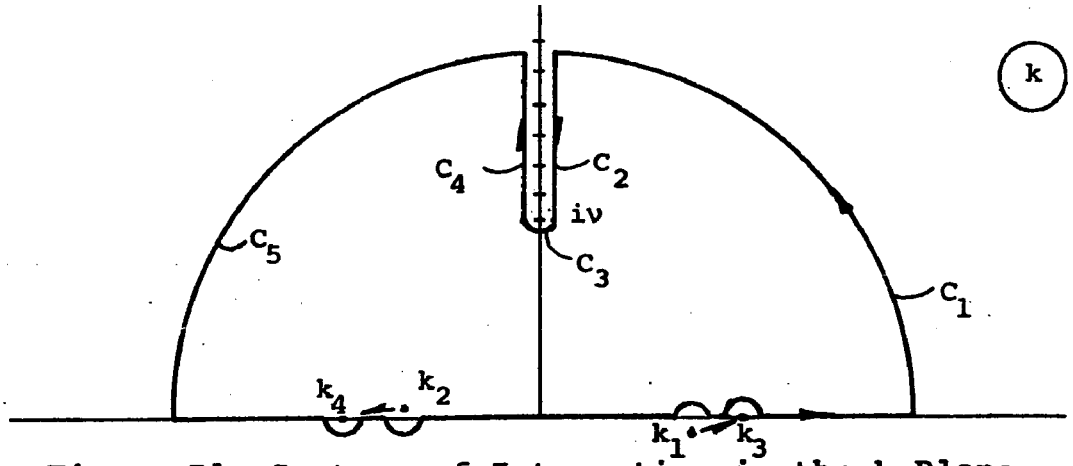

Figure B1: Contour of Integration in the k-Plane

We can now set $\mu=0$, since its primary purpose was to show us the direction in which to indent the contour on the real axis. The residue theorem then states

$$\int_{-\infty}^{\infty} + \int_{C_1} + \int_{C_2} + \int_{C_3} + \int_{C_4} + \int_{C_5} dk \frac{e^{iky+z\sqrt{\nu^2+k^2}}(2i\sqrt{\gamma^2-\nu^2})}{(k-k_1)(k-k_2)(-\kappa+\sqrt{\nu^2+k^2})}$$

$$= 2\pi i \left[\text{Res}(k_2) + \text{Res}(k_4) \right]$$

The arcs C_1, C_3, C_5 contribute nothing. In a method similar to the evaluation of (C1) in Appendix C, we can show that

$$\int_{C_2} dk \frac{e^{iky+z\sqrt{\nu^2+k^2}}(2i\sqrt{\gamma^2-\nu^2})}{(k-k_1)(k-k_2)(-\kappa+\sqrt{\nu^2+k^2})} = \int_{\infty}^{\nu} idk \frac{e^{-yk+iz\sqrt{k^2-\nu^2}}(2i\sqrt{\gamma^2-\nu^2})}{(ik-k_1)(ik-k_2)(-\kappa+i\sqrt{k^2-\nu^2})}$$

and

$$\int_{C_4} dk \frac{e^{iky+z\sqrt{\nu^2+\nu^2}}(2i\sqrt{\gamma^2-\nu^2})}{(k-k_1)(k-k_2)(-\kappa+\sqrt{\nu^2+k^2})} = \int_{\nu}^{\infty} idk \frac{e^{-yk-iz\sqrt{k^2-\nu^2}}(2i\sqrt{\gamma^2-\nu^2})}{(ik-k_1)(ik-k_2)(-\kappa-i\sqrt{k^2-\nu^2}}$$

The residue at k_2 is given as

$$\text{Res}(k_2) = \frac{e^{ik_2y+z\sqrt{\nu^2+k_2^2}}(2i\sqrt{\gamma^2-\nu^2})}{(k_2-k_1)(-\kappa+\sqrt{\nu^2+k_2^2})}$$

$$= \frac{e^{-iy\sqrt{\gamma^2-\nu^2}+\gamma z}(2i\sqrt{\gamma^2-\nu^2})}{(-2\sqrt{\gamma^2-\nu^2})(-\kappa+\gamma)}$$

As $\gamma \to \kappa$, the Res (k_2) term becomes singular. It should not be surprising that the Res (k_4) exactly cancels this

singular behavior. If we define $\gamma \equiv \kappa - \delta$ where $\delta/\kappa << 1$ and $|\delta y| << 1$ and $|\delta z| << 1$, then as $\delta \to 0$, it follows:

$$\sqrt{\gamma^2 - \nu^2} \simeq \sqrt{\kappa^2 - \nu^2} - \frac{\kappa\delta}{\sqrt{\kappa^2 - \nu^2}} + O(\delta^2)$$

and

$$\text{Res}(k_2) \sim \lim_{\delta \to 0} ie^{-i\sqrt{\kappa^2 - \nu^2}\, y + \kappa z} \left[1/\delta - (z - iy \frac{\kappa}{\sqrt{\kappa^2 - \nu^2}}) \right] .$$

In a similar manner, we can show that the residue at k_4 is the following

$$\text{Res}(k_4) = \frac{e^{-i\sqrt{\kappa^2 - \nu^2}\, y + \kappa z}}{(\kappa^2 - \gamma^2)} \cdot \left[\frac{-2i\kappa\sqrt{\gamma^2 - \nu^2}}{\sqrt{\kappa^2 - \nu^2}} \right]$$

$$\simeq \lim_{\delta \to 0} \frac{-ie^{-i\sqrt{\kappa^2 - \nu^2}\, y + \kappa z}}{\delta} .$$

The sum of the two residues is just

$$\text{Res}(k_2) + \text{Res}(k_4) = -ie^{-i|y|\sqrt{\kappa^2 - \nu^2} + \kappa z} (z - i|y| \frac{\kappa}{\sqrt{\kappa^2 - \nu^2}}) .$$

There are two comments. First, we have replaced y by $|y|$. The contour for $y<0$ is closed in the lower half of the k plane and since the details are similar, they were omitted.

Second, the contribution from the residues becomes unbounded if we formally let $\sqrt{y^2+z^2} \to \infty$. This does not matter since we only use this analysis to find the behavior of the diffraction potential near the body and it only has to match the inner expansion of the outer expansion.

Now, combining the contribution from the residues and the arcs C_2 and C_4 we find that the potential ϕ_s from (B4) is given as:

$$\phi_s(y,z) = p_o e^{-i|y|\sqrt{\kappa^2-\nu^2}-\kappa z}\left(z-i|y|\frac{\kappa}{\sqrt{\kappa^2-\nu^2}}\right)$$

$$\frac{-p_o\sqrt{\kappa^2-\nu^2}}{\pi}\int_\nu^\infty dk\, \frac{e^{-|y|k}}{(ik-\sqrt{\kappa^2-\nu^2})(ik+\sqrt{\kappa^2-\nu^2})}\left[\frac{e^{iz\sqrt{k^2-\nu^2}}}{-\kappa+i\sqrt{\nu^2+k^2}}+\frac{e^{-iz\sqrt{k^2-\nu^2}}}{\kappa+i\sqrt{\nu^2+k^2}}\right]$$

(B5)

To find the behavior of ϕ_s far from the origin, we see that the integral term in (B5) can be bounded as follows:

$$\left|\int_\nu^\infty dk\, \frac{e^{-|y|k\pm iz\sqrt{k^2-\nu^2}}}{(ik-\sqrt{\kappa^2-\nu^2})(ik+\sqrt{\kappa^2-\nu^2})(\pm\kappa+i\sqrt{\nu^2+k^2})}\right| \le \left|\int_\nu^\infty dk\, \frac{e^{-|y|k}}{\kappa(k^2+\kappa^2-\nu^2)}\right|$$

$$\le \left|\frac{e^{-|y|\nu}}{\kappa}\int_o^\infty dk\, \frac{e^{-|y|k}}{k^2+\kappa^2}\right|$$

$$= \left|\frac{e^{-|y|\nu}}{\kappa^2}\,\mathrm{Im}\left[e^{i\kappa|y|}E_1(i\kappa y)\right]\right|$$

The last equality comes from Abramowitz and Stegan (1964). In the near field $y = O(\varepsilon)$ and $O(\kappa y) = O(1) = O(\nu y)$, and both terms in (B5) are of order ε. In the outer expansion of the inner expansion, $O(y) = O(z) = O(1)$. As a result, the integral terms are bounded by $O(\varepsilon e^{-\varepsilon^{-1}})$ which is exponentially small and the residue terms are of order one. This assumes that the constant p_o is also of order one. Consequently, the asymptotic behavior of ϕ_S for large values of $\sqrt{y^2 + z^2}$ is

$$\phi_S(y,z) \simeq p_o e^{-i|y|\sqrt{\kappa^2-\nu^2} + \kappa z\left(z - i|y|\frac{\kappa}{\sqrt{\kappa^2-\nu^2}}\right)} \qquad \text{(B6)}$$

The problem of the anti-symmetric pressure distribution is similar to ϕ_S and some of the details will be omitted. The potential will be designated as ϕ_{AS} and the pressure on the free surface is given as follows:

$$p(y) = \operatorname{sgn}(y) p_o e^{-\mu|y| - i|y|\sqrt{\gamma^2-\nu^2}} \qquad \text{(B7)}$$

At an appropriate point we will let $\mu \to o$ and $\gamma \to \kappa$ as before. Since $p(y)$ is an odd function $p^*(k)$ can be found using a sine transform. Then, in an analysis similar to that preceding (B4) we find

$$\phi_{AS}(y,z) = \frac{-ip_o}{\pi} \int_{-\infty}^{\infty} dk \, \frac{k e^{iky + \sqrt{\nu^2+k^2}\, z}}{(k-k_1)(k-k_2)(-\kappa+\sqrt{\nu^2-k^2})} \qquad \text{(B8)}$$

where $k_1 = \sqrt{\gamma^2-\nu^2} - i\mu$ and $k_2 = -\sqrt{\gamma^2-\nu^2} + i\mu$.

Now we can evaluate (B8) as (B4) by using the residue theorem in connection with Figure B1. Using the same limiting procedure as before, we can show that

$$\phi_{AS}(y,z) = p_o \operatorname{sgn}(y) e^{-i|y|\sqrt{\kappa^2-\nu^2}+\kappa z}\left(z-i|y|\frac{\kappa}{\sqrt{\kappa^2-\nu^2}}\right)$$

$$+\frac{ip_o}{\pi}\operatorname{sgn}(y)\int_{\nu}^{\infty}\frac{dk\,k\,e^{-|y|k}}{(ik-\sqrt{\kappa^2-\nu^2})(ik+\sqrt{\kappa^2-\nu^2})}\cdot$$

$$\cdot\left[\frac{e^{iz\sqrt{k^2-\nu^2}}}{-\kappa+i\sqrt{\nu^2+k^2}}+\frac{e^{-iz\sqrt{k^2-\nu^2}}}{\kappa+i\sqrt{\nu^2+k^2}}\right]$$

(B9)

Similarly, it can also be shown that the asymptotic behavior of ϕ_{AS} for large values of $\sqrt{y^2+z^2}$ is

$$\phi_{AS}(y,z) \approx p_o \operatorname{sgn}(y) e^{-i|y|\sqrt{\kappa^2-\nu^2}+\kappa z}\left(z-i|y|\frac{\kappa}{\sqrt{\kappa^2-\nu^2}}\right)$$

With the information we have at hand, the potential, ϕ_L, for an arbitrary local pressure distribution can be written down. If the pressure is defined by P(y), then using the definition of the inverse Fourier transform we can write

$$\phi_L(y,z) = \frac{1}{2\pi}\int_{-\infty}^{\infty} dk \frac{e^{iky}}{(-\kappa+\sqrt{\nu^2+k^2})} P^*(k)$$

$$= \frac{1}{2\pi}\int_{-\infty}^{\infty} dk \frac{e^{iky}}{-\kappa+\sqrt{\nu^2+k^2}} \int_{-\infty}^{\infty} d\xi e^{-ik\xi} p(\xi)$$

(B10)

The integral has two poles and the contour is indented in such a manner as to insure outgoing waves.

APPENDIX C

Simplification of I(k)

The inner integrals of the potential for the line singularities given by (23a) and (67) can be simplified as a result of the assumptions of short waves from oblique headings. We will consider the case of zero speed first.

Make a change of variables of $k' = k + \nu$ and recall the dispersion relation. Then (23a) becomes

$$I_S(k') = \lim_{\mu \to 0} \int_{-\infty}^{\infty} d\ell \, \frac{e^{i\ell y + \sqrt{(k'-\nu)^2 + \ell^2}\, z}}{\sqrt{(k'-\nu)^2 + \ell^2} - (\kappa - i\mu')} \quad . \tag{C1}$$

Here $\frac{1}{g}(\omega_o - i\mu)^2 = \frac{1}{g}(\omega_o^2 - 2i\omega_o\mu + \mu^2)$, and since $\mu \to 0$, we drop the μ^2 term and define $\mu' \equiv \frac{2\omega_o \mu}{g}$.

We will now drop the primes, and note that (C1) contains both branch points where $\sqrt{(k-\nu)^2 + \ell^2}$ equals zero and simple poles where the denominator goes to zero. Through the use of the residue calculus we will evaluate $I_S(k)$.

The poles are given by values of ℓ equal to ℓ_o, where

$$\ell_o = \pm\sqrt{(\kappa - i\mu)^2 - (\nu - k)^2} \quad , \tag{C2}$$

and the branch points are given to ℓ equal to ℓ_1 where

$$\ell_1 = \pm i\sqrt{(\nu-k)^2} = \pm i|\nu - k| \quad . \tag{C3}$$

The branch cuts will be taken on the imaginary axis from $\pm i|\nu-k|$ to $\pm i\infty$.

Consider ℓ_o. If $[\kappa^2 - (\nu-k)^2] < 0$, then ℓ_o is imaginary and if $[\kappa^2 - (\nu-k)^2] > 0$ then ℓ_o is real. This gives the following intervals on k:

Case i) $k > \nu + \kappa$; ℓ_o is imaginary

Case ii) $\nu - \kappa < k < \nu + \kappa$; ℓ_o is real

Case iii) $\nu - \kappa > k$; ℓ_o is imaginary .

Case i) From (C2), define $\ell_o = +i\sqrt{(\nu-k)^2 - \kappa^2}$ and consider $y > 0$. Then the contour in Figure C1 will yield I(k).

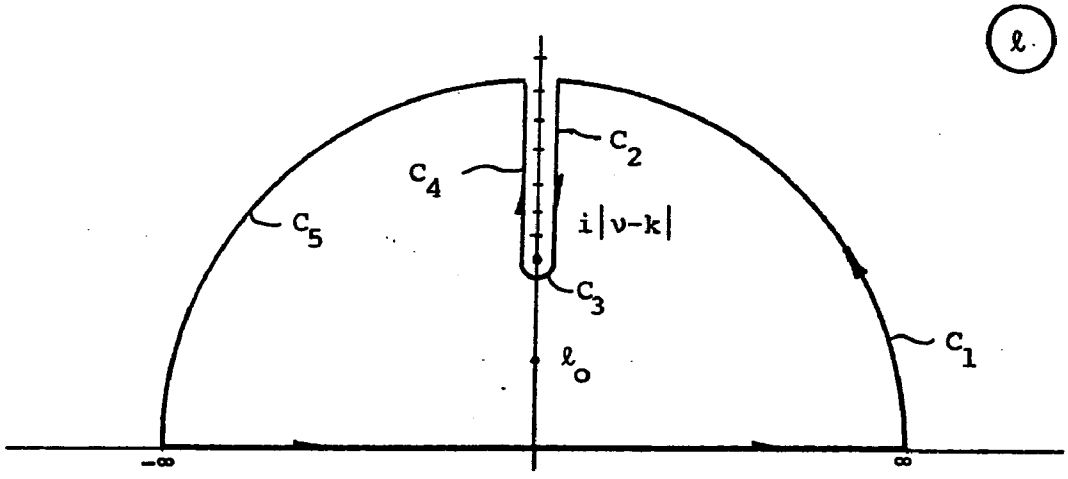

Figure C1: Contour of Integration for $k > \nu + \kappa$

The residue theorem states that

$$I_S(k) = 2\pi i \, \text{Res}(\ell_o) - \left[\int_{C_1} + \int_{C_2} + \int_{C_3} + \int_{C_4} + \int_{C_5}\right] d\ell \, \frac{e^{i\ell y + \sqrt{(\nu-k)^2 + \ell^2}\, z}}{\sqrt{(\nu-k)^2 + \ell^2} - \kappa}$$

To find the residue at ℓ_o, we know from l' Hospital's rule that

$$\text{Res}\ (\ell_o) = \lim_{\ell \to \ell_o} (\ell - \ell_o) \frac{e^{i\ell y + \sqrt{(\nu-k)^2 + \ell^2}\, z}}{\sqrt{(\nu-k)^2 + \ell^2} - \kappa}$$

$$= \frac{e^{i\ell_o y + \sqrt{(\nu-k)^2 + \ell_o^2}\, z}}{\ell_o} \sqrt{\ell_o^2 + (\nu-k)^2}$$

$$= \kappa \frac{e^{-y\sqrt{(\nu-k)^2 - \kappa^2} + z\kappa}}{i\sqrt{(\nu-k)^2 - \kappa^2}}$$

The contribution from C_3 is zero and since y is greater than zero, C_1 and C_5 also contribute nothing. On C_2 and C_4 we will get a non-zero contribution that will be shown to be of higher order.

If we make the substitution of $\ell = i\ell'$ into the radical $\sqrt{(\nu-\kappa)^2 + \ell^2}$ after considering Figure C2, then on C_2 the radical takes the value of

$$\sqrt{(\nu-\kappa)^2 + \ell^2} = i\sqrt{\ell'^2 - (\nu-k)^2}$$

and the integral along C_2 becomes

$$\int_{C_2} d\ell \frac{e^{i\ell y + \sqrt{(\nu-k)^2 + \ell^2}\, z}}{\sqrt{(\nu-k)^2 + \ell^2} - \kappa} = i \int_{\infty}^{|\nu-k|} d\ell' \frac{e^{-\ell' y + i\sqrt{\ell'^2 - (\nu-k)^2}\, z}}{i\sqrt{\ell'^2 - (\nu-k)^2} - \kappa}$$

$$= -i \int_{|\nu-k|}^{\infty} d\ell' \frac{e^{-\ell' y + i\sqrt{\ell'^2 - (\nu-k)^2}\, z}}{i\sqrt{\ell'^2 - (\nu-k)^2} - \kappa}$$

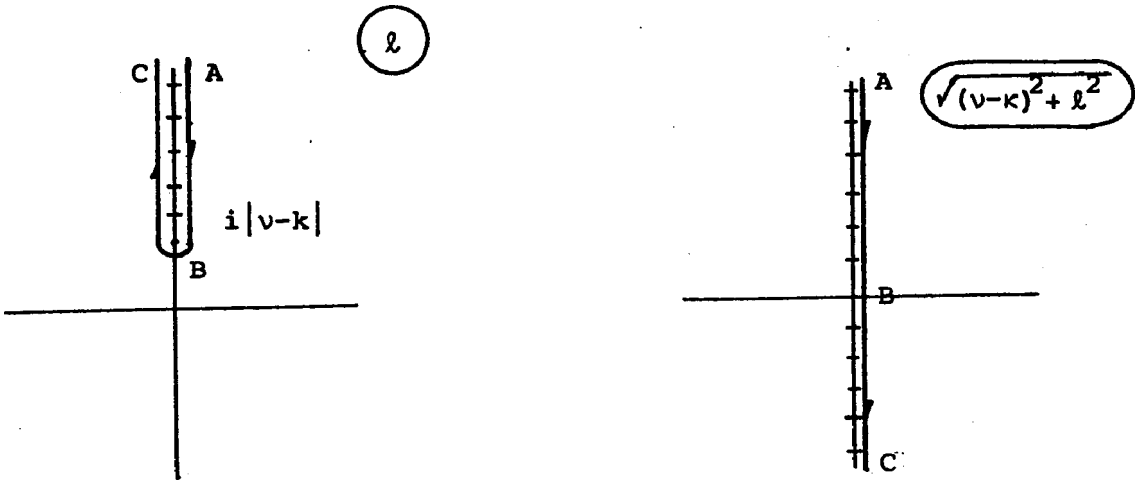

Figure C2: Contour Around the Branch Cut in the ℓ-Plane and $\sqrt{(\nu-\kappa)^2 + \ell^2}$ Plane

Similarly, along C_4, the radical takes the value of

$$\sqrt{(\nu-k)^2 + \ell^2} = -i\sqrt{\ell'^2 - (\nu-k)^2}$$

and the integral becomes

$$\int_{C_4} d\ell \, \frac{e^{i\ell y + \sqrt{(\nu-k)^2+\ell^2}\, z}}{\sqrt{(\nu-k)^2+\ell^2} - \kappa} = i \int_{|\nu-k|}^{\infty} d\ell' \, \frac{e^{-\ell' y - i\sqrt{\ell'^2 - |\nu-k|^2}\, z}}{-i\sqrt{\ell^2 - |\nu-k|^2} - \kappa}$$

Now, dropping the primes and recalling that $\kappa = O(\varepsilon^{-1})$ and $y = O(1)$, the two integrals can be bounded as follows:

$$\left| \int_{|\nu-k|}^{\infty} d\ell \, \frac{e^{-\ell y \pm i\sqrt{\ell'^2 - |\nu-k|^2}\, z}}{\pm i\sqrt{\ell'^2 - |\nu-k|^2} - \kappa} \right| \leq \int_{|\nu-k|}^{\infty} d\ell \, \frac{e^{-\ell y}}{\kappa}$$

$$= \frac{1}{\kappa} e^{-y|\nu-k|}$$

$$= o(\varepsilon e^{-1/\varepsilon})$$

Case ii) Here ℓ_o is real and the contour has to be deformed around the singularities. This is where the artificial vicosity will be useful. From equation (C2),

$$\ell_o = \pm \lim_{\mu \to o} \sqrt{(\kappa - i\mu)^2 - (\nu - k)^2}$$

$$= e^{i\left[\frac{o}{\pi}\right]} \left[\kappa^2 - |\nu - k|^2\right]^{1/2} \exp_{\lim \mu \to o} \left[\left[\tan^{-1}\left(-2\kappa\mu / (\kappa^2 - (\nu-k)^2)\right)\right]/2\right]$$

$$= \left[\kappa^2 - |\nu - k|^2\right]^{1/2} e^{i\left[\frac{o}{\pi}\right] + i\pi}$$

$$= \left[\kappa^2 - |\nu - k|^2\right]^{1/2} e^{i\left[\frac{\pi}{2\pi}\right]}$$

Consequently, ℓ_o, when negative, approaches the real axis from above and when positive approaches the real axis from below. Figure C3 defines the contour for evaluating $I_s(k)$.

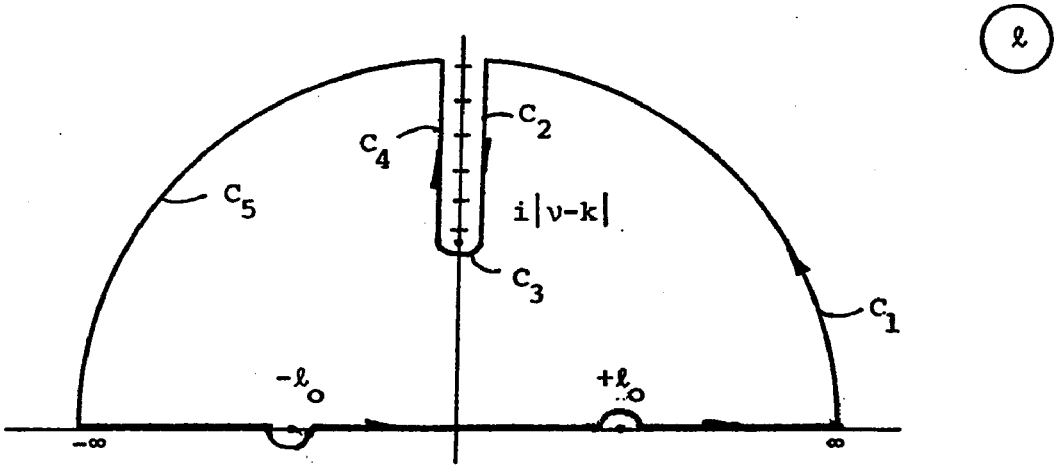

Figure C3: Contour of Integration for $\nu - \kappa < k < \nu + \kappa$

Again using the residue theorem, we find

$$I_s(k) = 2\pi i \,\mathrm{Res}\,(-\ell_o) - \left[\int_{C_1} + \int_{C_2} + \int_{C_3} + \int_{C_4} + \int_{C_5}\right] d\ell \, \frac{e^{i\ell y + \sqrt{(\nu-k)^2+\ell^2}\, z}}{\sqrt{(\nu-k)^2+\ell^2} - \kappa}$$

where $I_s(k)$ is now interpreted as a contour integral on the real axis as shown and $\ell_o = \sqrt{\kappa^2 - (\nu-k)^2}$. The residue can be calculated as before:

$$\mathrm{Res}(-\ell_o) = \lim_{\ell\to\ell_o} (\ell+\ell_o)\, \frac{e^{i\ell y + \sqrt{(\nu-k)^2+\ell^2}\, z}}{\sqrt{(\nu-k)^2+\ell^2} - \kappa}$$

$$= \frac{e^{-\ell_o y + \sqrt{(\nu-k)^2+\ell_o^2}\, z}}{-\ell_o} \left(\ell_o^2 + (\nu-k)^2\right)^{1/2}$$

$$= \frac{-\kappa\, e^{-iy\sqrt{\kappa^2-(\nu-k)^2}}}{\sqrt{\kappa^2-(\nu-k)^2}} + \kappa z$$

As in case i), the contours from C_1, C_3 and C_5 contribute nothing. The integrals on C_2 and C_4 can be bounded as follows:

$$\left|\left[\int_{C_2} + \int_{C_4}\right] d\ell \, \frac{e^{i\ell y + \sqrt{(\nu-k)^2+\ell^2}\, z}}{\sqrt{(\nu-k)^2+\ell^2} - \kappa}\right| \leq \frac{1}{\kappa} e^{-y|\nu-k|}$$

$$= O(\varepsilon),$$

since in the second case $0 \leq |\nu-k|$. Note that this is a weaker upper bound than that found for case i). However, it still is of higher order than the residue terms.

Case iii) This is very similar to case i) though the contour is indented in an opposite manner. The residue is given by:

$$\text{Res}(\ell_o) = \frac{\kappa e^{-y\sqrt{(\nu-k)^2 - \kappa^2}} + z\kappa}{i\sqrt{(\nu-k)^2 - \kappa^2}}$$

and the rest of the integrals are $O(\varepsilon e^{-1/\varepsilon})$ or higher.

The results are summarized in the following table:

TABLE C1

Values of $I_S(k)$ for Different Ranges of k and U Equal to Zero.

	$k>\nu+\kappa$ or $k<\nu-\kappa$	$\nu-\kappa<k<\nu+\kappa$
$I_S(k)$	$\dfrac{2\pi\kappa e^{-\lvert y\rvert\sqrt{(\nu-k)^2-\kappa^2}+z\kappa}}{\sqrt{(\nu-k)^2-\kappa^2}}$	$\dfrac{-2\pi i\kappa e^{-i\lvert y\rvert\sqrt{\kappa^2-(\nu-k)^2}+z\kappa}}{\sqrt{\kappa^2-(\nu-k)^2}}$

Here y has been replaced by $|y|$. For y negative, the contour is taken below the real axis instead of above. The details are very similar to those described in the preceding section and will be omitted.

To find the approximation to (23b), the dipole inner integral, an analysis similar to that for the source inner integral could be used. However, as noted in Chapter III, differentiation of the terms in Table C1, will give the same results. The dipole inner integral $I_D(k)$ is given in Table C2.

TABLE C2

Values of $I_D(k)$ for Different Ranges of k and U Equal to Zero.

	$k>\nu+\kappa$ or $k<\nu-\kappa$	$\nu-\kappa<k<\nu+\kappa$
$I_D(k)$	$-\mathrm{sgn}(y)\,2\pi\kappa e^{-\lvert y\rvert\sqrt{(\nu-k)^2-\kappa^2}+\kappa z}$	$-\mathrm{sgn}(y)\,2\pi\kappa e^{-i\lvert y\rvert\sqrt{\kappa^2-(\nu-k)^2}+\kappa z}$

If we include forward speed, then $I_S(k)$ is given by equation (67). We will now simplify $I_S(k)$ as in the zero speed case by assuming short waves from oblique headings. First, make the substitution $k' = k + \nu$ and recall that $\omega - \nu U = \omega_o$. Then (67) becomes

$$I_S(k') = \lim_{\mu\to o} \int_{-\infty}^{\infty} \frac{d\ell\, e^{i\ell y+\sqrt{(\nu-k')^2+\ell^2}\, z}}{\sqrt{(\nu-k')^2+\ell^2} - \frac{1}{g}(\omega_o+k'U-i\mu)^2} \qquad (C4)$$

We will drop the primes and note that (C4) contains both branch points and simple poles, just as (C1) did. The branch points given by ℓ_1 are the same as in the zero speed case:

$$\ell_1 = \pm\, i\sqrt{(\nu-k)^2} = \pm\, i\lvert\nu-k\rvert \quad . \qquad (C5)$$

As in (C3) the branch cut will be taken on the imaginary axis from $\pm i\lvert\nu-k\rvert$ to $\pm i\infty$

The poles are somewhat more complex than those given in (C2). Let the poles be designated by ℓ_o where

$$\ell_o = \pm\sqrt{\frac{1}{g2}(\omega_o + kU)^4 - (\nu-k)} \quad , \tag{C6}$$

Here, μ has been set equal to zero. It will be useful only in determining the path of integration which will be considered later.

Since k varies from $+\infty$ to $-\infty$; ℓ_o will be real or imaginary for various values of k. For example, when

$\frac{1}{g^2}(\omega_o + kU)^4 > (\nu-k)^2$, ℓ_o will be real and when

$\frac{1}{g^2}(\omega_o + kU)^4 < (\nu-k)^2$, ℓ_o will be imaginary. Consider

then, the values of k when

$$\frac{1}{g^2}(\omega_o + k\nu)^4 - (\nu-k)^2 = 0 \tag{C7}$$

There are two real and two complex roots to (C7). Since k is a real variable, we are only interested in the real roots which are as follows:

$$k = k_1 = \left[-(2\omega_o U+g) + \sqrt{4U^2\nu g + 4\omega_o Ug + g^2}\right]/2U^2$$

and

$$k = k_2 = -\left[(2\omega_o U+g) + \sqrt{4U^2\nu g + 4\omega_o Ug + g^2}\right]/2U^2$$

It is easily shown that for $k>k_1$, and $k<k_2$, ℓ_o is real and that for $k_2<k<k_1$, ℓ_o is imaginary. Consider the three intervals of k in evaluating $I_s(k)$ given in (C4) for $y>0$:

i) $k>k_1$

Note that $k_1<0$, which means that this interval includes the region around $k = 0$. The integration in (C4) is done on the real axis and its path will have to be indented around the poles. To find the direction of this indentation, let $\mu \to 0$. In a manner similar to that done for the zero speed problem, ℓ_o can be shown to approach the axis in the ℓ-plane from below for $\ell_o>0$ and from above for $\ell_o<0$. The contour on the real axis is given in Figure C4.

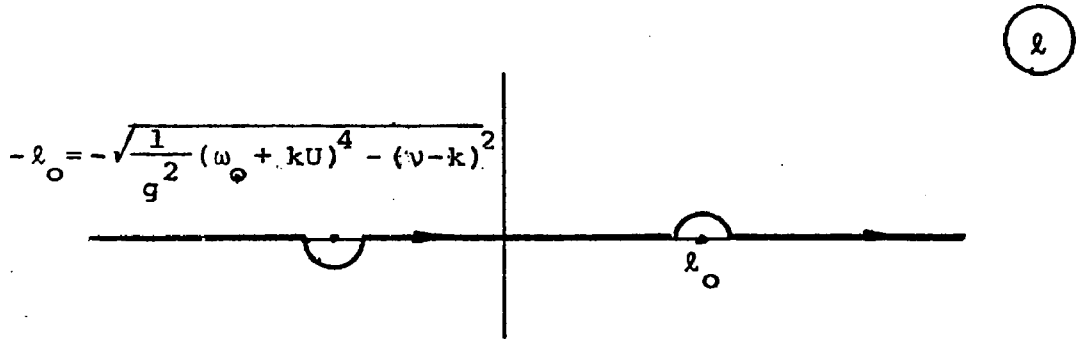

Figure C4: Contour of Integration on the Real Axis for $k>k_1$.

ii) $k_2<k<k_1$

Here ℓ_o is imaginary and the path of integretation does not have to be indented. For this range of k, define ℓ_o as

$$\ell_o = i\sqrt{(\nu-k)^2 - \frac{1}{g^2}(\omega_o + \kappa U)^4} \qquad \text{(C8)}$$

iii) $k<k_2$

As in the first interval, ℓ_o is real and the contour has to be indented as shown in Figure C5. The details for determining this are similar to that used in the zero speed case.

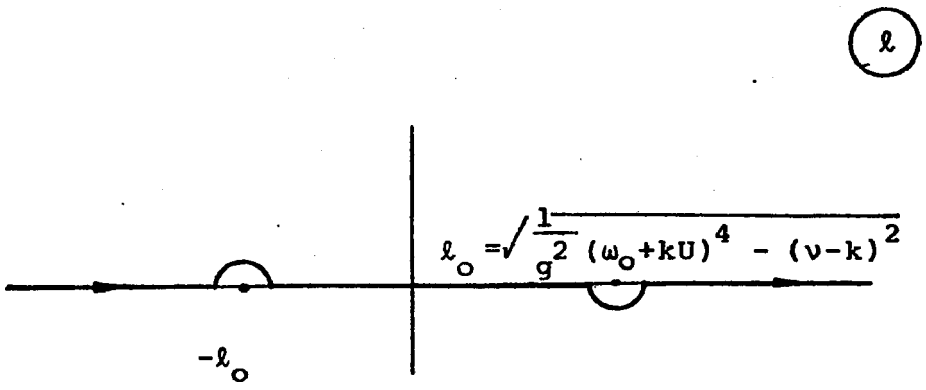

Figure C5: Contour of Integration on the Real Axis for $k<k_2$.

Equation (C4) can then be written in the following manner:

$$I_S(k) = \int_{C(k)} d\ell \, \frac{e^{i\ell y + \sqrt{(\nu-k)^2+\ell^2}\, z}}{\sqrt{(\nu-k)^2+\ell^2} - \frac{1}{g}(\omega_o+kU)^2}, \qquad \text{(C9)}$$

where C(k) is the contour given for the three ranges of k.

As in the zero speed problem (C9) can be simplified through the use of residue analysis. For $k>k_1$, use the contour given in Figure C3 and values of ℓ_o given in (C6). Then the arcs C_1, C_3, C_5 contribute nothing. The contribution from arcs C_2 and C_4 is $O(\varepsilon)$ and, consequently, dropped for being of higher order. $I_S(k)$ is then approximated by $2\pi i$ times the residue at $-\ell_o$. Similarly, for $k_2<k<k_1$, use the values of ℓ_o given in (C8) and the contour in Figure C1. Again the lowest order approximation to $I_S(k)$ is given by the residue at ℓ_o multiplied by $2\pi i$. For $k<k_2$, the contour is similar to that of Figure C3, though it is indented in an opposite manner, i.e., the indentation is above the axis for ℓ_o negative and below the axis for ℓ_o positive. The only contribution consistent with the level of approximation is from the residue. To summarize, the results are given in Table C3. This is for $y>0$.

TABLE C3

$I_S(k)$ for Different Values of k and U Not Equal to Zero.

	$I_S(k)$
$k>k_1$	$\dfrac{-2\pi i e^{-iy\sqrt{\frac{1}{g^2}(\omega_o+kU)^4-(\nu-k)^2}} \cdot e^{\frac{1}{g}(\omega_o+kU)^2 z} \cdot \frac{1}{g}(\omega_o+kU)^2}{\sqrt{\frac{1}{g^2}(\omega_o+kU)^4-(\nu-k)^2}}$
$k_2<k<k_1$	$\dfrac{2\pi\, e^{-y\sqrt{(\nu-k)^2-\frac{1}{g^2}(\omega_o+kU)^4}} \cdot e^{\frac{1}{g}(\omega_o+kU)^2 z} \cdot \frac{1}{g}(\omega_o+kU)^2}{\sqrt{(\nu-k)^2-\frac{1}{g^2}(\omega_o+kU)^4}}$
$k<k_2$	$\dfrac{2\pi i\, e^{iy\sqrt{\frac{1}{g^2}(\omega_o+kU)^4-(\nu-k)^2}} \cdot e^{\frac{1}{g}(\omega_o+kU)^2 z} \cdot \frac{1}{g}(\omega_o+kU)^2}{\sqrt{\frac{1}{g^2}(\omega_o+kU)^4-(\nu-k)^2}}$

BIBLIOGRAPHY

Abramowitz, M. and Stegun, I. 1964. Handbook of Mathematical Functions. Washington, D.C.: U.S. Government Printing Office.

Choo, K.Y. 1975. "Exciting Forces and Pressure Distribution on a Ship in Oblique Waves." Ph.D. Dissertation, Massachusetts Institute of Technology. 139 pp.

Faltinsen, O.M. 1971. A Rational Strip Theory of Ship Motions: Part 2, Report No. 113, Department of Naval Architecture and Marine Engineering, The University of Michigan, Ann Arbor, Michigan. 137 pp.

Frank, W. 1967. Oscillations of Cylinders in or Below the Free Surface of Deep Fluids, Report No. 2375, Naval Ship Research and Development Center, Washington, D.C. 45 pp.

Goodman, R.A. 1971. "Wave-Excited Main Hull Vibration in Large Tankers and Bulk-Carriers." Transactions, Royal Institute of Naval Architects 113:167-184.

Gradshteyn, I.S., Ryzhik, I.M. 1965. Tables of Integrals, Series, and Products, Academic Press, New York and London.

John, F. 1950. "On the Motion of Floating Bodies." Communications on Pure and Applied Mathematics. 3:45-101.

Kellogg, O.D. 1929. Foundations of Potential Theory. New York: Dover Publishing, Inc.

Khaskind, M.D. 1953. "The Diffraction of Waves About a Moving Cylindrical Vessel." Prikl. Mat. Mikh. 17:431-442.

_____. 1957. The Exciting Forces and Wetting of Ships in Waves. English translation: Report No. 307, David Taylor Model Basin. Washington, D.C.

Lamb, H. 1932. Hydrodynamics. Cambridge: Cambridge University Press.

McCreight, W.R. 1973. "Exciting Forces on a Moving Ship in Waves." Ph.D. Dissertation, Massachusetts Institute of Technology. 59 pp.

Nakamura, S., Takagi, M., Saito, K. and Ganno, M. 1973. "Hydrodynamic Pressures on a Restrained Ship in Oblique Waves." (J). Journal Society of Naval Architects of Japan. 133:85-100.

Newman, J.N. 1965. The Exciting Forces on a Moving Body in Waves. Journal of Ship Research. 9:190-199.

_____. 1970. Applications of Slender-Body Theory in Ship Hydrodynamics. Annual Review of Fluid Mechanics. 2:67-94.

Ogilvie, T.F. 1970. Singular Perturbation Problems in Ship Hydrodynamics. Report No. 096, Department of Naval Architecture and Marine Engineering, The University of Michigan, Ann Arbor, Michigan. 198 pp.

_____. 1974. The Fundamental Assumptions on Ship-Motion Theory. Report No. 148, Department of Naval Architecture and Marine Engineering, The University of Michigan, Ann Arbor, Michigan. 32 pp.

Ogilvie, T.F. and Tuck, E.O. 1969. A Rational Strip Theory of Ship Motions: Part 1. Report No. 013, Department of Naval Architecture and Marine Engineering, The University of Michigan, Ann Arbor, Michigan. 92 pp.

Ohmatsu, S. 1975. On the Irregular Frequencies in the Theory of Oscillating Bodies in a Free Surface. Papers of Ship Research Institute.

Porter, W.R. 1960. Pressure Distribution Added-Mass and Damping Coefficients for Cylinders Oscillating in a Free Surface: Report No. 82-16, University of California, Institute of Engineering Research, Berkeley, California.

Society of Ship Research of Japan (SSRJ). 1974. Measurement of Hydrodynamic Pressures Acting on the Hull of a Ship Which is Constrained in the Regular Waves. Committee Report of SR 131, 76-93.

Tricomi, F.G. 1957. Integral Equations. New York: Wiley: Interscience.

Tuck, E.O. 1965. The Application of Slender Body Theory to Steady Ship Motion. Report No. 2008, David Taylor Model Basin, Washington, D.C.

Ursell, F. 1962. Slender Oscillating Ships at Zero Forward Speed. Journal of Fluid Mechanics. 19:496-516.

_____. 1968. The Expansion of Water-Wave Potentials at Great Distances. Proceedings of the Cambridge Philosophical Society. 64:811-26.

Van Dyke, M. 1964. Perturbation Methods in Fluid Mechanics. New York: Academic Press.

Vugts, J.H. 1970. The Hydrodynamic Forces and Ship Motions in Waves. Ph.D. Dissertation. Technological University. Delft, Netherlands.

Wehausen, J.V. and Laitone, E.V. 1960. Surface Waves. Encyclopedia of Physics. Berlin: Springer-Verlag. IX:446-778.